D.1 Alkanes, Alkenes, Dienes and Diyenes

D.1.1 Acyclic Alkanes

The available proton affinities, gas basicities and resultant standard reaction enthalpy, entropy and Gibbs free energies for the non-dissociative proton transfer reaction of H_3O^+ with $C_1 - C_{12}$ acyclic alkanes are summarised in Table D.1.

Table D.1: A compilation of proton affinities (*PA*), gas basicities (*GB*), potential standard enthalpy (ΔH_r^Φ), potential standard entropy (ΔS_r^Φ) and Gibbs free energies (ΔG_r^Φ) of non-dissociative reaction of H_3O^+ with acyclic alkanes. Proton affinities and gas basicities are taken from Hunter and Lias, (1998) unless otherwise specified: [a]Hunter and East (2002), [b]Wróblewski *et al* (2006), [c]Arnold *et al* (1998). ΔG_r^Φ and ΔH_r^Φ are calculated from Eq. 2.88 and 2.89. ΔS_r^Φ is calculated from $\Delta S_r^\Phi = \left[\Delta H_r^\Phi - \Delta G_r^\Phi\right] / T$.

Compound	*PA* (eV)	*GB* (eV)	ΔH_r^Φ (eV)	ΔS_r^Φ (x 10^{-4} eV K^{-1})	ΔG_r^Φ (eV)
Methane	5.63	5.40	1.53	2.82	1.44
	5.42[b]		1.75		
	5.70[c]		1.46		
Ethane	6.18	5.91	0.98	1.60	0.93
	6.17[a]		0.99		
	5.82[b]		1.34		
	6.22[c]		0.94		
Propane	6.48	6.30	0.68	4.56	0.54
	6.51[a]		0.65		
	6.60[b]		0.56		
	6.53[c]		0.63		
n-Butane	6.85[a]		0.31		
	6.83[b]		0.33		
	6.74[c]		0.42		
iso-Butane (2-methyl propane)	7.02	6.96	0.14	8.52	-0.12
n-Pentane	6.91[a]		0.25		
	6.87[b]		0.30		
	6.98[c]		0.19		
n-Hexane	6.97[a]		0.19[a]		
	7.01[b]		0.15[b]		
	7.16[c]		0.00[c]		
n-Heptane	7.03[a]		0.13		
	7.36[c]		-0.20		
n-Octane	7.09[a]		0.08		
	7.57[c]		-0.40		
n-Nonane	7.11[a]		0.05		
n-Decane	7.16[a]		0.01		
n-Undecane	7.17[a]		-0.01		
n-Dodecane	7.18[a]		-0.02		

There are few gas bacisities available for the acyclic alkanes. Those available for the $C_1 - C_3$ *n*-alkanes and *iso*-butane correspond to a small positive change in entropy for the reaction of H_3O^+ with the alkanes. The proton affinities increase with the size of the alkane, this may be explained by the increasing number of electron donating methyl groups able to stabilise the positive charge of the donated proton. The extent and nature of the increase in *PA* for the larger alkanes is unclear. Hunter and Lias (1998) have reviewed available data and produced evaluated (experimentally and theoretically derived) proton affinities. Theoretical values calculated *via* the *ab initio* method have been obtained by Wróblewski *et al* (2006) (restricted Hartree-Fock method with 6-311G** split valence molecular orbitals basis sets) and Hunter and East (2002) (coupled-cluster theory with single, double and approximate triple excitations using cc-pVTZ basis sets). Arnold *et al* (1998) have estimated theoretical proton affinities using the known thermochemistry of alkanes and H^+ and estimated enthalpies of formation of $C_nH_{2n+3}{}^+$. These proton affinities are displayed in Figure D.1.

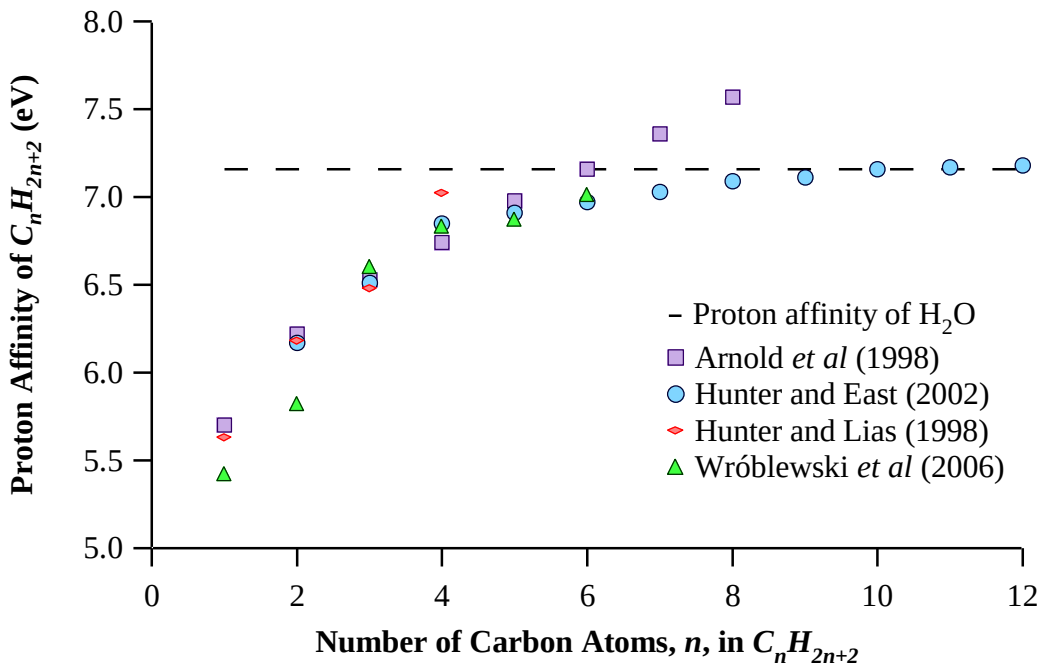

Figure D.1: The proton affinities of the $C_1 - C_{12}$ acyclic alkanes. Values correspond to the *n*- isomer alkanes except the C_4 value of Hunter and Lias (1998) which is the *PA* of *iso*-butane.

Evaluated proton affinity data is only available for the $C_1 - C_3$ straight chain alkanes and *iso*-butane in the review of Hunter and Lias (1998). The theoretical *PA* values for the $C_1 - C_3$ *n*-alkanes generally agree well with the evaluated data reviewed by Hunter and Lias (1998). The *PA* of these small alkanes is much less than that of water and the reaction with H_3O^+ is endothermic (Table D.1). The methane and ethane proton affinities calculated by Wróblewski *et al* (2006) are lower than the other theoretical and evaluated values. The

values derived by Wróblewski *et al* (2006) correspond to proton addition to one of the existing hydrogens in ethane and methane and to an outer carbon in the higher alkanes. Hunter and East (2002) found that proton affinity of *C-C* bonds is higher for central *C-C* bonds, outer *C-C* bonds having the lowest proton affinity. The Hunter and East (2002) values shown were derived for the central *C-C* bonds. This suggests the values derived by Wróblewski *et al* (2006) are low estimates and is a possible reason for the below average *PA* values for methane and ethane.

The theoretical *PA* values for the C_4 and C_5 *n*-alkanes are in good agreement and are less than the proton affinity of water, the reaction with H_3O^+ is therefore also endothermic. The theoretical *PA* values begin to diverge for the C_6 alkane and the divergence increases with increasing alkane size. The *ab initio* values for hexane are in close agreement and both less than the proton affinity of water while that derived by Arnold *et al* (1998) is equal to that of water indicating proton transfer from H_3O^+ is thermoneutral. The *PA* values derived by Arnold *et al* (1998) continue to increase and reaction with *n*-octane is exothermic by -0.40 eV. The *ab initio* values for the $C_7 – C_{12}$ alkanes increase by a decreasing amount: The H_3O^+ proton transfer reaction does not become thermoneutral until *n*-decane, and the reaction of *n*-dodecane is only slightly exothermic (-0.02 eV).

SIFT and VT-SIFT measurements of the reaction efficiencies and product distributions of the reaction of H_3O^+ with a number of acyclic alkanes are summarised in Tables D.2 and D.3 respectively. The reaction efficiencies of various acyclic alkanes with H_3O^+, H_3^+ and N_2H^+ from the SIFT and VT-SIFT are collated in Figure D2. No values are available in the presence of an electric field.

As discussed in § 2.9, a thermokinetic trend is generally observed in proton transfer reactions; the efficiency of proton transfer reaction is observed to increase with exoergicity, becoming efficient (k_m/k_c = 1) where the change in standard Gibbs free energy is less than -0.21 eV (Bouchoux *et al* 1996) to -0.43 eV (Bohme *et al* 1980). The reaction efficiency of the reaction of H_3O^+ with alkanes, C_nH_{2n+2} , reaction at 300 K (Figure C.2) in the absence of an electric field increases as *n*, the number of carbons, increases. Assuming changes in entropy remain relatively small and unimportant this appears to follow the general thermokinetic trend, given the increasing proton affinity and consequently decreasing reaction enthalpy with alkane size. The efficiency of the exothermic reactions of N_2H^+ and H_3^+ with propane and butane compared to the inefficiency of their reaction with H_3O^+ (Figure D2) also follows the trend.

Only the reaction of H_3O^+ with the C_{12} alkane is efficient at 298 K. If the proton affinities of Hunter and East (2002) are the closest to the true values for the higher alkanes following the thermokinetic trend suggests a lower limit of ΔS_r^{Φ} of 6.38 x 10^{-4} eV (ΔG_r^{Φ} = -0.21 eV) to 13.8 x 10^{-4} eV (ΔG_r^{Φ} = -0.43 eV). Conversely if the proton affinities derived by Arnold *et al* (1998) are closest to the true values and the thermokinetic trend is applied this suggests that ΔS_r^{Φ} is negative for the C_8 and possibly C_7 reaction with H_3O^+.

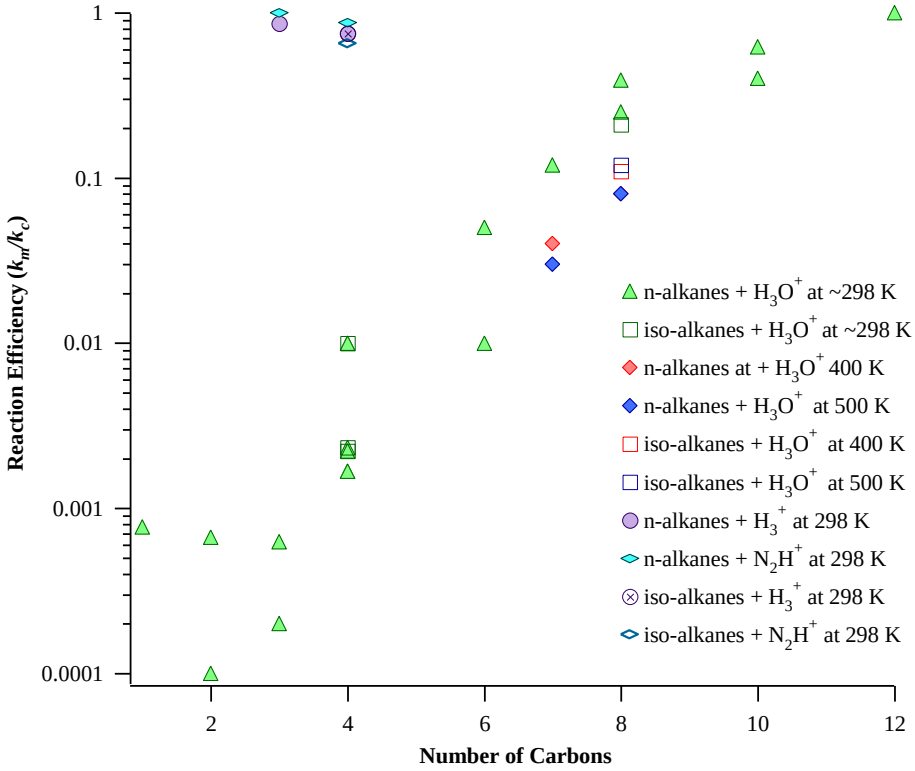

Figure D2: The reaction efficiencies of *n*- (transparent) and *iso*- (filled) acyclic alkanes with H_3O^+. The efficiencies of reaction with H_3^+ and N_2H^+ are calculated from collisional and measured rate constants in Milligan *et al* (2002), efficiencies of reactions with H_3O^+ at 400 K (red) and 500 K (blue) are taken from Arnold *et al* (1998). Efficiencies of reaction with H_3O^+ at 298 K (green) are taken from Wilson *et al* (2003), Španěl and Smith (1998), Milligan *et al* (2002) and Arnold *et al* (1998) as listed in Table D.2. k_m denotes measured rate constant and k_c collisional rate constant.

Table D.2: Reported reaction rate constants, reaction efficiencies and product distributions for the reactions of H_3O^+ with a series of acyclic alkanes measured using SIFT at ~298 K. P_{FT} denotes pressure in the flow tube, T_{FT} denotes temperature in the flow tube. NS denotes not specified, NR denotes no reaction, that is below the lowest limit that could be measured. k_m denotes the rate constant measured for the reaction of H_3O^+ with the alkane (C_nH_{2n+2}). k_c refers to the collisional rate constant (§ 2.4.1), k_L indicates that the collisional rate constant was derived from Langevin, Gioumousis, Stevenson theory (§ 2.4.1.2, Eq. 2.34) in the cited reference. k_{SC} indicates the collisional rate constant was derived using the results of Su and Chesnavich trajectory calculations (§ 2.4.1.4, Eq. 2.49 – 2.54) in the cited reference. * indicates that the method of collisional rate constant determination is not specified in the reference however since the dipoles of alkanes are close to zero all rate constant calculation theories yield a value close to k_L. k_m/k_c is the reaction efficiency (§ 2.9). δ_{k_c} denotes estimated uncertainty of the calculated collisional rate constant, δ_{k_m} denotes the estimated uncertainty of the measured rate constant. A helium carrier gas was used in all cases, small amounts of air were added by Španěl and Smith (1998) and Wilson *et al* (2003). Humidity was not specified by Španěl and Smith (1998) or Wilson *et al* (2003) though water vapour was present. The C_7-C_{12} alkanes employed by Arnold *et al* (1998) were anhydrous (water vapour content <0.005 %) and the helium carrier gas was passed through a molecular sieve to remove water. Milligan *et al* (2002) passed the helium carrier gas through a liquid nitrogen cooled zeolite resulting in a typical water vapour VMR of 150 ppb.

Alkane (C_nH_{2n+2})	P_{FT} (mbar)	T_{FT} (K)	k_m (x 10^{-9}m^3 s^{-1})	k_m/k_c	k_c	δ_{k_c} (%)	δ_{k_m} (%)	Observed Product Distribution : Product Ion (m/z): **Percentage of Product Total**, $C_nH_{2n+2}+H_3O^+ \rightarrow$				Reference
								$C_nH_{2n+2}.H_3O^+$	$C_nH^+_{2n+1}+H_2+H_2O$	$C_iH^+_{2i+1}+H_2O+C_{n-i}H_{2(n-i)+2}$	Other	
Methane (CH_4)	0.61	298	<0.001	<0.000769	k_L*	NS	NS	NR	NR	NR	NR	Wilson *et al* (2003)
Ethane (C_2H_6)	[a]0.61 [b]0.60	[a]298 [b]300	[a]<0.001 [b] <0.0001	[a]<0.000667 [b]<0.0001	[a]k_L* [b]k_L*	[a]NS [b]NS	[a]NS	[a]NR [b]NR	[a]NR [b]NR	[a]NR [b]NR	[a]NR [b]NR	[a]Wilson *et al* (2003) [b]Arnold *et al* (1998)
Propane (C_3H_8)	[a]0.61 [b]0.60	[a]298 [b]300	[a]<0.001 [b]0.0003	[a]<0.000625 [b]0.0002	k_L*[a] k_L*[b]	[a]NS [b]NS	[a]NS	[a]NR [b]100	[a]NR	[a]NR	[a]NR	[a]Wilson *et al* (2003) [b]Arnold *et al* (1998)

Table D.2 is continued on the following page

Alkane (C_nH_{2n+2})	P_{FT} (mbar)	T_{FT} (K)	k_m (x 10^{-9} m^3 s^{-1})	k_m/k_c	k_c	δ_{k_c} (%)	δ_{k_m} (%)	Observed Product Distribution : Product Ion (m/z): **Percentage of Product Total**, $C_nH_{2n+2} + H_3O^+ \rightarrow$ $C_nH_{2n+2}.H_3O^+$	$C_nH^+_{2n+1} + H_2 + H_2O$	$C_iH^+_{2i+1} + H_2O + C_{n-i}H_{2(n-i)+2}$	Other	Reference
n-Butane (C_4H_{10})	[a]0.61 [b]0.67 [c]0.64 [d]0.60	[a]298 [b]N/O [c]300±5 [d]300	[a]0.003 [b]0 [c]0.003 [d]0.0016	[a]0.00167 [b]0 [c]0.00167 [d]0.01	[d]k_L* [b]k_{SC} [c]k_{SC} [d]k_L*	[a]NS [b]20 [c]NS [d]NS	[c]15	$C_4H_{10}.H_3O^+$ (77): **[a]70** **[b]NR** **[c]30** **[d]100**	$C_4H_9^+$ (57) **[a]30** **[b]NR** **[c]70**			[a]Wilson *et al* (2003) [b]Španěl and Smith (1998) [c]Milligan *et al* (2002) [d]Arnold *et al* (1998)
iso-Butane (C_4H_{10})	[a]0.61 [b]0.67 [c]0.64 [d]0.60	[a] 298 [b]N/O [c]300±5 [d]300	[a] 0.0042 [b]0 [c]0.0040 [d]0.0018	[a]0.00233 [b]0 [c]0.00222 [d]0.01	[d]k_L* [b]k_{SC} [c]k_{SC} [d]k_L*	[a]NS [b]20 [c]NS [d]NS	[a]NS [b]NS [c]15	$C_4H_{10}.H_3O^+$ (77) **[a]55** **[b]NR** **[c]40** **[d]NR**	$C_4H_9^+$ (57) **[a]45** **[b]NR** **[c] 60** **[d]NR**	**[b]NR** **[d]NR**	**[b]NR** **[d]NR**	[a]Wilson *et al* (2003) [b]Španěl and Smith (1998eb [c]Milligan *et al* (2002) [d]Arnold *et al* (1998)
n-Pentane (C_5H_{12})	0.67	N/O	-	-	-	-	-	**NR**	**NR**	**NR**	**NR**	Španěl and Smith (1998)
iso-Pentane (C_5H_{12})	0.67	N/O	-	-	-	-	-	**NR**	**NR**	**NR**	**NR**	Španěl and Smith (1998)

Table D.2 is continued on the following page.

Alkane (C_nH_{2n+2})	P_{FT} (mbar)	T_{FT} (K)	k_m (x 10^{-9} m^3 s^{-1})	k_m/k_c	k_c	δ_{k_c} (%)	δ_{k_m} (%)	Observed Product Distribution : Product Ion (m/z): **Percentage of Product Total**, $C_nH_{2n+2} + H_3O^+ \rightarrow$				Reference
								$C_nH_{2n+2}.H_3O^+$	$C_nH^+_{2n+1} + H_2 + H_2O$	$C_iH^+_{2i+1} + H_2O + C_{n-i}H_{2(n-i)+2}$	Other	
n-Hexane (C_6H_{14})	[a]0.67 [b]0.60	[a]N/O [b]300	[a]<0.1 [b]0.03	[a]<0.05 [b]0.01	[a]k_{SC} [b]k_L*	[a]20 [b]NS	[a]NS	$C_6H_{14}.H_3O^+$ (105) [a]**100,** [b]**63**	$C_6H_{13}^+$(85) [b]**20**	$C_4H_9^+$ (57) [b]**4**	$C_3H_7.H_2O$ (61) [b]**10** $C_4H_9.H_2O$ (75) [b]**3**	[a]Španěl and Smith (1998) [b]Arnold *et al* (1998)
n-Octane (C_8H_{18})	0.67	N/O	0.9	0.39	k_{SC}	20	NS	$C_8H_{18}.H_3O^+$ (133) **100**				Španěl and Smith (1998)
n-Decane ($C_{10}H_{22}$)	[a]0.67 [b]0.60	[a]N/O [b]300	[a]1.6 [b]0.99	[a]0.62 [b]0.4	[a]k_{SC} [b]k_L*	[a]20 [b]NS	[a]NS	$C_{10}H_{22}.H_3O^+$ (161) [a]**100,** [b]**47**	$C_{10}H_{21}^+$ (141): [b]**2**	$C_4H_9^+$(57) [b]**8** $C_5H_{11}^+$(71) [b]**15** $C_6H_{13}^+$(85) [b]**18** $C_7H_{15}^+$(99) [b]**7** $C_8H_{17}^+$ (113) [b]**2**		[a]Španěl and Smith (1998) [b]Arnold *et al* (1998)
n-Dodecane ($C_{12}H_{26}$)	[a]0.67 [b]0.60	[a]N/O [b]300	[a]2.8 -	[a]1.0 -	[a]k_{SC}	[a]20	[a]NS	$C_{12}H_{26}.H_3O^+$ (189) [a]**100** [b]**58**		$C_4H_9^+$ (57): [b]**2** $C_5H_{11}^+$ (71): [b]**7** $C_6H_{13}^+$ (85): [b]**10** $C_7H_{15}^+$ (99): [b]**11** $C_8H_{17}^+$ (113): [b]**9** $C_9H_{19}^+$ (127): [b]**3**		[a]Španěl and Smith (1998) [b]Arnold *et al* (1998)

Table D.3: Reaction rate constants, reaction efficiencies and product distributions for the reactions of H_3O^+ with a series of acyclic alkanes measured using VT-SIFT by Arnold *et al* (1998). P_{FT} denotes pressure in the flow tube, T_{FT} denotes temperature in the flow tube. Helium carrier gas was employed. The helium was passed through a liquid nitrogen cooled zeolite trap to remove water resulting in typical water VMRs of 150 ppb . k_m denotes the measured rate constant for the reaction of H_3O^+ with the alkane (C_nH_{2n+1}). k_c refers to the collisional rate constant (§ 2.4.1) and k_m/k_c is the reaction efficiency. The method of collisional rate constant derivation was not specified in the cited reference, however, since the dipoles of alkanes are close to zero all collisional rate constant theories yield a value close to that derived from Langevin, Gioumousis, Stevenson theory, k_L, (§ 2.4.1.2, Eq. 2.34). δ_{k_m} denotes the estimated uncertainty of the measured rate constant, uncertainties associated with the collisional rate constants were not given but are generally in the order of 15 – 30 %.

Alkane C_nH_{2n+2}	P_{FT} (mbar)	T_{FT} (K)	k_m (x $10^{-9}m^3\ s^{-1}$)	k_m/k_c	δ_{k_m} (%)	Observed Product Distribution: Product Ion (m/z): **Percentage of Product Total**, $C_nH_{2n+2} + H_3O^+ \rightarrow$			
						$C_nH_{2n+2}.H_3O^+$	$C_nH^+_{2n+1} + H_2 + H_2O$	$C_iH^+_{2i+1} + C_{n-i}H_{2(n-i)+2} + H_2O$	$C_iH_{2i+1}.H_2O^+ + C_{n-i}H_{2(n-i)+2}$
n-heptane n-C_7H_{16}	0.60	300	0.26	0.12	15 *25*	$C_7H_{16}.H_3O^+$ (119): **77**	$C_7H_{15}^+$ (99): **5**	$C_4H_9^+$ (57): **7** $C_5H_{11}^+$ (71): **5**	$C_3H_7.H_2O^+$ (61): **2** $C_4H_9.H_2O^+$ (75): **4**
	0.60	400	0.079	0.04	15 *25*		$C_7H_{15}^+$ (99): **12**	$C_3H_7^+$ (43): **6** $C_4H_9^+$ (57): **49** $C_5H_{11}^+$ (71): **26** $C_6H_{13}^+$ (85):**2**	$C_3H_7.H_2O^+$ (61): **5**
	0.60	500	0.074	0.03	15 *25*			$C_3H_7^+$ (43): **15** $C_4H_9^+$ (57): **58** $C_5H_{11}^+$ (71): **27**	
n-octane n-C_8H_{18}	0.60	300	0.58	0.25	15 *25*	$C_8H_{18}.H_3O^+$ (133): **63**	$C_8H_{17}^+$ (113): **3**	$C_4H_9^+$ (57): **7** $C_5H_{11}^+$ (71):**16** $C_6H_{13}^+$ (85): **6**	$C_4H_9.H_2O^+$ (75): **5**
	0.60	400	0.18	0.08	15 *25*		$C_8H_{17}^+$ (113): **4**	$C_4H_9^+$ (57): **32** $C_5H_{11}^+$ (71):**33** $C_6H_{13}^+$ (85): **23**	
	0.60	500	0.19	0.08	15 *25*			$C_4H_9^+$ (57): **35** $C_5H_{11}^+$ (71):**42** $C_6H_{13}^+$ (85):**15**	

Table D.3 is continued on the following page

Alkane C_nH_{2n+2}	P_{FT} (mbar)	T_{FT} (K)	k_m (x 10^{-9}m^3 s^{-1})	k_m/k_c	δ_{k_m} (%)	Observed Product Distribution: Product Ion (m/z): **Percentage of Product Total**, $C_nH_{2n+2} + H_3O^+ \rightarrow$			
						$C_nH_{2n+2}.H_3O^+$	$C_nH^+_{2n+1} + H_2 + H_2O$	$C_iH^+_{2i+1} + C_{n-i}H_{2(n-i)+2} + H_2O$	$C_iH_{2i+1}.H_2O^+ + C_{n-i}H_{2(n-i)+2}$
iso-octane *i*-C_8H_{18}	0.60	300	0.49	0.21	15 *25*	$C_8H_{18}.H_3O^+$ (133): **32**	$C_8H_{17}^+$ (113): **22**	$C_4H_9^+$ (57): **27** $C_7H_{15}^+$ (99): **13**	$C_3H_7.H_2O^+$ (61): **6**
	0.60	400	0.26	0.11	15 *25*		$C_8H_{17}^+$ (113): **17**	$C_3H_7^+$ (43): **5** $C_4H_9^+$ (57): **57** $C_7H_{15}^+$ (99): 1**5**	$C_3H_7.H_2O^+$ (61): **6**
	0.60	500	0.27	0.12	15 *25*			$C_3H_7^+$ (43): **10** $C_4H_9^+$ (57): **85** $C_5H_{11}^+$ (71): **2** $C_7H_{15}^+$ (99): **3**	

However, the alkanes are unique in that the non-dissociative product is not observed from any of reactions of the C_1 – C_{12} alkanes with H_3O^+ studied to date and the associative reaction dominates. Thus the thermokinetic relationship between Gibbs free energy of non-dissociative proton transfer and reaction efficiency (Bohme *et al* 1980, Bouchoux *et al* 1996) may not exist. The explanatory theoretical thermokinetic relationship of Bouchoux *et al* (1996) defines the reaction efficiency in terms of the non-dissociative reaction and therefore applies only to it. However in the experimentally observed relationship between reaction efficiency and the Gibbs free energy of the non-dissociative reaction, the reaction efficiency is derived from the measured rate of disappearance of reactant ion (as it is here) and not specifically the measured rate of the non-dissociative reaction (e.g. Bohme *et al* 1980, Bouchoux *et al* 1996). The thermokinetic trend has been observed in reactions which proceed *via* dissociative and/or non-dissociative proton transfer, though the dissociative reaction unlike the associative does proceed through the non-dissociative products. Similarly reactions which proceed through more direct mechanisms such as hydride or alkide transfer may not follow the thermokinetic trend observed for non-dissociative proton transfer reactions. A reduction in the uncertainty in the proton affinities of the higher alkanes and entropic information is required.

H_3O^+ reacts with alkanes *via* one or more of three reaction pathways in SIFT and VT-SIFT; association (Eq. D.1), dissociation *via* loss of hydrogen (Eq. D.2) and dissociation to a $C_iH^+_{2i+1}$ carbocation and smaller alkane or alkene (Eq. D.3 a and b).

$$C_nH_{2n+2} + H_3O^+ + B \rightarrow C_nH_{2n+2}.H_3O^+ + B \qquad \text{(D.1)}$$

$$C_nH_{2n+2} + H_3O^+ \rightarrow C_nH^+_{2n+1} + H_2 + H_2O \qquad \text{(D.2)}$$

$$C_nH_{2n+2} + H_3O^+ \rightarrow C_iH^+_{2i+1} + C_{n-i}H_{2(n-i)+2} + H_2O \qquad \text{(D.3a)}$$

$$C_nH_{2n+2} + H_3O^+ \xrightarrow{B} C_iH^+_{2i+1} + C_{n-i}H_{2(n-i)} + H_2 + H_2O \qquad \text{(D.3b)}$$

Note that *B* denotes a buffer/carrier gas molecule and is helium in the case of most (VT)SIFT experiments. The standard enthalpies of the dissociation reactions of various alkenes are shown in Table D.4. The association reaction is exothermic and dominates at 298 K under thermal conditions (Table D.2). The rate of association increases with alkane size resulting in the efficient reaction with *n*-dodecane (Table D.2, Figure D.2). Španěl and Smith (1998) hypothesise that the rate of association reaction increases with increasing alkane size as a result of the increased degrees of vibrational freedom in which the energy of reaction (exothermicity and $\left\langle E_r^{SIFT} \right\rangle$) can be utilized thereby extending the lifetime of the transient

complex, $(C_nH_{2n+2}.H_3O^+)^*$, against unimolecular dissociation back to reactants. Since the dodecane reaction is efficient the lifetime of the transient complex $(C_{10}H_{22}.H_3O^+)^*$ (§ 2.6) must be at least sufficient for the collision with the buffer molecules to occur (Španěl and Smith, 1998e).

Milligan *et al* (2002) studied the dissociative reactions of D_3^+ with propane and other alkyl compounds including propene and propyne. Unlike the dissociative product ions of the unsaturated alkyl compounds almost no deuterium was retained in the $C_nH_{2n+1}^+$ products of propane. This indicates that in the dissociation reaction the transient complex is not sufficiently long lived for hydrogen scrambling to occur. Since hydride transfer could occur with similar ease in the other alkyl compounds and is not observed, Milligan *et al* (2002) hypothesise that dissociation occurs *via* protonation followed by rapid loss of the incoming hydrogen without scrambling, rather than hydride transfer.

$C_iH_{2i+1}^+$ ions could be formed *via* a direct reaction forming an alkane neutral and water (Eq. D.3a) and/or *via* dissociation of $C_nH_{2n+1}^+$ ions formed by elimination of hydrogen (Eq. D.3b) to give neutral products of hydrogen and an alkene (Eq. D.3b). Meot-Ner and Field (1976) found that $C_nH_{2n+1}^+$ ions where n = 7 – 10 undergo collisionally activated unimolecular decomposition at pressures of ~0.67 – 4.00 mbar in a propane carrier gas and temperatures greater than 480 K in a mass spectrometer (Meot-Ner, 1979). The increased temperature provided sufficient energy to overcome the endothermicity of the reactions (Table D.4). No dissociation of $C_nH_{2n+1}^+$ ions where $n \leq 6$ was observed up to 600 K. Meot-Ner and Field (1976) observed decomposition only if the fragment ion was $C_4H_9^+$ or larger and the neutral product was C_3H_6 or larger. Arnold *et al* (1997) formed $C_8H_{17}^+$ in the ion source of a VT-SIFT from *iso*-octane, injected the ions into the flow tube in a helium buffer at ~0.60 mbar and observed the product ions at 300 and 400 K. At 300 K $C_8H_{17}^+$ was the only ion detected, at 400 K $C_8H_{17}^+$ formed only 20 % of the product ions, 80 % were $C_4H_9^+$. Since these dissociation reactions are collisionally activated the rate increases with increasing pressure, thus the rate of dissociation may be increased and a greater abundance of dissociation products formed by Eq. D.3b at the higher pressures employed in PTR-MS compared to VT-SIFT at comparable energies ($\Delta\langle E_r \rangle$). The differing nature of the buffer is also likely to affect rates of dissociation and product distributions. The variation in the distribution of the energy available as a result of the electric field compared to that as a result of increased temperature may also affect the dissociation rates and product distributions.

Products of the reaction of H_3O^+ with C_1 – C_2 alkanes are below the detection levels of the SIFT (~298 K) due to the low reaction rates. Products were not observed from the reaction of propane by Wilson *et al* (2003). Arnold *et al* (1998) did observed products and found that only association occurs.

Products were not observed from the reaction of C_4 or C_5 alkanes by Španěl and Smith (1998). Wilson *et al* (2003) and Milligan *et al* (2002) observed products of association (Eq. D.1) and dissociation by loss of hydrogen (Eq. D.2) from the reaction of *n*-butane and *iso*-butane in the SIFT (~298 K). Arnold *et al* (1998) observed only the association product from reaction of *n*-butane in SIFT at 300 K. The enthalpy of the dissociative reaction of *n*-butane forming $C_4H_9^+$ by loss of hydrogen is uncertain; values range from -0.22 eV to +0.78 eV and depend on the structure of the ion (Table D.4). If the reaction proceeds *via* protonated *n*-butane an energy barrier in the range of the enthalpy of the non-dissociative reaction (0.56 to 0.67 eV) may be expected. The pressures and temperature in the (VT-)SIFT of Španěl and Smith (1998), Wilson *et al* (2003), Milligan *et al* (2002) and Arnold *et al* (1998) were similar (Table 3.2 and 3.3) and cannot explain the differences in product distributions.

Španěl and Smith (1998) observed only the association (Eq. D.1) product from the reaction of *n*-hexane, *n*-octane, *n*-decane and *n*-dodecane with H_3O^+ in SIFT at ~300 K. The association product was the dominant product ion from the reactions of *n*-hexane, *n*-heptane, *n*-octane, *n*-decane and *n*-dodecane with H_3O^+ in the experiments of Arnold *et al* (1998) at 300 K. However, Arnold *et al* (1998) also observed dissociation by loss of hydrogen (Eq. D.2) and dissociation to a number of smaller $C_iH_{2i+1}^+$ carbocations (Eq. D.3a,b) at 300 K. Dissociation by loss of hydrogen is endothermic for the C_6 – C_{10} *n*-alkanes, some of the dissociation reactions to $C_iH_{2i+1}^+$ carbocations (Eq. D.2a,b) are also endothermic (Table D.4). An energy barrier with the magnitude of the enthalpy of non-dissociation may also exist if the reactions proceed *via* the non-dissociative product. The lack of the non-dissociative product ($C_nH_{2n+3}^+$) and presence of dissociative ions in SIFT at 298 K suggests any additional barrier between $C_nH_{2n+3}^+$ and dissociative products is small. Positive entropy terms and $\left\langle E_r^{SIFT} \right\rangle$ (Eq. 3.18) (~0.089 eV + rovibrational energy of the alkane) may contribute to formation of the dissociative product ions. The dissociative reactions in which $C_iH_{2i+1}^+$ carbocations are formed by dissociation of the larger $C_nH_{2n+1}^+$ products of hydrogen elimination (Eq. D.3b) are more endothermic than the more direct reactions in which a smaller alkane is formed (Eq. D3a) (Table D.4). The discussed results of Arnold *et*

al (1997) and Moet-Ner and Field (1976) suggest that $C_nH^+_{2n+1}$ where n<10 carbocations do not dissociate at 300 K. $C_nH^+_{2n+1}$ product ions observed by Arnold *et al* (1998) at 300 K may be formed by the more direct mechanism (Eq. D.3b). The $\langle E_r^{SIFT} \rangle$ at 298 K may be sufficient to overcome the lower endothermicity of these reactions and/or any energy barrier corresponding to the transient non-dissociative product.

Arnold *et al* (1998) studied the reactions of H_3O^+ with *n*-heptane, *n*-octane and *iso*-octane at 400 and 500 K using VT-SIFT (Table D.3, Figure D.6). The reaction efficiency initially decreased between 300 and 400 K and then remained constant (Figure D.6, Table D.3). This corresponds to the disappearance of the association (Table D.2) product ($C_nH_{2n+2}.H_3O^+$) (Table D.3). Arnold *et al* (1998) measured the rate constants for the individual reaction pathways. The sum of rate constants for associative pathways did not change with temperature indicating the association pathway does not compete with dissociation. Rates of associative reactions have a negative temperature dependence (Meot-Ner, 1979). However a negative temperature dependence of $>T^{-19}$ would be needed for association products to completely disappear at 400 K thus it seems unlikely that this accounts for the reduction in efficiency between 300 and 400 K. Instead the decrease in overall reaction rate constant was attributed to thermal dissociation of association products back to initial reactants (H_3O^+ + C_nH_{2n+2}) between 300 and 400 K (Arnold *et al* 1998)

The increase in energy in the VT-SIFT at 400 and 500 K is comparable to the increase of energy ($\Delta\langle E_r \rangle$) in the PTR-MS under normal operating conditions (§ D.1.2, § D.1.3, § D.2). Product distributions from reactions of *n*-octane, *n*-decane, *n*-dodecane and *n*-hexadecane with H_3O^+ have been observed in the PTR-MS and are reviewed in Table D.5. The association product was only observed from the reaction of *n*-octane and was a minor product (0.6 %). A similar decrease in efficiency relative to SIFT at 298 K to that in VT-SIFT at 400 and 500 K may therefore be expected in PTR-MS. Given the three-body nature of association the disappearance of the association channel may be a result of the changes in buffer, pressure and collision times in the PTR-MS as well as the increase in energy available, the importance of the distribution of energy is also unknown. The product of dissociation by loss of hydrogen (Eq. D.2) was only observed from reaction of *n*-octane in PTR-MS and formed a minor product (1%). Arnold *et al* (1998) observed a similar disappearance of the dissociation product formed by loss of hydrogen from *n*-heptane and *n*-octane between 400 K and 500 K (Table D.3). The disappearance of the product of dissociation by hydrogen elimination (Eq. D.2) may indicate its dissociation to smaller

$C_iH^+_{2i+1}$ ions at the elevated energies (overall reaction Eq. D.3b). This is consistent with the previously discussed observations of Moet-Ner and Field (1976) and Arnold *et al* (1997) which suggest $C_nH^+_{2n+1}$ ions dissociate to smaller $C_iH^+_{2i+1}$ carbocations where *i* is ≥ 4 at temperatures of 400 to 600 K. At 500 K *n*-heptane reacted with H_3O^+ by dissociation *via* Eq. D.3 a and/or b alone producing $C_3H_7^+$, $C_4H_9^+$ and $C_5H_{11}^+$ (Table D.3). Similarly $C_4H_9^+$ (35 %), $C_5H_{11}^+$ (42 %) and $C_6H_{13}^+$ (15 %) were the sole products from *n*-octane reaction with H_3O^+. Moet-Ner and Field (1976) did not observe dissociation of $C_nH^+_{2n+1}$ ions to $C_iH^+_{2i+1}$ions where $i \leq 3$; it is possible that the $C_3H_7^+$ observed from reactions of *n*-heptane and *iso*-octane in VT-SIFT at 400 and 500 K (Table D.3) and from *n*-octane, *n*-dodecane and *n*-hexadecane in the PTR-MS (*E/N* 150 Td, P_{dt} 2.3 mbar and T_{dt} 323 K, Table D.5) were formed by reaction Eq. 2.29a.

Warneke *et al* (2003) observed a similar product distribution from *n*-octane in the PTR-MS at *E/N* of 106 Td and P_{dt} of 2.4 mbar (Table D.5) to that in VT-SIFT at 500 K and P_{FT} 0.60 mbar (Table D.3); though $C_5H_{11}^+$ was increased by 19 % and $C_6H_{13}^+$ was not observed. At the higher *E/N* of 150 Td and P_{dt} of 2.1 mbar Jobson *et al* (2005) observed predominantly products of dissociation *via* Eq. D.3; $C_3H_7^+$ (20.6 %), $C_4H_9^+$ (36.1 %), $C_5H_{11}^+$ (15.5 %) and $C_6H_{13}^+$ (5.2 %), minor products of association (0.6%) and dissociation by loss of hydrogen (1.0 %) were observed (Table D.5). The product distribution from reaction of *n*-heptane and *iso*-octane have not been measured in the PTR-MS but under normal operating conditions products of dissociation *via* Eq. D.3a,b are expected as in VT-SIFT at 400 to 500 K where $\Delta\langle E_r \rangle$ is similar. However, as discussed the increase in pressure and change of buffer may affect the relative abundancies.

A calculated sensitivity of 8.3 ncps ppb^{-1} and a measured sensitivity (using count rates at m/z 71 and m/z 57) of 2.8 ncps ppb^{-1} were determined by Warneke *et al* (2003) for *n*-octane in the PTR-MS (*E/N* 106 Td). Taking into account the uncertainties of 20% (± 0.56) in measured sensitivities and 30% (± 2.5) in calculated sensitivities the measured sensitivity is a minimum of 2.44 ncps ppb^{-1} less than the calculated value. This may indicate that the rate constant is less than collisional as observed in SIFT and hypothesised from VT-SIFT data. However, as discussed in the introduction to this chapter a number of other factors may have caused this relatively small difference in calculated and measured sensitivities. Warneke *et al* (2003) overlooked fragments of <5% and additional fragmentation e.g. to $C_6H_{13}^+$ (m/z 85) may have contributed to an underestimation of the measured sensitivity. Experimental data is

required to determine reaction efficiencies of alkanes in the PTR-MS as a function of *E/N* and T_{dt}.

Experimental product distributions resulting from H_3O^+ with $<C_8$ alkanes in the PTR-MS could not be found. Milligan *et al* (2002) determined the product distributions from reaction of N_2H^+ and H_3^+ as well as H_3O^+ at 298 K, the results are displayed in Figure D.3a-c. Product distributions are displayed as a function of change in energy relative to reaction with H_3O^+ at 298 K which corresponds to $GB(H_2O)$-GB(reagent ion neutral) where the reagent ion neutral is N_2 or H_2. Fragments are unlikely to increase linearly as the energy increases as indicated by the full lines, rather dissociation products will increase from some point at which their production is energetically possible. The enthalpies of dissociation reactions with H_3O^+ are also shown in Figure D.3a-c; these are an indication of the point at which the products become thermodynamically feasible (neglecting entropy, $\langle E_r \rangle$, collisional stabilization, activation energies, and/or loss of energy in inactive modes such as translation or radiation). Abundancies may not increase in a linear fashion and points are joined to guide the eye.

Product ions $C_2H_5^+$ from propane and $C_2H_5^+$ and $C_3H_5^+$ from *n*- and *iso*-butane are not observed from N_2H^+ reaction despite being exothermic. This may be due to an activation energy barrier, loss of energy in translation or radiation or collisional stabilization. As at elevated energies in VT-SIFT at the increased energies of reaction with N_2H^+ and H_3^+ the association product is not observed. At an increase in energy of 2.03 eV $C_3H_7^+$ is the only product from propane reaction, at an increase of 2.75 eV $C_2H_5^+$ is also observed. These increases in energy are large compared to that in the drift tube, $\Delta\langle E_r \rangle$ (Eq. 3.4, T_{dt} 298 K) of propane and H_3O^+ at *E/N* 120 -140 Td in air is 0.25 – 0.37 eV (Figure 3.4). At *E/N* of 120 Td and T_{dt} 298 K in an air buffer $KE^r_{c.m.}$ of propane is 0.18 eV (Figure 3.2) and $KE^b_{c.m.}$ (Figure 3.3) is 0.16 eV totalling 0.34 eV, this is less than the enthalpy of dissociation reaction with H_3O^+ to form $C_2H_5^+$ and $C_3H_7^+$, thus formation is unlikely in normally operated PTR-MS. However, positive entropy and/or the internal energy of propane may contribute to dissociation to $C_2H_5^+$ or $C_3H_7^+$. The lack of $C_2H_5^+$ from the N_2H^+ reaction suggests this is unlikely for $C_2H_5^+$ at least.

a: propane

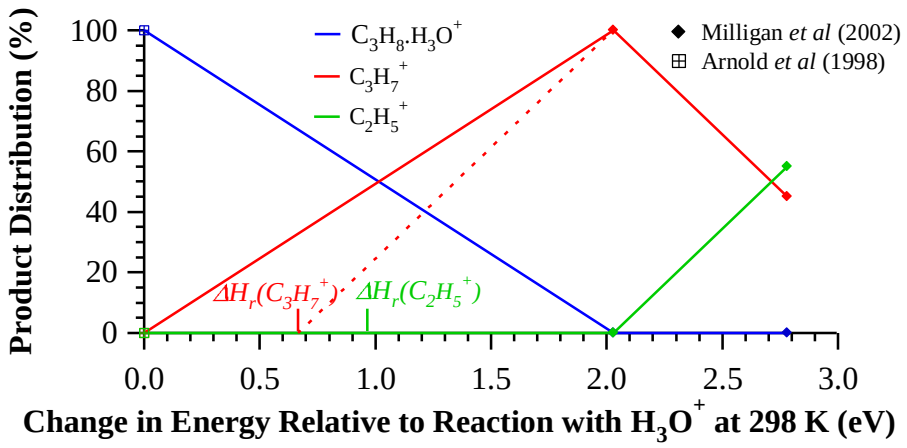

b: *n*-butane

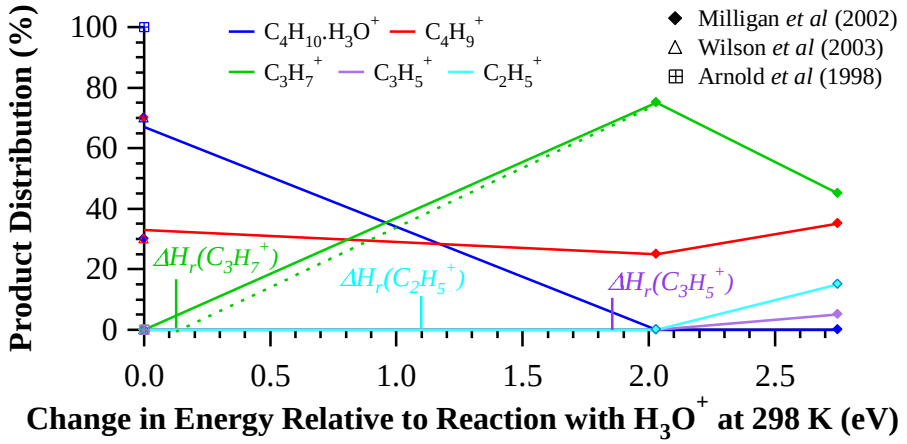

c: *iso*-butane

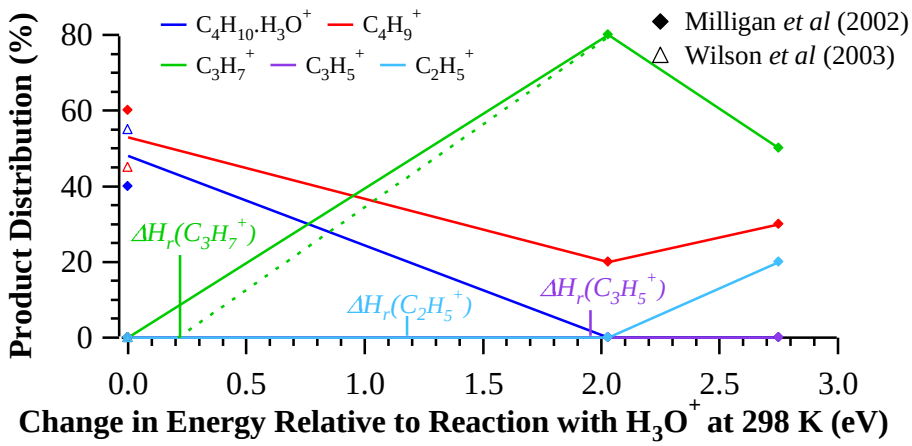

Figure D.3a-c: Product distributions from reactions of N_2H^+, H_3^+ and H_3O^+ with propane, *n*-butane and *iso*-butane respectively (~298 K). Change in energy relative to reaction at 298 K is $GB(H_2O)$ – $GB(reagent\ ion\ neutral)$ $\Delta H_r\ (F^+)$ denotes the standard enthalpy of the reaction of H_3O^+ with the alkane to form the fragment , F^+. $\Delta H_r\ (F^+)$ is an indication of the energy required for the abundance of F^+ to increase above zero as indicated by the dashed lines. Abundancies are unlikely to increase linearly from zero as change in zero increase from zero as is indicated by the full line.

At an increase in energy of 2.03 eV $C_3H_7^+$ and $C_4H_9^+$ are observed from *n*- and *iso*-butane reaction; at an increase of 2.75 eV $C_2H_5^+$ and a small amount of $C_3H_5^+$ is also observed. Since $C_4H_9^+$ is produced from butane reaction with H_3O^+ in the SIFT at 298 K and is observed from the reactions of N_2H^+ and H_3^+ it is likely to be formed in the PTR-MS. $\Delta\langle E_r \rangle$ (Eq. 3.4, T_{dt} 298 K, air buffer) of butane and H_3O^+ at *E/N* 120 -140 Td in air is 0.26 – 0.39 eV (Figure 3.4), this is small compared to the increases in energy by change of reagent ion to N_2H^+ and H_3^+. The enthalpy of dissociation reaction of butane with H_3O^+ to form $C_3H_7^+$ (Table 3.4) is less than $\Delta\langle E_r \rangle$ (Eq. 3.4, T_{dt} 298 K) at *E/N* 120 -140 Td in air. If the reaction proceeds *via* the non-dissociative product, $C_4H_{11}^+$, an energy barrier of similar magnitude to the enthalpy of non-dissociation (+ 0.31 to 0.41 eV, Table D.1 and D.4) may be expected. The sum of $KE^r_{c.m.}$ of propane (0.19 eV, Figure 3.2) and $KE^b_{c.m.}$ (0.16 eV, Figure 3.3) at *E/N* of 120 Td and T_{dt} 298 K in an air buffer is sufficient to overcome such a barrier. Thus $C_3H_7^+$ may be observed from butane in normally operated PTR-MS (depending on the role of collisional stabilization/activation and/or loss of energy in inactive modes such as translation or radiation).

The endothermicities of the dissociative reactions of butane with H_3O^+ to form $C_2H_5^+$ and $C_3H_5^+$ are greater than $\Delta\langle E_r \rangle$ and the sum of $KE^r_{c.m.}$ and $KE^b_{c.m.}$, indicating formation is unlikely in normally operated PTR-MS. Positive entropy and/or the internal energy of butane may contribute to dissociation to $C_2H_5^+$ or $C_3H_5^+$ and formation in the PTR-MS. The lack of $C_2H_5^+$ or $C_3H_5^+$ from the N_2H^+ reaction suggests this is unlikely, though the role of collisional activation/stabilization in the PTR-MS is unknown.

Given the lack of products above the lower detection limit of SIFT from the C_1-C_6 alkanes in a number of studies and since reaction efficiency is likely to remain similar to that in SIFT or decrease, lower alkanes are unlikely to make a large contribution to PTR-MS spectra.

Production of the lower $C_nH^+_{2n+1}$ ion $C_2H_5^+$ at m/z 29 is endothermic by more than ~ 1 eV (Table D.4) from reaction of H_3O^+ with all of the C_3 – C_{10} alkanes (Table D.4) and it has not been observed in SIFT (Table D.2), VT-SIFT (Table D.3) or PTR-MS (Table D.5) studies-to-date.

Jobson *et al* (2005) observed a product ion at m/z 41 ($C_3H_5^+$, 12 – 15.9 %) from the reactions of *n*-octane, *n*-dodecane and *n*-hexadecane with H_3O^+ in the PTR-MS at *E/N* of 150 Td and T_{dt} of 323 K in dry nitrogen. Minor products were also observed at m/z 55, 69, 83, 97. These

product ions may result from an additional dissociation reaction (not observed in thermal SIFT at 298 K), Eq. D.4:

$$C_nH_{2n+2} + H_3O^+ \rightarrow C_iH^+_{2i-1} + C_{n-i}H_{2(n-i)+2} + H_2 + H_2O \qquad \text{(D.4)}$$

The reaction to form $C_3H_5^+$ from any of the C_5 - C_{10} *n*-alkanes is endothermic by ~ 2 eV (Table D.4), this is greater than the energy available in the drift tube under the conditions employed by Jobson *et al* (2005) ($KE^r_{c.m.}$>0.34 eV, and $KE^b_{c.m.}$>0.29 eV). A positive entropy term, the internal energy of the neutral reactant and collisional activation may contribute to $C_3H_5^+$ formation.

O_2^+ reactions with alkanes occur at collisional rate and O_2^+ is present in the PTR-MS at ≤ 3 % (§ 2.3.1). Jobson *et al* (2005) measured product distributions in air, as in normal PTR-MS operation, and in nitrogen. The use of a nitrogen buffer reduced O_2^+ from the ion source (§ 2.3.1) to 0.02 % compared to ~ 3 % in air. Product distributions were unaffected by the change in buffer excluding the possibility that product ions result from the reaction of O_2^+ alone.

Jobson *et al* (2005) compared relative abundancies of $C_iH^+_{2i+1}$ from the reactions of *n*-octane, *n*-dodecane and *n*-hexadecane with H_3O^+ in the PTR-MS (*E/N* of 150 Td, T_{dt} of 323 K, P_{dt} 2.1 mbar and therefore *E* ~70 V cm^{-1}) with those from EI-MS (Mallard and Linstrom 2005) and found excellent agreement. $C_iH^+_{2i-1}$ ions are also minor products of EI-MS for example, m/z 41 forms 9.3 %, m/z 55 3.2 %, m/z 69 0.9 % and m/z 83 0.2 % of product ions from EI-MS of *n*-decane (Mallard and Linstrom 2005).

In summary, < C_6 alkanes are unlikely to contribute appreciably to PTR-MS spectra as their reactions with H_3O^+ are inefficient and proceed slowly. >C_6 alkanes are expected to contribute significantly to spectra, but experimental efficiencies in the PTR-MS are required. Reaction of the C_6 – C_{12} ions with H_3O^+ produces predominantly $C_nH^+_{2n+1}$ (*n*>2) ions at m/z 43, 57, 71, 85, 99 etc and $C_3H_5^+$ ions (m/z 41). Other $C_nH^+_{2n-1}$ (n>3) ions (m/z 55, 69, 83, 97 etc) are minor products of alkane reaction in the PTR-MS. The isobaric nature of product ions and low reaction efficiencies prevent quantification of individual alkanes but products should be considered in spectra interpretation.

Table D.4: The standard (298 K) enthalpy of reaction of various non-dissociative (Table 3.1) and dissociative proton transfer reactions of alkanes with H_3O^+. Values are derived from [a] Milligan *et al* (2002), [b]Arnold *et al* (1998) [c]calculations using proton affinities and standard enthalpies of formation, [d]calculation from enthalpies of formation and appearance energies. The enthalpies of formation of $C_2H_5^+$, $C_3H_7^+$, $C_4H_9^+$ and $C_6H_{13}^+$ were calculated using the proton affinities (Hunter and Lias 1998) and standard enthalpies of formation (Mallard and Linstrom 2005) of ethene, propene, 2-butene (*PA* of 1-butene is unknown) and 1-hexene and are 9.41 eV, 8.34 eV, 8.07 eV and 7.14 eV respectively. The enthalpies of formation of $C_3H_7^+$ and $C_6H_{13}^+$ calculated from proton affinities and enthalpies of formation of cyclopropane and cyclohexane are 8.70 eV and 7.52 - 7.71 eV (depending on *PA* employed, § 3.1.4) and the standard enthalpies of dissociation reactions producing $C_3H_7^+$ and $C_6H_{13}^+$ are then endothermic by 0.36 eV and 0.38 – 0.57 eV respectively more than shown. Standard enthalpies of formation of $C_4H_9^+$ and $C_5H_{11}^+$ could not be derived from proton affinities and standard enthalpies of formation of cyclobutane and cyclopentane as the proton affinities of these compounds are unknown. The proton affinities of 1- and 2- pentene are unknown and the standard enthalpy of formation of $C_5H_{11}^+$ was approximated from the appearance energy for formation of $C_5H_{11}^+$ from the alkane reactant. *No *AE* data was available for $C_5H_{11}^+$ formation from these alkanes and the mean of enthalpies of formation of $C_5H_{11}^+$ calculated from appearance energies of the C_6 –C_9 alkanes was employed and is 7.83 eV. The proton affinity of heptene is unknown and no *AE* was available for formation of $C_7H_{15}^+$ from *n*-heptane so the enthalpy of formation of $C_7H_{15}^+$ was calculated from the *AE* of $C_7H_{15}^+$ from *n*-octane and is between 7.12 eV and 7.32 eV (the range of *AE*). The enthalpy of formation of $C_3H_5^+$ was calculated from the proton affinity (Hunter and Lias 1998) and standard enthalpy of formation (Mallard and Linstrom 2005) of propyne and is 10.09 eV. The $C_3H_5^+$ standard enthalpy of formation calculated from the proton affinity (Hunter and Lias 1998) and standard enthalpy of formation (Mallard and Linstrom 2005) of cyclopropene is 10.31 eV and the standard enthalpies of dissociation reactions producing cyclic $C_3H_5^+$ are thus 0.22 eV more endothermic than those shown. Neutral $C_{n-i}H_{2(n-i)+2}$ products of dissociation were taken to be linear *n* isomer alkanes. A standard enthalpy of formation of H^+ of 15.92 eV from CRC Handbook of Chemistry And Physics (1986-1987), a standard enthalpy of formation of H_3O^+ of 6.25 eV calculated as described in § 3 and by convention a standard enthalpy of formation of hydrogen of 0 were employed. The standard enthalpy of formation of *n*-nonane was not available from Mallard and Linstrom (2005) and was taken from CRC Handbook of Chemistry and Physics (1986-1987). All other standard enthalpies of formation were taken from Mallard and Linstrom (2005) and proton affinities were taken from Hunter and Lias (1998), appearance energies were taken from Mallard and Linstrom (2005).

Alkane	Product ion, ΔH_r^ϕ (eV), $C_nH_{2n+2} + H_3O^+ \rightarrow$				
(C_nH_{2n+2})	$C_nH_{2n+3}^+ + H_2O$	$C_nH_{2n+1}^+ + H_2 + H_2O$	$C_iH_{2i+1}^+ + C_{n-i}H_{2(n-i)+2} + H_2O$	$C_iH_{2i+1}^+ + C_{n-i}H_{2(n-i)} + H_2 + H_2O$	$C_iH_{2i-1}^+ + C_{n-i}H_{2(n-i)+2} + H_2 + H_2O$
Propane (C_3H_8)	+0.56,+0.63, +0.65, +0.68	$C_3H_7^+$ +0.67[a], +0.66[c], -1.02 to +0.98[d]	$C_2H_5^+$ +0.96[a], +0.95[c], -1.06 to +0.94[d]		
n-Butane (C_4H_{10})	+0.31, +0.33, +0.42	$C_4H_9^+$ −0.02[a], +0.61[c], _ 0.22 to + 0.78[d]	$C_2H_5^+$ +1.10[a], +1.09[c], +1.69[d] $C_3H_7^+$ +0.12[a], +0.11[c], -0.01 to +0.15[d]	$C_2H_5^+$ 2.50[c], 3.1[d]	$C_3H_5^+$ +1.86[c]

Table D.4 is continued on the following page.

Alkane (C_nH_{2n+2})	Product ion, ΔH_r^{ϕ} (eV), $C_nH_{2n+2} + H_3O^+ \rightarrow$				
	$C_nH_{2n+3}^+ + H_2O$	$C_nH_{2n+1}^+ + H_2 + H_2O$	$C_iH_{2i+1}^+ + C_{n-i}H_{2(n-i+2)} + H_2O$	$C_iH_{2i+1}^+ + C_{n-i}H_{2(n-i)} + H_2 + H_2O$	$C_iH_{2i-1}^+ + C_{n-i}H_{2(n-i+2)} + H_2 + H_2O$
n-Pentane (C_5H_{12})	+0.19, +0.25, +0.30	$C_5H_{11}^+$ +0.56[d]*	$C_2H_5^+$ +1.10[c] $C_3H_7^+$ +0.24[c], +0.20 to +0.30[d] $C_4H_9^+$ +0.06[c], -0.16 to +0.07[d]	$C_2H_5^+$ +2.39[c] $C_3H_7^+$ +1.65[c], +1.61 to +1.71[d]	$C_3H_5^+$ +1.99[c]
n-Hexane (C_6H_{14})	0.00, +0.15, +0.19	$C_6H_{13}^+$ +0.39[b], +0.11[c]	$C_2H_5^+$ +1.08[c] $C_3H_7^+$ +0.24[c], +0.40 to +0.55[d] $C_4H_9^+$ 0.17[b, c], +0.10 to +0.24[d] $C_5H_{11}^+$ -0.10 to +0.07[d]	$C_2H_5^+$ +2.38[c] $C_3H_7^+$ +1.53[c], +1.69 to +1.83[d] $C_4H_9^+$ +1.58[c], +1.51 to 1.65[d]	$C_3H_5^+$ +1.99[c]
n-Heptane (C_7H_{16})	-0.20, +0.13	$C_7H_{15}^+$ +0.34[b], +0.30 to +0.50[d]	$C_2H_5^+$ +1.07[c] $C_3H_7^+$ +0.28[b], +0.23[c] $C_4H_9^+$ +0.17[b,c], -0.37 to +0.37[d] $C_5H_{11}^+$ +0.03[b], -0.48 to +0.18[d] $C_6H_{13}^+$ -0.17[b], -0.45[c], -0.46 to -0.02[d]	$C_2H_5^+$ +2.38[c] $C_3H_7^+$ +1.52[c] $C_4H_9^+$ +1.47[c], +0.93 to 1.68[d] $C_5H_{11}^+$ +0.93 to 1.60[d]	$C_3H_5^+$ +1.98[c]
n-Octane (C_8H_{18})	-0.40, +0.08	$C_8H_{17}^+$ +0.24[b]	$C_2H_5^+$ +1.08[c] $C_3H_7^+$ +0.29[b], +0.22[c] $C_4H_9^+$ +0.16[b], +0.17[c], +0.34 to +0.69[d] $C_5H_{11}^+$ [b]+0.03, -0.16 to +0.43[d] $C_6H_{13}^+$ -0.04[b], -0.33[c], +0.01 to +0.08[d]	$C_2H_5^+$ +2.38[c] $C_3H_7^+$ +1.53[c] $C_4H_9^+$ +1.46[c], +1.64 to 1.99[d] $C_5H_{11}^+$ +1.45 to 1.71[d] $C_6H_{13}^+$ +1.08[c], +1.43 to +1.50[d]	$C_3H_5^+$ +1.97[c]

Table D.4 is continued on the following page.

Alkane (C_nH_{2n+2})	Product ion, ΔH_r^{ϕ} (eV), $C_nH_{2n+2} + H_3O^+ \rightarrow$				
	$C_nH_{2n+3}^+ + H_2O$	$C_nH_{2n+1}^+ + H_2 + H_2O$	$C_iH_{2i+1}^+ + C_{n-i}H_{2(n-i+2)} + H_2O$	$C_iH_{2i+1}^+ + C_{n-i}H_{2(n-i)} + H_2 + H_2O$	$C_iH_{2i-1}^+ + C_{n-i}H_{2(n-i+2)} + H_2 + H_2O$
n-Nonane (C_9H_{20})	+ 0.05		$C_2H_5^+$ +1.08[c] $C_3H_7^+$ +0.22[c] $C_4H_9^+$ +0.16[c] $C_5H_{11}^+$ +0.32[d] $C_6H_{13}^+$ -0.77[c]	$C_2H_5^+$ +2.39[c] $C_3H_7^+$ +1.52[c] $C_4H_9^+$ +1.46[c] $C_5H_{11}^+$ +1.62[d] $C_6H_{13}^+$ +0.97[c]	$C_3H_5^+$ +1.97[c]
n-Decane ($C_{10}H_{22}$)	+0.01	$C_{10}H_{21}^+$ +0.02[b]	$C_2H_5^+$ +1.08[c] $C_3H_7^+$ +0.22[c] $C_4H_9^+$ +0.17[b], +0.16[c] $C_5H_{11}^+$ +0.02[b], +0.10[d]* $C_6H_{13}^+$ -0.06[b], -0.33[c]	$C_2H_5^+$ +2.38[c] $C_3H_7^+$ +1.53[c] $C_4H_9^+$ +1.46[c] $C_5H_{11}^+$ +1.41[d]* $C_6H_{13}^+$ +0.96[c]	$C_3H_5^+$ +1.97[c]

Table D.5: The product distributions resulting from the reaction of a series of acyclic alkanes with H_3O^+ in the PTR-MS. P_{dt} denotes drift tube pressure, T_{dt} denotes drift tube temperature, V_{drift} denotes voltage applied to the drift tube and E the resultant electric field strength. *Percentage product distributions from Jobson *et al* (2005) are estimated here from count rates derived from spectra shown in reference and given to 1 decimal place and are therefore approximate values: Product ions with count rates < 100 counts s^{-1} were neglected as were m/z corresponding to ^{13}C isotopes and $H_3O^+(H_2O)_n$ clusters and their isotopes. A significant number of product ions were present with count rates < 100 counts s^{-1} and the distributions here only represent dominant product ions. The minor products, not shown here, include longer chain $C_iH^+_{2i+1}$ ions but also small amounts at m/z 69, 83, 97 corresponding to unsaturated carbocations of formula $C_iH^+_{2i-1}$. A T_{dt} of 323 K, P_{dt} of 2.1 mbar and E/N of 150 Td were specified by Jobson *et al* (2005) for sensitivity and diesel exhaust measurements within the reference and are assumed to apply for product distribution measurements, E was derived from these values. However, Jobson *et al* (2005) give a $KE^{ion}_{.}$ of 0.35 eV for the product distribution measurements, here a $KE^{ion}_{.}$ of ~0.40 eV is derived for T_{dt} of 323 K, P_{dt} of 2.1 mbar and E/N of 150 Td using a reduced H_3O^+ mobility of 2.96 cm^2 / Vs in nitrogen (Dotan *et al*, 1976), the difference may be a result of a difference in the reduced mobility employed in calculation of $KE^{ion}_{.}$ rather than a d ifference in drift tube conditions employed for product distribution measurements. A $KE^{ion}_{.}$ of 0.35 eV corresponds to E/N of 140 Td at a T_{dt} of 323 K here. Product distributions from Jobson *et al* (2005) were measured in dry nitrogen buffer as opposed to air as is employed in normal operation of PTR-MS thereby reducing O_2^+. Product distributions in Warneke *et al* (2003) were measured in synthetic air.

Alkane C_nH_{2n+2}	P_{dt} (mbar)	T_{dt} (K)	V_{drift} (V)	E (V cm^{-1})	E/N (Td)	Observed Product Distribution: Product Ion , (m/z): **Percentage of Product Total** $C_nH_{2n+2} + H_3O^+ \rightarrow$ $C_nH_{2n+2}.H_3O^+$	$C_nH^+_{2n+1} + H_2 + H_2O$	$C_iH^+_{2i+1} + C_{n-i}H_{2(n-i)+2} + H_2O$	Other	Reference
n-octane n-C_8H_{18}	[a]2.4 [b]2.1	[a]NS [b]323	[a]NS [b]NS	[a]NS [b]~70	[a]106 [b]150	$C_8H_{18}.H_3O^+$ (133): **[b]0.6**	$C_8H_{17}^+$ (113): **[b]1.0**	$C_3H_7^+$ (43): **[b]20.6** $C_4H_9^+$ (57): **[a]39, [b]36.1** $C_5H_{11}^+$ (71): **[a]61, [b]15.5** $C_6H_{13}^+$ (85): **[b]5.2**	$C_3H_5^+$ (41): **[b]15.5** $C_4H_9.H_2O^+$ (75): **[b]5.7**	[a]Warneke *et al* (2003) [b]Jobson *et al* (2005)*
n-decane n-$C_{10}H_{22}$	2.4	NS	NS	NS	106			$C_4H_9^+$ (57): **21** $C_5H_{11}^+$ (71): **15** $C_6H_{13}^+$ (85): **19** $C_7H_{15}^+$ (99):**45**		Warneke *et al* (2003)

Table D5 is continued on the following page.

Alkane C_nH_{2n+2}	P_{dt} (mbar)	T_{dt} (K)	V_{drift} (V)	E (V cm^{-1})	E/N (Td)	Observed Product Distribution: Product Ion , (m/z): **Percentage of Product Total** $C_nH_{2n+2} + H_3O^+ \rightarrow$ $C_nH_{2n+2}.H_3O^+$	$C_nH^+_{2n+1} + H_2 + H_2O$	$C_iH^+_{2i+1} + C_{n-i}H_{2(n-i)+2} + H_2O$	Other	Reference
n-dodecane n-$C_{12}H_{26}$	2.1	323	NS	~70	150			$C_3H_7^+$ (43): **20.0** $C_4H_9^+$ (57): **40.0** $C_5H_{11}^+$ (71): **16.0** $C_6H_{13}^+$ (85): **12.0**	$C_3H_5^+$ (41): **12.0**	Jobson *et al* (2005)*
n-hexa-decane n-$C_{16}H_{34}$	2.1	323	NS	~70	150			$C_3H_7^+$ (43): **20.5** $C_4H_9^+$ (57): **45.5** $C_5H_{11}^+$ (71): **11.4** $C_6H_{13}^+$ (85): **6.8**	$C_3H_5^+$(41): **15.9**	Jobson *et al* (2005)*

D.1.2. Alkenes

The available proton affinities, gas basicities and resultant standard reaction enthalpy, entropy and Gibbs free energies for the non-dissociative proton transfer reaction of H_3O^+ with several alkenes are displayed in Table D.6.

Table D.6 A compilation of proton affinities (*PA*), gas basicities (*GB*), potential standard enthalpy (ΔH_r^Φ), potential standard entropy (ΔS_r^Φ) and Gibbs free energies (ΔG_r^Φ) of the non-dissociative H_3O^+ reaction with alkenes. Proton affinities and gas basicities are taken from Hunter and Lias, (1998) ΔG_r^Φ and ΔH_r^Φ are calculated from Eq. 2.88 and 2.89, ΔS_r^Φ are calculated from $\Delta S_r^\Phi = \left(\Delta H_r^\Phi - \Delta G_r^\Phi\right)/T$

Compound	*PA* (eV)	*GB* (eV)	ΔH_r^Φ (eV)	ΔS_r^Φ (x 10^{-4} eV K^{-1})	ΔG_r^Φ (eV)
Ethene	7.05	6.75	0.11	0.70	0.09
Propene	7.79	7.49	-0.63	0.73	-0.65
2-Butene	7.74	7.46	-0.58	1.36	-0.62
2-Methyl-2-butene	8.38	8.08	-1.22	0.73	-1.24
1-Hexene	8.35	8.05	-1.18	0.73	-1.21
Cyclopropene	8.48	8.16	-1.32	0.10	-1.32
Cyclobutene	8.13	7.81	-0.97	0.0070	-0.97
Cyclopentene	7.94	7.61	-0.78	-0.52	-0.76
Cyclohexene	8.13	7.79	-0.97	-0.52	-0.95

The product distributions, measured rate constants and resultant reaction efficiencies of the reaction of various alkenes with H_3O^+ measured in SIFT at 298 K in helium are reviewed in Table D.7. The Gibbs free energy of the reactions of $>C_2$ alkenes with H_3O^+ are less than –0.43 eV (Table D.6) and as expected from thermokinetic trends (§ 2.9, Bohme *et al* 1980, Bouchoux *et al* 1996) react efficiently (Table D.7). The reaction of ethene with H_3O^+ is endothermic and the reaction is inefficient at 298 K (Table D.6, D.10).

VT-SIFT investigations of alkene reactions with H_3O^+ could not be found. Some alkene-proton transfer reactions have been investigated at various energies by variation of the reagent ion. Milligan *et al* (2002) studied the product distributions and reaction rate constants of reaction of alkenes with H_3O^+, N_2H^+ and H_3^+ in SIFT (298 K, helium carrier gas) Figure D.4 displays the reaction efficiencies of various alkenes with H_3O^+, N_2H^+, H_3^+ at 298 K. The reactions of the C_3 – C_5 alkenes are exothermic with N_2H^+, H_3^+ and H_3O^+ efficiency is one within experimental uncertainty. The reaction of ethene with H_3^+ is exoergic and is efficient. An increase in the rate of the non-dissociative reaction of ethene with H_3O^+ may occur under the elevated energy of the PTR-MS as energy is put into the endothermic reaction (Eq.2.90). Conversely the rate of the association reaction (observed in

SIFT) is likely to decrease at the increased energy in the drift tube (if the association product is stable under the increased energy of PTR-MS). Experimental data is required to determine the effect of increased energy on overall rate of disappearance of ethene and efficiency of the ethene reaction with H_3O^+ in the PTR-MS.

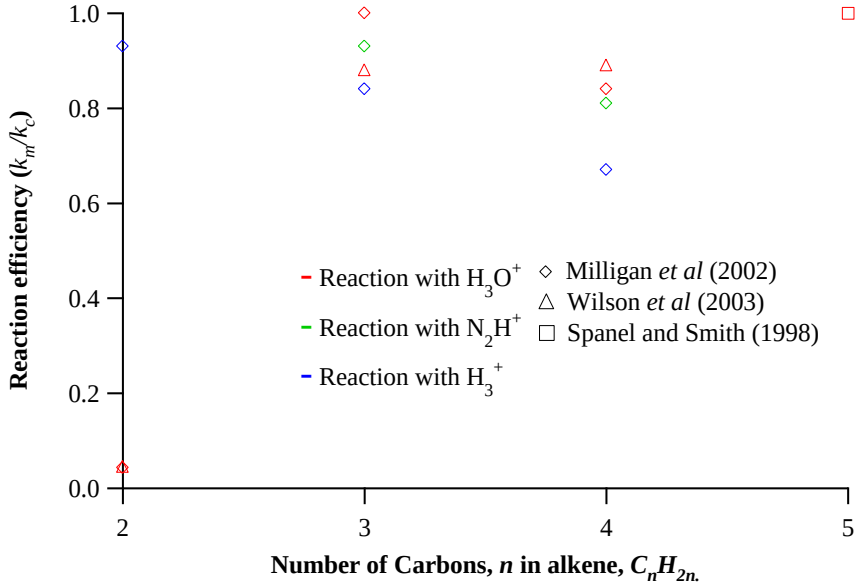

Figure D.4: The reaction efficiency (§ 2.9) of proton transfer reactions of C_2 – C_5 alkenes with N_2H^+, H_3^+ and H_3O^+ at ~ 298 K in SIFT with a helium carrier gas. Reaction efficiencies with H_3O^+ are calculated from measured and collisional rate constants from Španěl and Smith (1998), Wilson *et al* (2003) and Milligan *et al* (2002). Reaction efficiencies with N_2H^+ and H_3^+ are calculated from measured and collisional rate constants from Milligan *et al* (2002). Except for the C_4 alkene which refers to the reaction of 2-butene, the values correspond to reaction of the straight chain alkene with the double bond between carbons one and two.

Deuterium labelling of H_3^+ in reaction with ethene and propene by Milligan *et al* (2002) showed full hydrogen scrambling suggesting the proton transfer reactions with alkenes proceed through a non-dissociated excited intermediate rather than by a direct mechanism hydride transfer or rapid proton transfer (as with propane, § D.1.1).

The alkenes react with H_3O^+ by one or more of three reaction pathways in the SIFT at 298 K in helium (Table D.7); associative (Eq. D.5), non-dissociative (Eq. D.6) and dissociation to a carbocation and smaller alkene (Eq. D.7)

$$C_nH_{2n} + H_3O^+ + B \rightarrow C_nH_{2n}.H_3O^+ + B \tag{D.5}$$

$$C_nH_{2n} + H_3O^+ \rightarrow C_nH_{2n+1}^+ + H_2O \tag{D.6}$$

$$C_nH_{2n} + H_3O^+ \rightarrow C_iH_{2i+1}^+ + C_nH_{2(n-i)} + H_2O \tag{D.7}$$

In SIFT at 298 K the associative and non-dissociative product ions are observed from the reaction of ethene with H_3O^+. The associative reaction product is not observed from reaction of the higher alkenes for which the non-dissociative reaction is exothermic and the association product is not stable. The C_3 – C_6 alkenes react only by non-dissociation (Eq. D.6, Table D.7). C_7 – C_{10} alkenes react by non-dissociation and dissociation *via* Eq. D.7 (Table D.7). As discussed in § D.1.1, dissociation of $C_nH^+_{2n+1}$ to smaller $C_iH^+_{2i+1}$ ions where $i \geq 4$ and alkenes have been observed (Moet-Ner and Field 1976 and Arnold *et al* 1997) but at temperatures greater than 400 K. Dissociation of C_7 – C_{10} alkenes by Eq. D.7 to form e.g. $C_4H_9^+$ are endothermic by ≤ + 0.16 eV and $\langle E_r^{SIFT} \rangle$ at 298 K appears to be sufficient to overcome any endothermicity of dissociation.

As alkene chain length increases, the complexity of dissociation increases as product carbocations of varying size are produced through dissociation *via* Eq. D.7. The extent of dissociation increases with increasing chain length from C_7 – C_{10} alkenes (Table D.7).

The product distributions from ethene reaction with various reagent ions (Milligan *et al* 2002), are displayed as a function of change in energy relative to H_3O^+ at 298 K in Figure D.5. In this case the change in energy is the difference in gas basicities of the reagent ion neutrals, that is $GB(H_2O) - GB(N_2 \text{ or } H_2)$. The standard enthalpy of reaction of ethene with H_3O^+ to form $C_2H_3^+$, H_2 and H_2O is also shown, as an indication of the energy required for formation (neglecting entropy, thermal $\langle E_r \rangle$ at 298 K, collisional stabilization/activation, activation energies, and/or loss of energy in translation or radiation). The increase in energy of proton transfer due to the change in reagent ion to NH_2^+, H_3^+ (2.03 eV and 2.75 eV respectively) is large compared to the increase in energy in the PTR-MS, even at *E/N* of 200 Td $\Delta\langle E_r \rangle$ (Eq. 3.4, T_{dt} 298 K) of ethene is only 0.82 eV. $\Delta\langle E_r \rangle$ (Eq. 3.4, T_{dt} 298 K) of ethene and H_3O^+ at *E/N* 120 -140 Td in air is 0.23 – 0.34 eV (Figure 3.4). Under the normal operating conditions of PTR-MS the dissociative product ion $C_2H_3^+$ is not expected. Using $\Delta\langle E_r \rangle$ (Eq. 3.4, T_{dt} 298 K) as an approximation of the change in energy in the drift tube Figure D.5 suggests the non-dissociative product ion $C_2H_5^+$ (m/z 29) will form ~80 % of products and the associative product, $C_2H_4.H_3O^+$ (m/z 47), ~ 20% at *E/N* 120 -140 Td. Product ion abundancies may not vary linearly even from the thresholds, experimentally derived product distributions at the lower changes in energy are required.

As with the reaction with H_3^+ m/z 27 ($C_2H_3^+$) is the most dominant fragment from EI-MS of ethene at ~26.9 %, the parent ion at m/z 28 forms ~ 43.2 % of the product ions. Additionally

m/z 26 forms ~22.9 % of the total products and minor fragments (totalling ~ 7%) are observed at the elevated energies in EI-MS (Mallard and Linstrom 2005). This fragmentation is not expected at the lower energy in PTR-MS.

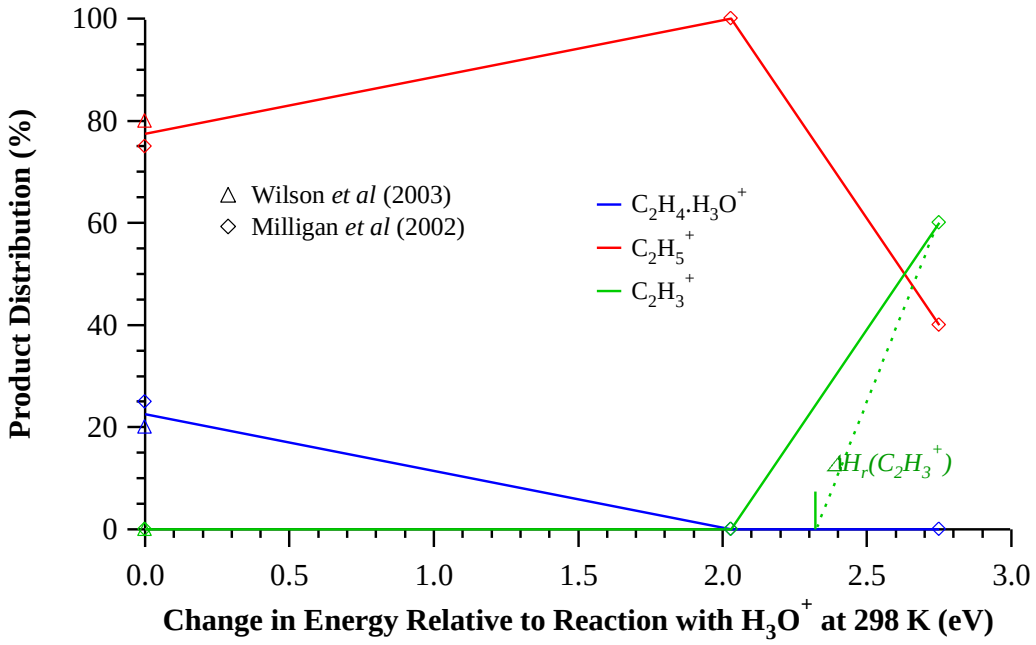

Figure D.5: Product distributions resulting from the reaction of ethene with H_3O^+, N_2H^+ and H_3^+ in SIFT at 298 K in helium carrier gas. Product distributions from reaction with H_3O^+ are taken from Milligan *et al* (2002) and Wilson *et al* (2003), those from reaction with H_3^+ and N_2H^+ are taken from Milligan *et al* (2002). The change in energy relative to reaction with H_3O^+ is the difference in gas basicities of H_3O^+ and the reagent ion (H_3O^+, N_2H^+ or H_3^+). ΔH_r $(C_2H_3^+)$ is the standard enthalpy of the reaction of H_3O^+ with ethene to form the $C_2H_3^+$ taken from Milligan *et al* (2002). ΔH_r $(C_2H_3^+)$ is an indication of the energy required for the abundance to increase above zero as indicated by the dashed line.

Product ion distributions from the reaction of propene with H_3O^+, N_2H^+ and H_3^+ (Milligan *et al* 2002) are displayed in Figure D.6 as a function of the change in energy relative to reaction H_3O^+ at 298 K. The relative abundance of the fragment product ions, $C_3H_5^+$ and $C_2H_3^+$, are unlikely to increase linearly from zero as energy available for reaction is increased as depicted by the solid lines in Figure D.6. Rather the fragment abundancies are likely to increase from some threshold where sufficient energy is available to overcome the endothermicity of the dissociation and any associated entropy and/or activation energy barrier. The standard enthalpies of the reactions of H_3O^+ with propene, to form the fragments are shown as an approximation of this threshold. Note that the enthalpies of reaction will depend on the structure of the fragment product ion, e.g. cyclic or acyclic, the values shown correspond to the most thermodynamically favourable structure i.e. a lower limit of the threshold enthalpy.

Table D.7 Reported reaction rate constants, reaction efficiencies and product distributions for the reactions of H_3O^+ with a series of alkenes measured using SIFT. P_{FT} denotes pressure in the flow tube, T_{FT} denotes temperature in the flow tube. k_m denotes the rate constant measured for the reaction of H_3O^+ with the alkene (C_nH_{2n}). k_c refers to the collisional rate constant (§ 2.4.1), k_L indicates that the collisional rate constant was derived from Langevin, Gioumousis, Stevenson theory (§ 2.4.1.2, Eq. 2.34) in the cited reference. k_{SC} indicates the collisional rate constant was derived using the results of Su and Chesnavich trajectory calculations (§ 2.4.1.4, Eq. 2.49 – 2.54) in the cited reference. * indicates that the method of collisional rate constant determination is not specified in the reference however since the dipoles of cyclic alkanes are close to zero all rate constant calculation theories will yield a value close to k_L. k_m/k_c is the reaction efficiency (§ 2.9) δ_{k_c} denotes estimated uncertainty of the calculated collisional rate constant, δ_{k_m} denotes the estimated uncertainty of the measured rate constant. A helium carrier was used in all cases, small amounts of air were added by Wilson *et al* (2003) and Španěl and Smith (1998); Španěl and Smith (1998) and Diskin *et al* (2002) used air to dilute VOC vapours entering the flow tube. Diskin *et al* (2002) performed experiments with dry air dilutant and repeated with humid laboratory air (1 % water content) and breathe (6 % water content), no products were observed at m/z corresponding to $MH^+.H_2O$ hydrates and/or $M.H_3O^+$complexes in the presence of water and it is assumed product distributions were unchanged. Humidity was not specified by Španěl and Smith (1998) or Wilson *et al* (2003) though water vapour was present. Milligan *et al* (2002) used helium alone and the helium was passed through a liquid nitrogen cooled zeolite resulting in a typical water vapour VMR of 150 ppb. *Lindinger *et al* (1998) specify thermal rate constants, measurements conditions are not given.

Alkene (C_nH_{2n})	P_{FT} (mbar)	T_{FT} (K)	k_m (x 10^{-9}m^3 s^{-1})	k_m/k_c	k_c	δ_{k_c} (%)	δ_{k_m} (%)	Observed Product Distribution: Product Ion, (m/z): **Percentage of Product Total**, $C_nH_{2n} + H_3O^+ \rightarrow$ $C_nH_{2n}.H_3O^+$	$C_nH_{2n+1}^+ + H_2O$	$C_iH_{2i+1}^+ + C_{n-i}H_{2(n-i)} + H_2O$	Reference
Ethene (C_2H_4)	[a]0.61 [b]0.64	[a]298 [b]300±5	[a]0.063, [b]0.06	[a]0.045, [b]0.043	k_L*		[b]15	$C_2H_4.H_3O^+$ (47): **[a]20, [b]25**	$C_2H_5^+$, (29): **[a]80, [b]75**		[a]Wilson *et al* (2003) [b]Milligan *et al* (2002)
Propene (C_3H_6)	[a]0.61 [b]0.64 [c]NS	[a]298, [b]300±5 [c]NS	[a]1.5, [b]1.7 [c]1.5	[a]0.88 [b]1 [c]0.88	k_L*		[b]15		$C_3H_7^+$, (43): **[a and b]100**		[a]Wilson *et al* (2003) [b]Milligan *et al* (2002) [c]Lindinger *et al* (1998)*

Table D.7 is continued on the following page.

Alkene (C_nH_{2n})	P_{FT} (mbar)	T_{FT} (K)	k_m (x 10^{-9} m^3 s^{-1})	k_m/k_c	k_c	δ_{k_c} (%)	δ_{k_m} (%)	Observed Product Distribution: Product Ion, (m/z): **Percentage of Product Total**, $C_nH_{2n} + H_3O^+ \rightarrow$ $C_nH_{2n}.H_3O^+$	$C_nH_{2n+1}^+ + H_2O$	$C_iH_{2i+1}^+ + C_{n-i}H_{2(n-i)} + H_2O$	Reference
2-Butene (C_4H_8)	[a]0.61 [b]0.64	[a]298, [b]300±5	[a]1.6 [b]1.6	[a]0.89, [b]0.84	k_L*		[b]15		$C_4H_9^+$, (57): **[a and b]100**		[a]Wilson *et al* (2003) [b]Milligan *et al* (2002)
1-Pentene (C_5H_{10})	[c]0.67[d] 0.93	[c]N/O [d]RT	[c]1.9	[c]1	[c]k_{SC} [d]k_{SC}	[c]20[d]2 5			$C_5H_{11}^+$ (71): **[c and d]100**		[c]Španěl and Smith (1998) [d]Diskin *et al* (2002)
2-Pentene (C_5H_{10})	0.93	RT			k_{SC}				$C_5H_{11}^+$ (71): **100**		Diskin *et al* (2002)
2-Methyl-2-Butene (C_5H_{10})	0.67	N/O	1.9	1	k_{SC}	20			$C_5H_{11}^+$, (71): **100**		Španěl and Smith (1998)
1-Hexene (C_6H_{12})	0.93	RT							$C_6H_{13}^+$, (85): **100**		Diskin *et al* (2002)
2-Hexene (C_6H_{12})	0.93	RT							$C_6H_{13}^+$ (85): **100**		Diskin *et al* (2002)
1-Heptene (C_7H_{14})	0.93	RT							$C_7H_{15}^+$ (99): **25**	$C_4H_9^+$ (57): **75**	Diskin *et al* (2002)
2-Heptene (C_7H_{14})	0.93	RT							$C_7H_{15}^+$ (99): **35**	$C_4H_9^+$ (57): **65**	Diskin *et al* (2002)
1-Octene (C_8H_{16})	0.93	RT							$C_8H_{17}^+$ (113): **30**	$C_4H_9^+$ (57): **35** $C_5H_{11}^+$ (71): **35**	Diskin *et al* (2002)
2-Octene (C_8H_{16})	0.93	RT							$C_8H_{17}^+$ (113): **35**	$C_4H_9^+$ (57): **30** $C_5H_{11}^+$ (71): **35**	Diskin *et al* (2002)

Table D.7 is continued on the following page.

Alkene (C_nH_{2n})	P_{FT} (mbar)	T_{FT} (K)	k_m (x 10^{-9} m^3 s^{-1})	k_m/k_c	k_c	δ_{k_c} (%)	δ_{k_m} (%)	Observed Product Distribution: Product Ion, (m/z): **Percentage of Product Total**, $C_nH_{2n} + H_3O^+ \rightarrow$ $C_nH_{2n}.H_3O^+$	$C_nH^+_{2n+1} + H_2O$	$C_iH^+_{2i+1} + C_{n-i}H_{2(n-i)} + H_2O$	Reference
1-Nonene (C_9H_{18})	0.93	RT							$C_9H_{19}^+$ (127): **30**	$C_4H_9^+$ (57): **20** $C_5H_{11}^+$ (71): **30** $C_6H_{13}^+$ (85): **20**	Diskin *et al* (2002)
2-Nonene (C_9H_{18})	0.93	RT							$C_9H_{19}^+$ (127): **40**	$C_4H_9^+$ (57): **20** $C_5H_{11}^+$ (71): **25** $C_6H_{13}^+$ (85): **15**	Diskin *et al* (2002)
1-Decene ($C_{10}H_{20}$)	0.93	RT							$C_{10}H_{21}^+$ (141): **45**	$C_4H_9^+$ (57): **10** $C_5H_{11}^+$ (71): **20** $C_6H_{13}^+$ (85): **15** $C_7H_{15}^+$ (99): **25**	Diskin *et al* (2002)

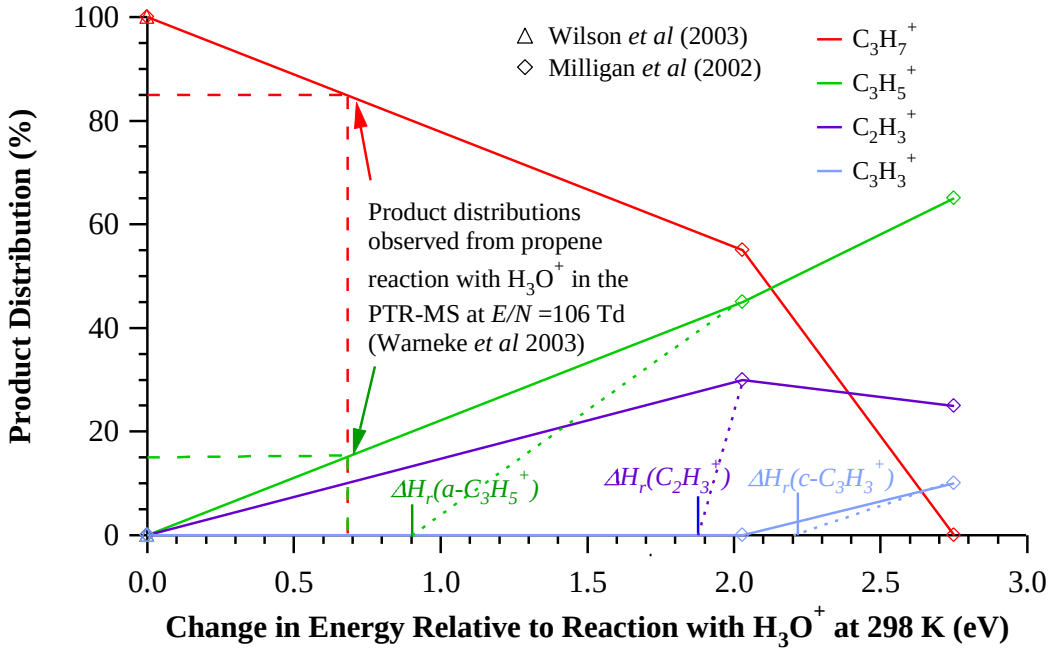

Figure D.6: Product distributions resulting from the reaction of propene with H_3O^+, N_2H^+ and H_3^+ in SIFT at 298 K in helium carrier gas. Product distributions from reaction with H_3O^+ are taken from Milligan *et al* (2002) and Wilson *et al* (2003), those from reaction with H_3^+ and N_2H^+ are taken from Milligan *et al* (2002). The change in energy relative to reaction with H_3O^+ is the difference in gas basicities of H_3O^+ and the reagent ion (H_3O^+, N_2H^+ or H_3^+). $\Delta H_r\ (F^+)$ denotes the standard enthalpy of the reaction of H_3O^+ with propene, C_3H_6, to form the fragment, F^+. $\Delta H_r\ (F^+)$ were taken from Milligan *et al* (2002). The value of $\Delta H_r\ (F^+)$ is dependent on the structure of F^+, *a* denotes that the value of $\Delta H_r\ (F^+)$ corresponds to allyl F^+, *c* denotes that the value corresponds to cyclic F^+. $\Delta H_r\ (F^+)$ is an indication of the energy required for the abundance of F^+ to increase above zero as indicated by the dashed lines, abundancies are unlikely to increase linearly from zero as change in energy increases from zero as is indicated by the full line, changes in product distributions may be non linear from the threshold.

$\Delta\langle E_r\rangle$ of propene in the PTR-MS under normal operating *E/N* of 120 – 140 Td in an air buffer (T_{dt} 298 K) is 0.25 eV – 0.37 eV (Figure 3.4). $C_3H_3^+$ is only observed from reaction with H_3^+ corresponding to an increase in energy relative to reaction with H_3O^+ (298 K) of 2.75 eV. Milligan *et al* (2002) did not observe $C_3H_3^+$ from the reaction of H_3^+ with propene when a hydrogen buffer was used in place of helium and Milligan *et al* (2002) suggest excited H_3^+ ions may have resulted in its formation in helium. The reaction of H_3O^+ with propene to form cyclic $C_3H_3^+$, $2H_2$ and H_2O is endothermic by + 2.24 eV (Milligan *et al* 2002) which is greater than the sum of $KE^r_{c.m.}$ (Figure 3.2) and $KE^b_{c.m.}$ (Figure 3.3) of 0.34 eV at *E/N* 120 Td and T_{dt} 298 K in an air buffer. Thus $C_3H_3^+$ is not expected in normally operated PTR-MS and was not observed by Warneke *et al* (2003) at *E/N* of 106 Td.

The standard enthalpy of the reaction of H_3O^+ with propene to form $C_2H_3^+$, CH_4 and H_2O is endothermic by + 1.88 eV and $C_2H_3^+$ is not observed in H_3O^+ reaction of propene in SIFT at 298 K. $C_2H_3^+$ is observed from the reactions of N_2H^+ and H_3^+ with propene, corresponding to an increase in energy relative to reaction with H_3O^+ > 1.88 eV (2.03 and 2.75 eV respectively). The relative abundance is expected to increase as energy is increased by >~1.88 eV as shown by the dashed line (depending on thermal $\langle E_r \rangle$ at 298 K, the role of entropy, activation energy and/or collisional activation/stabilization) rather than linearly as the increase in energy increases from zero as shown by the solid line. Formation of $C_2H_3^+$ is therefore unlikely under normal operating *E/N* of PTR-MS and was not observed by Warneke *et al* (2003) at *E/N* of 106 Td.

$C_3H_5^+$ is observed from the reaction of propene with N_2H^+ and H_3^+ (Figure D.6). The standard enthalpy of reaction of H_3O^+ with propene to form allyl $C_3H_5^+$, H_2 and H_2O is endothermic by +0.89 eV and not observed in SIFT at 298 K (Table D.7). Warneke *et al* (2003) observed $C_3H_5^+$ with a relative abundance of 15 % in PTR-MS at *E/N* of 106 Td (P_{dt} 2.4 mbar). Warneke *et al* (2003) obtained a measured sensitivity of 16.6 ± 3.32 (20 %) ncps ppb^{-1} from ion count rates at m/z 43 and an additional 15% due to fragmentation to m/z 41 ($C_3H_5^+$), this compared with a calculated sensitivity of 20.7 ± 6.21 (30 %) ncps ppb^{-1}. The agreement of the calculated and measured sensitivity within the uncertainties substantiates the fragmentation to m/z 41 and suggests no additional fragmentation occurs. The $\Delta\langle E_r \rangle$ (T_{dt} 298 K) of propene at *E/N* of 106 Td in an air buffer is 0.19 eV and less than the +0.89 eV endothermicity of dissociation to $C_3H_5^+$. If the relative abundance of $C_3H_5^+$ increased linearly as change in energy increased above +0.89 eV toward the abundance observed at an increase in energy of 2.03 eV (dashed line) an increase in energy of ~1.3 eV would be required to give a 15 % abundance of $C_3H_5^+$. Even if the abundance of $C_3H_5^+$ increased linearly from zero as the increase in energy increased from zero, a 15 % abundance of $C_3H_5^+$ would require a change in energy of ~0.7 eV as shown in Figure D.6. The $\langle E_r \rangle$ of reactants at 298 K if thermalised may contribute to dissociation as well as $\Delta\langle E_r \rangle$ i.e. $\langle E_r^{PTR-MS} \rangle$ (Eq. 3.2) may contribute as a whole. $KE_{c.m.}^{r}$ is 0.14 eV at *E/N* of 106 Td (T_{dt} 298 K, air buffer, Figure 3.2), $KE_{c.m.}^{b}$ is 0.13 eV (Figure 3.3) the sum of $KE_{c.m.}^{b}$ and $KE_{c.m.}^{r}$ is 0.27 eV, a further 0.62 eV is required to overcome the endothermicity of dissociation to $C_3H_5^+$. There may be a positive entropy term in addition to the internal energy of the reactant neutral, propene.

Warneke *et al* (2003) employed a drift tube pressure of 2.4 mbar compared to 0.64 mbar in the flow tube of the SIFT used by Milligan *et al* (2002) and it is possible that the dissociation to $C_3H_5^+$ is collisionally activated in the PTR-MS. Milligan *et al* (2002) compared product distributions they obtained at a flow tube pressure of 0.64 mbar in helium with those from earlier studies obtained in other CI-MS techniques at pressures of $<10^{-5}$ mbar and found a good correlation. For example, the reaction of ethene and H_3^+ was studied by Fiaux *et al* (1976) using ion cyclotron resonance mass spectrometry at ~ 1 x 10^{-6} mbar in a hydrogen buffer and when H_3^+ was completely deactivated before reaction the $C_2H_3^+$ formed 69 % of the products and $C_3H_5^+$ ~31 %. This compares well with the 60 % $C_2H_3^+$ and 40 % $C_2H_5^+$ observed by Milligan *et al* (2002) (Figure D.5). The similar product distributions, despite the change in buffer and pressure, indicate collisional activation is not important in the SIFT experiments at 0.64 mbar in helium or in the ICR experiments. However, the lifetime of the excited non-dissociated transient in relation to the time required for collisions with buffer molecules may differ in the PTR-MS, and collisionally activated dissociation may be important. This is difficult to assess without experimental pressure dependencies of product distributions in the PTR-MS at fixed energies, the effect of the diverse nature of the air buffer also requires investigation.

The dominant product ions in EI-MS of propene are similar to those from reaction of H_3^+ and likewise reduced fragmentation is observed in the PTR-MS due to the reduced energy. In EI-MS m/z 27 ($C_2H_3^+$) is ~ 10.2 %, m/z 39 ($C_3H_3^+$) is ~19.1 % and m/z 41 ($C_3H_5^+$) is ~26.3 of the total ion signal but the parent ion at m/z 42 is ~18.5 % of the total product ion signal and other minor products totalling 25.9 % are observed at the increased energy (Mallard and Linstrom 2005).

Milligan *et al* (2002) also studied the product distributions from reaction of N_2H^+ with propene using SIFDT as a function of electric field strength. As the electric field strength was increased, product distributions approached those observed from the reaction of H_3^+. This verifies that the increase in energy of the reactant ion due to the electric field can contribute to increased dissociation in a similar manner to the increase in energy due to variation of reaction Gibbs free energy by change of reagent ion.

The percentage product distributions from the reactions of H_3O^+, N_2H^+ and H_3^+ with 2-butene in SIFT at 298 K are displayed in Figure D.7 Distributions are displayed as a function of change in energy relative to reaction with H_3O^+ (298 K) due to the difference in gas basicities of the reagent ion. The standard enthalpies of reaction with H_3O^+ to produce observed dissociation products are shown. Though production of $C_2H_5^+$ from the reaction of

N_2H^+ is thermodynamically favourable, $C_2H_5^+$ is not observed; this could be a result of an activation energy barrier, loss of energy through inactive modes such as radiation, or translation of a non-dissociated transient species, collisional stabilization or due to competition from other dissociation reactions. There is sufficient energy in the reaction of 2-butene with H_3^+ for formation of $C_2H_5^+$. $\Delta\langle E_r \rangle$ of 2-butene in the PTR-MS at *E/N* 120 – 140 Td is 0.26 – 0.39 eV (298 K, air buffer, Figure 3.4), less than the change in energy due to change of reagent ion to H_3^+ (2.75 eV), $C_2H_5^+$ formation is not expected in the PTR-MS and was not observed by Warneke *et al* (2003) at *E/N* of 106 Td in air. Though there is some uncertainty in the standard enthalpy required for the dissociative reactions to form $C_3H_5^+$ and $C_4H_7^+$ and the value depends on the structure of the ion, the values calculated here (0.67 eV and 0.74 eV respectively, Table D.9) are greater than $\Delta\langle E_r \rangle$ (0.26 eV – 0.39 eV) and the sum of $KE^r_{c.m.}$ (0.19 eV – 0.26 eV) and $KE^b_{c.m.}$ (0.16 eV – 0.22 eV) in PTR-MS at *E/N* 120 – 140 Td in air at T_{dt} 298 K. Only the non-dissociated product was observed by Warneke *et al* (2003) at *E/N* 106 Td.

The product distributions from reaction of various alkenes with H_3O^+ in the PTR-MS and CIR-TOF-MS are reviewed in Table D.8. The standard enthalpies of some of the potential non-dissociative and dissociative reactions are displayed in Table D.9. The change in buffer, pressure and increase in energy in the PTR-MS based techniques result in greater dissociation than in the SIFT at 298 K. 2-butene was the only alkene to react non-dissociatively at the relatively low *E/N* of 106 Td. In addition to the non-dissociative (Eq. D.6) and dissociative (Eq. D.7) reaction observed in SIFT, some alkenes in the PTR-MS react dissociatively to form an unsaturated carbocation and alkane (Eq. D.8).

$$C_nH_{2n} + H_3O^+ \rightarrow C_iH^+_{2i-1} + C_{n-i}H_{2(n-i)+2} + H_2O \qquad \text{(D.8)}$$

It is noteworthy that in the reactions of higher alkenes a $C_iH^+_{2i-1}$ product ion may also be formed by loss of hydrogen from a $C_iH^+_{2i+1}$ product ion formed in dissociation reaction Eq. D.7. For example, $C_3H_7^+$ and $C_3H_5^+$ have both been observed from the reaction of 1-dodecene at *E/N* of ~150 Td (Jobson *et al* 2005, Table D.8), $C_3H_5^+$ may be formed indirectly from $C_3H_7^+$ (Eq. D.9 – D10) or directly by dissociation (Eq. D.11)

$$C_{12}H_{24} + H_3O^+ \rightarrow C_3H^+_7 + C_9H_{18} + H_2O \qquad \text{(D.9)}$$

$$C_3H^+_7 \rightarrow C_3H^+_5 + H_2 \qquad \text{(D.10)}$$

$$C_{12}H_{24} + H_3O^+ \rightarrow C_3H^+_5 + C_9H_{20} + H_2O \qquad \text{(D.11)}$$

The overall reaction (Eq. D.12) for the indirect reaction (Eq. D.9 – D10) is endothermic by 1.97 eV the direct dissociation reaction (Eq. D.11) is endothermic by 0.67 eV.

$$C_{12}H_{24} + H_3O^+ \rightarrow C_3H_5^+ + H_2 + C_9H_{18} + H_2O \qquad \text{(D.12)}$$

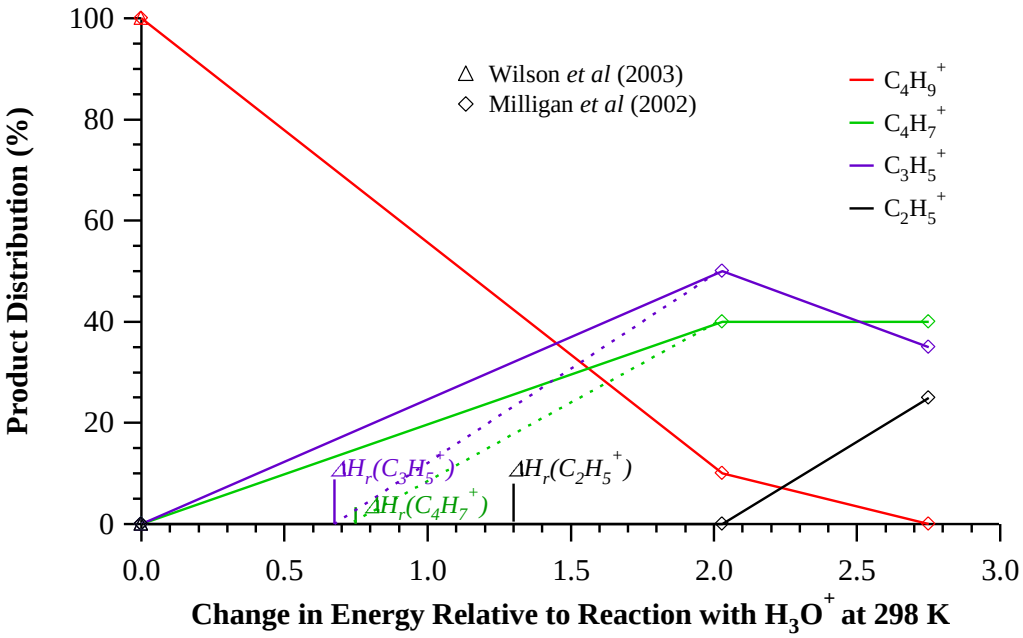

Figure D.7: Product distributions resulting from the reaction of 2-butene with H_3O^+, N_2H^+ and H_3^+ in SIFT at 298 K in helium carrier gas. Product distributions from reaction with H_3O^+ are taken from Milligan *et al* (2002) and Wilson *et al* (2003), those from reaction with H_3^+ and N_2H^+ are taken from Milligan *et al* (2002). The change in energy relative to reaction with H_3O^+ is the difference in gas basicities of H_3O^+ and the reagent ion (H_3O^+, N_2H^+ or H_3^+). $\Delta H_r\ (F^+)$ denotes the standard enthalpy of the reaction of H_3O^+ with 2-butene to form the fragment, F^+. $\Delta H_r\ (F^+)$ is an indication of the energy required for the abundance of F^+ to increase above zero as indicated by the dashed lines, abundancies are unlikely to increase linearly from zero as change in zero increase from zero as is indicated by the full line.

The indirect reaction (Eq. D.12) is unlikely at the energies in the PTR-MS and assuming entropy effects are negligible, the observed $C_3H_5^+$ is probably formed *via* the less endothermic direct dissociation mechanism (Eq. D.8 and D.11). Blake *et al* (2006) observed $C_3H_5^+$ (30%) from reaction of 1-butene with H_3O^+ at *E/N* of 165 Td (Table D.8). Dissociation to $C_3H_7^+$ is not possible in this case and $C_3H_5^+$ formation must be occurring by the direct mechanism (Eq. D.8). The dissociative reaction of 1-butene to form $C_3H_5^+$ is endothermic by ~0.56 eV (Table D.9) this is comparable with the increase in energy in the drift tube (assuming a drift tube temperature of 298 K $\Delta\langle E_r \rangle$ is 0.56 eV at *E/N* of 165 Td in nitrogen buffer) and less than the sum of $KE^b_{c.m.}$ (0.29 eV) and $KE^r_{c.m.}$ (0.36 eV) which is 0.65 eV at *E/N* 165 Td in a nitrogen buffer at T_{dt} of 313 K. Similarly in EI-MS m/z 41

Table D.8 The product distributions resulting from the reaction of a series of alkenes with H_3O^+ in the PTR-MS (Warneke *et al* 2003, Jobson *et al* 2005) and CIR-TOF-MS (§ 2.8) (Blake *et al* 2006). * not specified in the cited reference but derived from the cited T_{dt}, E and E/N. ** Percentage product distributions from Jobson *et al* (2005) are estimated here from count rates derived from spectra shown in reference and given to on decimal place and are therefore approximate values. Product ions with count rates < 100 counts s^{-1} were neglected as were m/z corresponding to ^{13}C isotopes and $H_3O^+(H_2O)_n$ clusters and their isotopes. A significant number of product ions were present with count rates < 100 counts s^{-1} and the distributions here only represent dominant product ions. The minor products, consist mainly of other $C_iH^+_{2i+1}$ ions and $C_iH^+_{2i-1}$ ions, in the case of tridecane the non-dissociative product, $C_{13}H_{27}^+$, is also a minor product. A T_{dt} of 323 K, P_{dt} of 2.1 mbar and E/N of 150 Td were specified by Jobson *et al* (2005) for sensitivity and diesel exhaust measurements within the reference and are assumed to apply for product distribution measurements, E was derived from these values. However, Jobson *et al* give a $KE_{.}^{ion}$ of 0.35 eV for the product distribution measurements, here a $KE_{.}^{ion}$ of 0.40 eV is derived for T_{dt} of 323 K and E/N of 150 Td using a reduced H_3O^+ mobility of 2.96 cm^2 / Vs in nitrogen (Dotan *et al*, 1976), the difference may be a result of a difference in the reduced mobility employed in calculation of $KE_{.}^{ion}$ rather than a difference in drift tube conditions employed for product distribution measurements. A $KE_{.}^{ion}$ of 0.35 eV corresponds to E/N of 140 Td at a T_{dt} of 323 K here. Product distributions from Jobson *et al* (2005) were measured in dry nitrogen buffer as opposed to air as is employed in normal operation of PTR-MS thereby reducing O_2^+. Product distributions in the CIR-TOF-MS (Blake *et al* 2006) were also measured in dry nitrogen, product distributions in Warneke *et al* (2003) were measured in air as in normally operated PTR-MS. Measurements by Lindinger *et al* (1998) are assumed to be made in PTR-MS measurement conditions are not specified.

Alkene (C_nH_{2n})	P_{dt} (mbar)	T_{dt} (K)	E (V cm^{-1})	E/N (Td)	Observed Product Distribution: Product Ion , (m/z): **Percentage of Product Total** $C_nH_{2n} + H_3O^+ \rightarrow$				Reference
					$C_nH^+_{2n+1} + H_2O$	$C_nH^+_{2n-1} + H_2 + H_2O$	$C_iH^+_{2i+1} + H_2O + C_{n-i}H_{2(n-i)}$	$C_iH^+_{2i-1} + H_2O + C_{n-i}H_{2(n-i)+2}$	
Propene (C_3H_6)	[a]2.4 [b]NS	[a]NS [b]NS	[a]NS [b]NS	[a]106 [b]NS	$C_3H_7^+$ (43): [a]**85** [b]**100**	$C_3H_5^+$ (41): [a]**15**			[a]Warneke *et al* (2003) [b]Lindinger *et al* (1998)
1-Butene (C_4H_8)	~7.09 *	313	270	165	$C_4H_9^+$ (57): **25**		$C_2H_5^+$ (29): **45**	$C_3H_5^+$ (41):**30**	Blake *et al* (2006)
E- 2-Butene (C_4H_8)	2.4	NS	NS	106	$C_4H_9^+$ (57): **100**				Warneke *et al* (2003)

Table D.8 is continued on the following page.

Alkene (C_nH_{2n})	P_{dt} (mbar)	T_{dt} (K)	E (V cm^{-1})	E/N (Td)	Observed Product Distribution: Product Ion , (m/z): **Percentage of Product Total** $C_nH_{2n} + H_3O^+ \rightarrow$				Reference
					$C_nH^+_{2n+1} + H_2O$	$C_nH^+_{2n-1} + H_2 + H_2O$	$C_iH^+_{2i+1} + H_2O + C_{n-i}H_{2(n-i)}$	$C_iH^+_{2i-1} + H_2O + C_{n-i}H_{2(n-i)+2}$	
Z- 2-Butene (C_4H_8)	2.4	NS	NS	106	$C_4H_9^+$ (57): **100**				Warneke *et al* (2003)
1-Pentene (C_5H_{10})	2.4	NS	NS	106	$C_5H_{11}^+$ (71): **85**		$C_3H_7^+$ (43): **15**		Warneke *et al* (2003)
3-Methyl-1-butene (C_5H_{10})	2.4	NS	NS	106	$C_5H_{11}^+$ (71): **80**		$C_3H_7^+$ (43): **20**		Warneke *et al* (2003)
2-Methyl-1-butene (C_5H_{10})	2.4	NS	NS	106	$C_5H_{11}^+$ (71): **80**		$C_3H_7^+$ (43): **20**		Warneke *et al* (2003)
E- 2-Pentene (C_5H_{10})	2.4	NS	NS	106	$C_5H_{11}^+$ (71): **80**		$C_3H_7^+$ (43): **20**		Warneke *et al* (2003)
Z-2-Pentene (C_5H_{10})	2.4	NS	NS	106	$C_5H_{11}^+$ (71): **80**		$C_3H_7^+$ (43): **20**		Warneke *et al* (2003)
2-Methyl-2-Butene (C_5H_{10})	2.4	NS	NS	106	$C_5H_{11}^+$, (71): **79**		$C_3H_7^+$ (43): **21**		Warneke *et al* (2003)
Dodecene ($C_{12}H_{24}$)	2.1**	323**	~70**	150**	$C_{12}H_{25}^+$ (169): **1.4**		$C_3H_7^+$ (43): **15.4** $C_4H_9^+$ (57): **54.0** $C_5H_{11}^+$ (71): **7.7** $C_6H_{13}^+$ (85): **9.3** $C_7H_{15}^+$ (99): **1.5** $C_8H_{17}^+$ (113): **1.4**	$C_3H_5^+$ (41): **9.3**	Jobson *et al* (2005) **

Table D.8 is continued on the following page.

Alkene (C_nH_{2n})	P_{dt} (mbar)	T_{dt} (K)	E (V cm^{-1})	E/N (Td)	Observed Product Distribution: Product Ion , ΔH_r^{Φ} (eV), (m/z): **Percentage of Product Total** $C_nH_{2n} + H_3O^+ \rightarrow$				Reference
					$C_nH_{2n+1}^+ + H_2O$	$C_nH_{2n-1}^+ + H_2 + H_2O$	$C_iH_{2i+1}^+ + H_2O + C_{n-i}H_{2(n-i)}$	$C_iH_{2i-1}^+ + H_2O + C_{n-i}H_{2(n-i)+2}$	
Tridecene ($C_{13}H_{26}$)	2.1**	323**	~70**	150**			$C_3H_7^+$ (43): **16.4** $C_4H_9^+$ (57): **46.7** $C_5H_{11}^+$ (71): **14.0** $C_6H_{13}^+$ (85): **8.2** $C_8H_{17}^+$ (113): **1.2**	$C_3H_5^+$ (41): **8.2** $C_5H_9^+$ (69): **1.3** $C_7H_{13}^+$ (97): **1.2** Also (59): 2.9	Jobson *et al* (2005) **
Cyclopentene *c*-C_5H_8	2.4	NS	NS	106	$C_5H_9^+$ (69): **100**				Warneke *et al* (2003)
Cyclohexene *c*-C_6H_{10}	2.4	NS	NS	106	$C_6H_{11}^+$ (83): **100**				Warneke *et al* (2003)

Table D.9: The standard (298 K) enthalpy of reaction of non-dissociative and dissociative proton transfer reactions of various alkenes with H_3O^+. Values derived from [a]Milligan *et al* (2002), [b]Diskin *et al* (2002), [c]using proton affinities and where applicable standard enthalpies of formation, [d]calculation from enthalpies of formation and appearance energies. The enthalpies of formation of $C_2H_5^+$, $C_3H_7^+$ and $C_4H_9^+$ were calculated using the proton affinities (Hunter and Lias 1998) and standard enthalpies of formation (Mallard and Linstrom 2005) of ethene, propene and 2-butene (*PA* of 1-butene is unknown) and are 9.41 eV, 8.34 eV and 8.07 eV respectively. The enthalpies of formation of $C_2H_3^+$, $C_3H_5^+$ and $C_4H_7^+$ were calculated from proton affinities (Hunter and Lias 1998) and standard enthalpies of formation (Mallard and Linstrom 2005) of ethyne, propyne and 2-butyne (*PA* of 1-butyne is unknown) and are 11.62 eV, 10.09 eV and 9.38 eV respectively. The enthalpy of formation of $C_3H_7^+$ calculated from the proton affinity and enthalpy of formation of cyclopropane is 8.70 eV and the standard enthalpies of dissociation reactions producing $C_3H_7^+$ are then endothermic by 0.36 eV more than shown. Standard enthalpies of formation of $C_4H_9^+$ and $C_5H_{11}^+$ could not be derived from proton affinities and standard enthalpies of formation of cyclobutane and cyclopentane as the proton affinities of these compounds are unknown. The $C_3H_5^+$ and $C_4H_7^+$ standard enthalpies of formation calculated from the proton affinities (Hunter and Lias 1998) and standard enthalpies of formation (Mallard and Linstrom 2005) of cyclopropene and cyclobutene are 10.31 eV and 9.41 eV respectively, the standard enthalpies of dissociation reactions producing cyclic $C_3H_5^+$ and $C_4H_7^+$ are thus 0.22 eV and 0.03 eV more endothermic than those shown. Neutral $C_{n-i}H_{2(n-i)}$ products of dissociation were taken to be linear alkenes with the double bond between carbons one and two. Neutral $C_{n-i}H_{2(n-i)+2}$ products of dissociation were taken to be linear *n* isomer alkanes. A standard enthalpy of formation of H^+ of 15.92 eV from CRC Handbook of Chemistry And Physics (1986-1987), a standard enthalpy of formation of H_3O^+ of 6.25 eV calculated as described in § 3 and by convention a standard enthalpy of formation of hydrogen of 0 were employed. The standard enthalpies of formation of 1-pentene, 1-dodecene, 1-nonene and *n*-nonane were not available from Mallard and Linstrom (2005) and were taken from CRC Handbook of Chemistry and Physics (1986-1987). All other standard enthalpies of formation were taken from Mallard and Linstrom (2005) and proton affinities were taken from Hunter and Lias (1998), appearance energies were taken from Mallard and Linstrom (2005).

Alkene (C_nH_{2n})	Product ion, ΔH_r^ϕ (eV), $C_nH_{2n} + H_3O^+ \rightarrow$				
	$C_nH_{2n+1}^+ + H_2O$	$C_iH_{2i+1}^+ + C_{n-i}H_{2(n-i)} + H_2O$	$C_iH_{2i-1}^+ + H_2O + C_{n-i}H_{2(n-i)+2}$	$C_nH_{2n-1}^+ + H_2 + H_2O$	$C_nH_{2n-3}^+ + 2H_2 + H_2O$
Ethene (C_2H_4)	$C_2H_5^+$ +0.11[a, c]			$C_2H_3^+$ +2.32[a, c], +2.00 to +3.18[d]	
Propene (C_3H_6)	$C_3H_7^+$ -0.63[a, c]		$C_2H_3^+$ +1.88[a, c], +2.10 to +3.14[d]	$C_3H_5^+$ +1.12[c], +0.76 to +0.93[d] Allyl $C_3H_5^+$ +0.89[a] 2-propenyl $C_3H_5^+$ +1.12[a] Cyclopropyl $C_3H_5^+$ +2.17[a]	$C_3H_3^+$ +1.91 to +3.57[d] Cyclic $C_3H_3^+$ +2.24[a] Propargyl $C_3H_3^+$ +3.32[a]
1-Butene (C_4H_8)		$C_2H_5^+$ +1.20[c] +2.85 to +2.97	$C_3H_5^+$ +0.56[c] +0.14 to +0.74[d]	$C_4H_7^+$ +0.63[c] +0.09 to +0.24[d]	

Table D.9 is continued on the following page.

Alkene (C_nH_{2n})	Product ion, ΔH_r^{ϕ} (eV), $C_nH_{2n} + H_3O^+ \rightarrow$				
	$C_nH_{2n+1}^+ + H_2O$	$C_iH_{2i+1}^+ + C_{n-i}H_{2(n-i)} + H_2O$	$C_iH_{2i-1}^+ + H_2O + C_{n-i}H_{2(n-i)+2}$	$C_nH_{2n-1}^+ + H_2 + H_2O$	$C_nH_{2n-3}^+ + 2H_2 + H_2O$
2-Butene (C_4H_8)	$C_4H_9^+$ -0.58[c]	$C_2H_5^+$ +1.31[a, c]	$C_3H_5^+$ +0.45[a] +0.67[c] +0.24[d]	$C_4H_7^+$ +0.18[a] +0.74[c] +0.22[d]	
1-Pentene (C_5H_{10})		$C_2H_5^+$ +1.17[b], +1.08[c] $C_3H_7^+$ +0.34[c]	$C_3H_5^+$ +0.68[c]		
2-Pentene (C_5H_{10})		$C_2H_5^+$ +1.25[b] *Z*-2-pentene $C_2H_5^+$ + 1.15[c] *E*-2-pentene $C_2H_5^+$ + 1.21[c] *Z*-2-pentene $C_3H_7^+$ +0.42[c] *E*-2-pentene $C_3H_7^+$ +0.47[c]	$C_3H_5^+$ *Z*-2-pentene + 0.75[c] *E*-2-pentene +0.81[c]		
1-Heptene (C_7H_{14})		$C_2H_5^+$ +1.08[c] $C_3H_7^+$ +0.22[c] $C_4H_9^+$ +0.16[c]	$C_3H_5^+$ +0.67[c]		
1-Octene (C_8H_{16})		$C_2H_5^+$ +1.08[c] $C_3H_7^+$ +0.23[c] $C_4H_9^+$ +0.16[c]	$C_3H_5^+$ +0.67[c]		
1-Dodecene ($C_{12}H_{24}$)		$C_2H_5^+$ +1.08[c] $C_3H_7^+$ +0.23[c] $C_4H_9^+$ +0.16[c]	$C_3H_5^+$ +0.67[c]		

($C_3H_5^+$) forms 32.6 % of the product ions from 1-butene, the $C_2H_3^+$ m/z 27 is also observed (8.2 %) at the higher energies (Mallard and Linstrom 2005). The production of $C_3H_5^+$ from reactions of H_3O^+ with >C_4 1-alkenes are endothermic by ~0.67 eV (Table D.9). Jobson *et al* (2005) observed $C_3H_5^+$ and larger $C_iH_{2i-1}^+$ product ions from H_3O^+ reaction with 1-undecene, 1-dodecene and 1-tridecene at *E/N* of ~150 Td (P_{dt} of 2.1 mbar and T_{dt} ~323 K – refer to Table D.8) and $\Delta\langle E_r\rangle$ ~0.51 eV (neglecting the increase in T_{dt} above 298 K). $C_3H_5^+$ was not observed from the reaction of 2-butene or C_5 alkenes with H_3O^+ by Warneke *et al* (2003) at *E/N* of 106 Td ($\Delta\langle E_r\rangle$ ~ 0.20 eV, $KE_{c.m.}^r$ ~0.16 eV, $KE_{c.m.}^b$ 0.13 eV at T_{dt} 298 K)(Blake *et al* 2006). Given the dissociation of 1-butene at higher *E/N* (Blake *et al* 2006) some $C_3H_5^+$ production might be expected at higher *E/N* and/or T_{dt}. as $\Delta\langle E_r\rangle$ approaches the endothermcitiy of the dissociation.

Dissociation by Eq. D.7 to $C_2H_5^+$ is a more endothermic reaction than dissociation to other $C_iH_{2i+1}^+$ ions or $C_3H_5^+$ (Table D.9). $C_2H_5^+$ (45 %) was observed from reaction of 1-butene by Blake *et al* (2006) at *E/N* 165 Td, T_{dt} 313 K, P_{dt} ~7.09 mbar. The standard enthalpy of dissociation of 1-butene to $C_2H_5^+$ is 1.20 eV and greater than $\Delta\langle E_r\rangle$ (0.56 eV) at *E/N* of 165 Td (in nitrogen) assuming a drift tube temperature of 298 K. The drift tube was operated at 313 K in these measurements and the increase in energy will therefore be greater than $\Delta\langle E_r\rangle$ calculated on the assumption that drift tube temperature is 298 K (so that 1-butene internal energy is unchanged). The total $\langle E_r^{PTR-MS}\rangle$ may be available for dissociation, at *E/N* of 165 Td and T_{dt} 313 K, in nitrogen $\langle E_r^{PTR-MS}\rangle$ is 0.65 eV ($KE_{c.m.}^b$ (0.29eV) + $KE_{c.m.}^r$ (0.36 eV)) plus the internal energy of 1-butene. A positive entropy term may contribute to the energy available to overcome the 1.20 eV endothermicity of $C_2H_5^+$. In EI-MS m/z 29 ($C_2H_5^+$) forms only 4.1 % of the product ions, however this may be due to the increase in competing dissociation reactions not observed in PTR-TOF-MS (m/z 27 (8.2 %), m/z 39 (11.1 %), m/z 28 (8.8 %), minor (22.5%) (Mallard and Linstrom 2005). The pressure in the CIR-TOF-MS employed by Blake *et al* (2006) is ~ 5 mbar greater than that generally employed in conventional PTR-MS and if collisional activation is involved a reduction in $C_2H_5^+$ abundance may be observed at lower pressures.

The standard enthalpies of dissociation reactions of the higher alkenes are comparable to that of 1-butene (Table D.9). $C_2H_5^+$ was not observed from reaction of H_3O^+ with 2-butene or the C_5H_{10} alkenes by Warneke *et al* (2003), though this may be due to the substantially lower

E/N of 106 Td employed (and possibly the reduced pressure). Jobson *et al* (2005) studied the product abundancies from the reaction of H_3O^+ with 1-undecene, 1-dodecene and 1-tridecene under similar drift tube conditions to Blake *et al* (2006); *E/N* of ~150 Td in nitrogen ($\Delta\langle E_r \rangle$ ~ 0.51 eV neglecting the increase in drift tube temperature above 298 K), T_{dt} ~323 K, though P_{dt} was 2.1 mbar. No product ion was observed at m/z 29 from reaction of 1-tridecene, a minor product ion was observed at m/z 29 from reaction of 1-undecene and 1-dodecene. However, the larger number of competing dissociation channels for the higher alkenes may explain the reduced abundance of $C_2H_5^+$ relative to that from reaction of 1-butene. Similarly the elevated energies in EI-MS result in production of $C_2H_5^+$ from lower order alkenes as well as the larger alkenes but in all cases $C_2H_5^+$ is a relatively minor product (e.g. m/z 29 is ~ 4.1 %, 5.9 % and 5.4 % of total ion products from 1-butene, 1-pentene and 1-dodecene respectively, Mallard and Linstrom 2005), possibly due to the large number of competing dissociation channels accessible at the higher energies.

Standard enthalpies of dissociation of the C_5 alkenes to $C_3H_7^+$ are 0.34 to 0.56 eV (Table D.9) and $C_3H_7^+$ is not observed under the thermal conditions of SIFT at 298 K. The increase in energy in PTR-MS at *E/N* of 106 Td ($\Delta\langle E_r \rangle$ 0.20 eV at 298 K in air, Figure 3.4) enables dissociation to $C_3H_7^+$ to occur and Warneke *et al* (2003) observed a 15 – 20 % abundance of $C_3H_7^+$ from the C_5H_{10} alkenes. Standard enthalpies of dissociation of the C_6 – C_{12} 1-alkenes to $C_3H_7^+$ are ~ 0.23 eV (Table D.9) compared with a sum of $KE^r_{c.m.}$ (>0.23 eV, Figure 3.2) and $KE^b_{c.m.}$ (0.18 eV, Figure 3.3) of >0.41 eV at *E/N* 120 Td and T_{dt} 298 K in air. $C_3H_7^+$ was observed from reaction of H_3O^+ with 1-undecene, 1-dodecene and 1-tridecene at *E/N* of ~150 Td and T_{dt} 323 K in nitrogen ($\Delta\langle E_r \rangle$ ~0.51 eV neglecting the increase in T_{dt} above 298 K).

As the chain length of the alkene increases an increasing number of product ions can be formed from dissociation by Eq. D.7. The dissociative reaction of H_3O^+ with 1-hexene to form $C_4H_9^+$ is endothermic by 0.29 eV which is less than sum of $KE^r_{c.m.}$ (Figure 3.2) and $KE^b_{c.m.}$ of 0.41 – 0.50 eV (Figure 3.3) at normal operating *E/N* of 120 – 140 Td and T_{dt} 298 K in air. The dissociative reactions of H_3O^+ with the C_7 – C_{12} alkenes to form $C_4H_9^+$ are endothermic by 0.16 eV (Table D.9), less than the energy available in the drift tube under normal operating conditions ($KE^r_{c.m.} + KE^b_{c.m.}$ > 0.42 eV at *E/N* 120 Td and T_{dt} 298 K in air). The enthalpies of the dissociation reaction decrease with increasing alkene size and the energy available in the drift tube increases with alkene size therefore the extent of

dissociation and number of product ions increases with alkene size as well as with increasing *E/N* and T_{dt} (Table D.8, D.9).

In summary, >C_2 alkenes react to form $C_nH^+_{2n+1}$ carbocations (m/z 29, 43, 57, 71, 85, 99 etc) by non-dissociative and dissociative reaction. $C_iH^+_{2i-1}$ product ions (m/z 41, 55, 69, 83, 97 etc) are also formed from dissociative reactions of higher alkenes and of lower alkenes at higher *E/N*. Dissociation to $C_iH^+_{2i+1}$ with the double bond remaining in the neutral (Eq. D.7) is the dominant dissociation pathway for the alkenes studied to-date under normal operating drift tube conditions (Table D.9) Conversely in EI-MS the $C_iH^+_{2i-1}$ product ions dominate over $C_iH^+_{2i+1}$ ions. For example m/z 27 and 41 form a total of 40.8 % and 17.4 % of products from EI-MS of 1-butene and 1–pentene respectively compared to the sum at m/z 29 and m/z 43 of 4.1 % and 7.0 % from 1-butene and 1-pentene respectively (Mallard and Linstrom 2005). The relative abundance of $C_iH^+_{2i-1}$ is expected to increase as energy in the drift tube is increased by increasing *E/N* and or T_{dt}.

The effects of drift tube pressure and buffer require further investigation to determine the role of buffer molecules in alkene dissociation in the PTR-MS and CIR-TOF-MS. Further investigation of dissociation of $C_nH^+_{2n+1}$ to $C_iH^+_{2i+1}$ and $C_iH^+_{2i-1}$ as a function of energy, distribution of energy, pressure at fixed energies and buffer would be of interest.

The isobaric nature of the product ions of the alkenes prevents quantification of individual alkenes or differentiation of isomers in the PTR-MS. The VMR of the sum of >C_2 alkenes can potentially be quantified from ion count rates at m/z corresponding to the $C_nH^+_{2n+1}$ and $C_iH^+_{2i-1}$ product ions. However a number of other compounds, e.g. alkanes, alcohols, aldehydes, carboxylic acids etc, react with H_3O^+ to produce ions at the same m/z corresponding to $C_nH^+_{2n+1}$ and $C_iH^+_{2i-1}$. Quantification of >C_2 alkenes in ambient air masses is therefore not possible without complimentary techniques such as GC or FTIR.

Christian *et al* (2004) compared VMRs of propene in smoke from generated fires obtained from OP-FTIR with those obtained in the PTR-MS (*E/N* 130 Td, P_{dt} 2 mbar) by calculation from count rates at m/z 43. Count rates at m/z 43 were reduced by 30 % to account for the increase in the signal from fragmentation from ethanoic acid and glycoaldehyde before calculation of propene VMR. The VMR of propene derived in the PTR-MS was generally higher than that from OP-FTIR indicating the contribution of other compounds at m/z 43.

The study average for the integrated PTR-MS excess VMRs divided by the integrated OP-FTIR excess VMRs (PT/FT) was 2.33± 0.89. 'Excess' here refers to VMRs from generated fires minus the VMRs measured prior to fire start. Propene measured by GC-FID analysis of canister samples was ~ 80 % of OP-FTIR VMRs. No note of instrumental background quantification or subtraction is made by Christian *et al* (2004) this may also have contributed to the higher propene VMRs. Kuster *et al* (2004) compared propene VMRs in suburban air of La Porte Texas measured by application of a calibration derived sensitivity to m/z 43 count rates in PTR-MS (*E/N* 123 Td, P_{dt} 2.5 mbar) with those obtained from online GC-FID and derived a gradient of 0.91, intercept 270 ppt and r^2 0.74. Background measurements were made every 30 min to 2 h by passing measurement air through a Pt wool catalyst at 430°C in the PTR-MS. The gradient is within uncertainty of one but the relatively large intercept and relatively poor correlation coefficient suggests other compounds may have contributed to m/z 43. Propene was the most abundant lightweight hydrocarbon measured by Kuster *et al* (2004) and VMRs were relatively high, peaking at 100 ppb. There is considerable variation in propene VMRs in the troposphere but mean VMRs are generally between 0.1 and 10 pbb (Bonsang and Boissard, 1999). At the lower propene VMRs where other contributions to m/z 43 are comparable, propene VMRs derived from m/z 43 will be less accurate without measurement and subtraction of all other contributors by alternative techniques such as FTIR or GC. m/z 41 ($C_3H_5^+$) count rates were not considered by Christian *et al* (2004) or Kuster *et al* (2004).

Rogers *et al* (2006) compared the sum of methyl tertiary butyl ether (MTBE) and C_4H_8 isomers in the Mexico City metropolitan area derived by GC-FID with VMRs derived by calculation from m/z 57 count rates in the PTR-MS (*E/N* 145 Td, P_{dt} 1.9 mbar, T_{dt} ~295 – 300 K). Instrument background was measured every 20 min by flooding the inlet with zero air. A gradient of 0.97, intercept of 160 ppt and correlation coefficient of 0.99 was obtained. The gradient and correlation coefficient of close to one suggest good agreement between the GC-FID and PTR-MS VMRs. The intercept may result from interference at m/z 43 from compounds other than MTBE and C_4H_8 but could be a result of random underestimation of the instrument background. A gradient of >1 and lower correlation coefficient might be expected if other contributors were present. The gradient is only slightly less than one (~1 given the uncertainty in the VMRs) suggesting any fragmentation of alkenes to m/z 29 or 41 is minor at this *E/N* (Table D.8)

D.1.3 The Reaction of Acyclic Alkanes and Alkenes in the Presence of Water.

The majority of alkanes and alkenes do not react with $H_3O^+(H_2O)_n$ by proton transfer at 298

K as their proton affinities (Table D.1 and D.6) are less than those of the clusters (>8.57 eV at n > 1). The proton transfer reactions of $H_3O^+(H_2O)_n$ with alkanes and alkenes have not been studied at the higher energies in PTR-MS, where $\Delta\langle E_r \rangle$ may be sufficient to overcome the endothermicity of non-dissociative transfer to alkenes.

There is little evidence of $C_nH_{2n}.H_3O^+$ or $C_nH_{2n+2}.H_3O^+$ formation *via* ligand switching reactions in SIFT or $C_nH^+_{2n+1}.H_2O$ or $C_iH^+_{2i-1}H_2O$ formation by three-body association reactions with water (e.g. Diskin *et al* 2002, Wang *et al* 2004a, Španěl *et al* 2002). The lack of ligand switching is unsurprising given the non-polar nature of the alkanes and alkenes (§ 2.6, Španěl and Smith 1995c). In fact the reverse ligand switching reaction (Eq. D.13) has been observed from the alkane association products formed by reaction with H_3O^+ in SIFT (Španěl and Smith 1998e) thereby catalyzing $H_3O^+.H_2O$ formation:

$$C_nH_{2n+2}.H_3O^+ + H_2O \rightarrow C_nH_{2n+2} + H_3O^+.H_2O \qquad \text{(D.13)}$$

Jobson *et al* (2005) noted only a small or no degree of $C_nH_{2n+2}.H_3O^+$ formation from *n*-octane, *n*-dodecane and *n*-hexadecane reaction with H_3O^+ at m/z 133, 189, 245 (Table D.5) in PTR-MS (*E/N* 150 Td, 323 K in dry nitrogen and air) and an increase in the m/z 37 ($H_3O^+.H_2O$) indicating that reaction Eq. D.13 also occurs in the PTR-MS.

Hydrates of smaller hydrocarbons with *PA* close to water e.g. $C_2H_5^+$ are stable (Španěl and Smith 1995c). The formation of hydrates of $C_2H_5^+$, $C_3H_7^+$ and $C_4H_9^+$ is exothermic (Keesee and Castleman 1986). A number of SIFT studies have shown that most hydrocarbon ions do not associate with water at sufficient rates to be observed in SIFT (e.g. Diskin *et al* 2002, Španěl *et al* 2002). Španěl and Smith (2000) conclude that when *M* is a saturated aliphatic MH^+ hydrates are not formed at a significant rate under SIFT-MS conditions by association of MH^+ with water or by ligand switching of *M* with $H_3O^+(H_2O)$. Given the negative energy dependence of association reaction rates (e.g. Meot-Ner 1979) significant formation of clusters such as $C_nH^+_{2n+1}.H_2O$ and $C_iH^+_{2i-1}H_2O$ maybe less likely (at a given water vapour VMR) in PTR-MS than SIFT at 298 K, as exemplified by the reduction in $H_3O^+(H_2O)_n$ n= 1-3 in PTR-MS (Warneke *et al* 2001b). At the elevated energies of PTR-MS, the lifetime of excited $(MH^+.H_2O)^*$ transients with respect to dissociation to MH^+ and H_2O is likely to be reduced and fewer species will be sufficiently long lived for stabilizing collisions with buffer molecules to form $MH^+.H_2O$. Likewise ligand switching reactions with $H_3O^+(H_2O)$ may be reduced due to the reduction of $H_3O^+(H_2O)$ at a given humidity and the decrease in rate as energy is put to the exothermic reaction and as collisional rate decreases. Arnold *et al* (1998) and Jobson *et al* (2005) observed minor products at m/z corresponding to hydrates of the

smaller $C_nH^+_{2n+1}$ ions formed by dissociative reactions of alkanes with H_3O^+ in VT-SIFT at 300 to 500 K (Table D.3) and PTR-MS respectively (Table D.5). Three-body association of $C_3H_7^+$ ions produced from propanol reactions with H_3O^+ in SIFDT with H_2O have been noted by Warneke *et al* (1996). The rate of association may increase with increased pressure as the number density of buffer molecules and therefore stabilization increases, pressure in PTR-MS is increased compared to SIFT. The change in buffer may also affect the extent of stabilization, many of the molecules in the PTR-MS buffer are polyatomic and have more vibrational energy levels into which energy can be removed compared to monatomic helium in SIFT. Further investigation is warranted, however these $C_nH^+_{2n+1}$ hydrates formed < 6 % of total product ions in PTR-MS and contribution to the corresponding m/z is likely to be relatively small.

D.1.4. Cyclic Alkanes

The available thermodynamic data for the non-dissociative proton transfer reactions of H_3O^+ with various cyclic alkanes are displayed in Table D.10. The efficiencies and product distributions of H_3O^+ reaction with a range of cyclic alkanes measured using SIFT and VT-SIFT are displayed in Tables D.11 and D.12 respectively. The standard enthalpies of various dissociation reactions are given in Table D.13.

Table D.10: A compilation of proton affinities (*PA*), gas basicities (*GB*), potential standard enthalpy (ΔH_r^Φ), potential standard entropy (ΔS_r^Φ) and Gibbs free energies (ΔG_r^Φ) of the non-dissociative reaction of H_3O^+ with various cyclic alkanes. Proton affinities and gas basicities are taken from Hunter and Lias, (1998) unless otherwise specified: [a]Španěl *et al* (1995a), [c]Španěl *et al* (1995b). ΔG_r^Φ and ΔH_r^Φ are calculated from Eq. 2.88 and 2.89, except in the case of [c]Španěl *et al* (1995b) and [e]values calculated here from data of Španěl *et al* (1995b), see in text for details. [b] ΔH_r^Φ values taken from Midey *et al* (2003) and proton affinity calculated from $PA_{(O)VOC} = PA_{H_2O} + \Delta H_r^\Phi$. ΔS_r^Φ are calculated from $\Delta S_r^\Phi = \left(\Delta H_r^\Phi - \Delta G_r^\Phi\right)/T$

Compound	*PA* (eV)	*GB* (eV)	ΔH_r^Φ (eV)	ΔS_r^Φ (x 10^{-4} eV K^{-1})	ΔG_r^Φ (eV)
Cyclopropane	7.78	7.48	-0.61	1.01	-0.64
Cyclohexane	7.12	6.91	0.04	3.83	-0.07
	6.94[a]		0.22		
Cyclooctane	7.81[b]		-0.65[b]		
Methylcyclohexane	7.11 to 7.16[c]	6.73 to 6.81[e]	0.03 to 0.11[c]		0.11 to 0.03[e]
	7.81[b]		-0.65 [b]		

Proton affinities of cyclooctane (C_8H_{16}) and methylcyclohexane (C_7H_{14}) have been derived here from the enthalpies of non-dissociative reaction given by Midey *et al* (2003). Midey *et*

al (2003) employed enthalpies of formation to calculate the enthalpies of non-dissociative proton transfer. The enthalpy of formation of $C_7H_{15}^+$ used corresponded to a tertiary structure, the enthalpy of formation of $C_8H_{17}^+$ to a linear structure, theoretical calculations showed that the minimum energy structure of both protonated cycloalkanes do not favour a cyclic structure (Midey *et al* 2003).

Španěl *et al* (1995a,b) calculated proton affinities of methylcyclohexane and cyclohexane (C_6H_{12}) from enthalpies of non-dissociative reactions derived by re-arrangement of Eq. 2.90 (which applies to endothermic reactions) and assuming entropy is negligible to give Eq. D.14:

$$\Delta H_r = RT \left[\ln k_c - \ln k_m \right] \qquad \text{(D.14)}$$

where ΔH_r is the enthalpy of the non-dissociative reaction and has units kJ mol^{-1}, R is the gas constant and is 8.314 34 x 10^{-3} kJ K^{-1} mol^{-1}, T is temperature in units K, k_c is the collisional rate constant and k is the rate constant for non-dissociative proton transfer.

Table D.11: Reported reaction rate constants, reaction efficiencies and product distributions for the reactions of H_3O^+ with a series of cyclic alkanes measured using SIFT at 298 K. P_{FT} denotes pressure in the flow tube, T_{FT} denotes temperature in the flow tube. k_m denotes the rate constant measured for the reaction of H_3O^+ with the cyclic alkane (C_nH_{2n}). k_c refers to the collisional rate constant (§ 2.4.1), k_L indicates that the collisional rate constant was derived from Langevin, Gioumousis, Stevenson theory (§ 2.4.1.2, Eq. 2.34) in the cited reference. k_{SC} indicates the collisional rate constant was derived using the results of Su and Chesnavich trajectory calculations (§ 2.4.1.4, Eq. 2.49 – 2.54) in the cited reference. * indicates that the method of k_{coll} is not specified in the reference however since the dipoles of cyclic alkanes are close to zero all rate constant calculation theories will yield a value close to k_L. k_m/k_c is the reaction efficiency (§ 2.9). δ_{k_m} denotes the estimated uncertainty of the measured rate constant, uncertainties associated with the collisional rate constants were not given but are generally in the order of 15 – 30 %. A helium carrier gas was used in all cases, small amounts of moist air were added by Wilson *et al* (2003). Milligan *et al* (2002) passed the helium carrier gas through a liquid nitrogen cooled zeolite resulting in a typical water vapour VMR of 150 ppb. Humidity was not specified by Španěl *et al* (1995 a, b) or Wilson *et al* (2003).

Compound (C_nH_{2n})	P_{FT} (mbar)	T_{FT} (K)	k_m (x 10^{-9} m^3 s^{-1})	k_m/k_c	k_c	δ_{k_m} (%)	Observed Product Distribution : Product Ion (m/z): **Percentage of Product Total**, $C_nH_{2n} + H_3O^+ \rightarrow$ $C_nH_{2n+1} + H_2O$	$C_nH^+_{2n-1} + H_2 + H_2O$	Reference
Cyclopropane C_3H_6	[a~]0.67 [b]0.61 [c]0.64 [d]0.67	[a]300 [b]298 [c]300±5 [d]300	[a]1.3 [b]1.5 [c]1.6 [d]1.5	[a]1.00 [b]0.87 [c]1.1 [d]0.98	[a]k_{SC} [b]k_L* [c]k_{SC} [d]k_L	 [c]15 [d]20	$C_3H_7^+$ (43): [a, b, c and d]**100**		[a]Španěl *et al* (1995b) [b]Wilson *et al* (2003) [c]Milligan *et al* (2002) [d]Španěl *et al* (1995a)
Cyclohexane C_6H_{12}	[a]~0.67 [d]0.67	[a]300 [d]300	[a]<0.0001 [d]≤0.0001	[a]<0.0000513 [d]≤0.0000513	[a]k_{SC} [d]k_L	 [d]20	*c*-$C_6H_{13}^+$ (85) **[a]~50** **[d]~50**	*c*-$C_6H_{11}^+$ (83) **[a]~50** **[d]~50**	[a]Španel *et al* (1995b) [d]Španěl *et al* (1995a)
Methyl cyclohexane C_7H_{14}	[a]~0.67[c]0.64	[a]300 [c]300±5	[a]0.7 [c]0.71	[a]0.32 [c]0.32	[a]k_{SC} [c]k_{SC}	 [c]15	$C_7H_{15}^+$ (99) **[a]5** **[c]10**	$C_7H_{13}^+$ (97) **[a]95** **[c]90**	[a]Španěl *et al* (1995b) [c]Milligan *et al* (2002)

Table D.12: Reaction rate constants, reaction efficiencies and product distributions for the reactions of H_3O^+ with cyclooctane (C_8H_{16}) and methylcyclohexane (C_7H_{14}) measured using VT-SIFT by Midey *et al* (2003). Pressure in the flow tube (P_{FT}) was not stated but is generally ~0.5 - 0.6 mbar in VT-SIFT. T_{FT} denotes temperature in the flow tube. A helium carrier gas was used and water vapour was removed by passing the helium through a liquid nitrogen cooled sieve, cyclic alkanes were diluted with helium. k_m denotes the measured rate constant for the reaction of H_3O^+ with the cyclic alkane (C_nH_{2n}). k_c refers to the collisional rate constant (§ 2.4.1) and k_m/k_c is the reaction efficiency: Midey *et al* (2003) derived the collisional rate constant using the results of Su and Chesnavich trajectory calculations (§ 2.4.1.4, Eq. 2.49 – 2.54). The measured rate constants have relative errors of ± 15 % and absolute errors of ±25%, uncertainties of the collisional rate constants were not given but are generally in the order of 15 – 30 %.

Cyclic alkane C_nH_{2n}	T_{FT} (K)	k_m (x 10^{-9} m^3 s^{-1})	k_m/k_c	Observed Product Distribution: Product Ion (m/z): **Percentage of Product Total**, $C_nH_{2n} + H_3O^+ \rightarrow$								
				$C_nH_{2n}.H_3O^+$	$C_nH^+_{2n+1} + H_2O$	$C_nH^+_{2n-1} + H_2 + H_2O$	$C_nH^+_{2n} + H + H_2O$	$C_iH^+_{2i-2} + C_{n-i}H^+_{2(n-i)+2} + H_2O$	$C_iH^+_{2i-1} + C_{n-i}H^+_{2(n-i)+2} + H_2O$	$C_iH^+_{2i} + C_{n-i}H^+_{2(n-i)+1} + H_2O$	$C_iH^+_{2i+1} + C_{n-i}H^+_{2(n-i)} + H_2O$	$C_iH^+_{2i+2} + C_{n-i}H^+_{2(n-i)-1} + H_2O$
C_8H_{16}	***298***	0.50	0.22	$C_8H_{16}.H_3O^+$ (131): **30**	$C_8H_{17}^+$ (113): **45**	$C_8H_{15}^+$ (111): **6**			$C_5H_9^+$ (69): **3**		$C_5H_{11}^+$ (71):**16**	
	400	0.30	0.13		$C_8H_{17}^+$ (113): **20**	$C_8H_{15}^+$ (111): **10**			$C_4H_7^+$ (55): **4** $C_5H_9^+$ (69): **5** $C_6H_{11}^+$ (83): **2**	$C_4H_8^+$ (56): **7** $C_6H_{12}^+$ (84): **1**	$C_4H_9^+$ (57): **16** $C_5H_{11}^+$ (71): **35**	
	500	0.30	0.13			$C_8H_{15}^+$ (111): **15**			$C_4H_7^+$ (55): **5** $C_5H_9^+$ (69): **6** $C_6H_{11}^+$ (83): **3**	$C_4H_8^+$ (56): **5** $C_5H_{10}^+$ (70): **4** $C_6H_{12}^+$ (84): **3**	$C_4H_9^+$ (57): **25** $C_5H_{11}^+$ (71): **34**	

Table D.12 is continued on the following page.

Cyclic alkane C_nH_{2n}	T_{FT} (K)	k_m (x 10^{-9} m^3 s^{-1})	k_m/k_c	Observed Product Distribution: Product Ion (m/z): **Percentage of Product Total**, $C_nH_{2n} + H_3O^+ \rightarrow$								
				$C_nH_{2n}.H_3O^+$	$C_nH^+_{2n+1}$ + H_2O	$C_nH^+_{2n-1}$ + H_2 + H_2O	$C_nH^+_{2n}$ + H + H_2O	$C_iH^+_{2i-2}$ + $C_{n-i}H^+_{2(n-i)+2}$ + H_2O	$C_iH^+_{2i-1}$ + $C_{n-i}H^+_{2(n-i)+2}$ + H_2O	$C_iH^+_{2i}$ + $C_{n-i}H^+_{2(n-i)+1}$ + H_2O	$C_iH^+_{2i+1}$ $C_{n-i}H^+_{2(n-i)}$ + H_2O	$C_iH^+_{2i+2}$ + $C_{n-i}H^+_{2(n-i)-1}$ + H_2O
C_7H_{14}	***298***	0.8	0.38	$C_7H_{14}.H_3O^+$ (117): **1**	$C_7H_{15}^+$ (99): **5**	$C_7H_{13}^+$ (97): **88**			$C_6H_{11}^+$ (83): **6**			
	400	0.6	0.29		$C_7H_{15}^+$ (99): **8**	$C_7H_{13}^+$ (97): **75**	$C_7H_{14}^+$ (98): **1**	$C_5H_8^+$ (68): **1**	$C_5H_9^+$ (69): **1** $C_6H_{11}^+$ (83): **7**	$C_5H_{10}^+$ (70): **1**	$C_4H_9^+$ (57): **4**	$C_4H_{10}^+$ (58): **1**
	500	0.4	0.19		$C_7H_{15}^+$ (99): **1**	$C_7H_{13}^+$ (97): **68**		$C_5H_8^+$ (68): **1**	$C_5H_9^+$ (69): **1** $C_6H_{11}^+$ (83): **10**	$C_4H_8^+$ (56): **2** $C_5H_{10}^+$ (70): **3**	$C_4H_9^+$ (57): **11** $C_4H_7^+$ (43): **2**	

Table D.13: The standard (298 K) enthalpy of reaction of dissociative proton transfer reactions of various cyclic alkanes with H_3O^+. Values derived from [a]proton affinities and standard enthalpies of formation[b], threshold proton affinities and *PA(H_2O)* in Španěl *et al* (1995a), [c]Milligan *et al* (2002), [d]Midey *et al* (2003), [e]enthalpies of formation and appearance energies. The enthalpies of formation of $C_3H_5^+$, $C_4H_7^+$, $C_5H_9^+$ and $C_6H_{11}^+$ used to derive enthalpies of dissociation to $C_3H_5^+$, $C_4H_7^+$, $C_5H_9^+$ and $C_6H_{11}^+$ were calculated from the proton affinities (Hunter and Lias 1998) and standard enthalpies of formation (Mallard and Linstrom 2005) of cyclopropene, cyclobutene, cyclopentene and cyclohexene and were 10.31 eV, 9.42 eV, 8.33 eV and 7.75 eV respectively. Bracketed values of enthalpies of dissociation to $C_3H_5^+$, $C_4H_7^+$, $C_5H_9^+$ and $C_6H_{11}^+$ were calculated using enthalpies of formation of $C_3H_5^+$, $C_4H_7^+$, $C_5H_9^+$ and $C_6H_{11}^+$ derived from proton affinities (Hunter and Lias 1998) and standard enthalpies of formation (Mallard and Linstrom 2005) of propyne, 2-butyne, 2-pentyne and 1-hexyne of 10.09 eV, 9.38 eV, 8.86 eV and 8.90 eV respectively. The enthalpy of formation of $C_2H_3^+$ was calculated from the proton affinity (Hunter and Lias 1998) and standard enthalpy of formation (Mallard and Linstrom 2005) of ethyne and is 11.62 eV. The enthalpy of formation of $C_3H_7^+$ used to derive the enthalpy of dissociation to $C_3H_7^+$ was calculated from the proton affinity and standard enthalpy of formation of cyclopropane and is 8.70 eV. The bracketed value of enthalpy of dissociation to $C_3H_7^+$ was calculated using an enthalpy of formation of $C_3H_7^+$ derived from the proton affinity and standard enthalpy of formation of propene of 8.34 eV. The enthalpy of formation of $C_4H_9^+$ was calculated using the proton affinity (Hunter and Lias 1998) and standard enthalpy of formation (Mallard and Linstrom 2005) of 2-butene (*PA* of 1-butene and cyclobutane is unknown) and is 8.07 eV. Neutral products $C_{n-i}H_{2(n-i)\pm 2}$ are assumed to be n-alkanes. Neutral products $C_{n-i}H_{2(n-i)}$ are taken to be linear alkenes with the double bond between carbons one and two except for C_6H_{12} produced from the butylcyclohexane reaction with H_3O^+ which was assumed to be cyclohexane. A standard enthalpy of formation of H^+ of 15.92 eV from CRC Handbook of Chemistry and Physics (1986-1987), a standard enthalpy of formation of H_3O^+ of 6.25 eV calculated as described in § 3 and by convention a standard enthalpy of formation of hydrogen of 0 were employed. All other standard enthalpies of formation were taken from Mallard and Linstrom (2005) and proton affinities were taken from Hunter and Lias (1998).

Cyclic Alkane (C_nH_{2n})	Product ion, ΔH_r^ϕ (eV), $C_nH_{2n} + H_3O^+ \rightarrow$			
	$C_nH_{2n-1}^+ + H_2 + H_2O$	$C_iH_{2i-1}^+ + C_{n-i}H_{2(n-i)\pm 2} + H_2O$	$C_iH_{2i+1}^+ + C_{n-i}H_{2(n-i)} + H_2O$	$C_iH_{2i}^+ + C_{n-i}H_{2(n-i)+1}^+ + H_2O$
Cyclopropane C_3H_6	$C_3H_5^+$ +1.00 (+0.78)[a], +0.37 to +0.47[e]	$C_2H_3^+$ +1.54[a], +1.57[b], +1.53[c], +1.53 to +2.44[e]		
Cyclopropane C_3H_6	*a*-$C_3H_5^+$ +0.61[b], +0.55[c] *c*-$C_3H_5^+$ +1.87[b], +1.83[c] *p*-$C_3H_5^+$ +0.78[c]			
continued				
Cyclopentane C_5H_{10}	$C_5H_9^+$ +0.36 (+0.89)[a]	$C_2H_3^+$ +2.58[a] $C_3H_5^+$ +1.47 (+1.25)[a] $C_4H_7^+$ +0.68 (+0.64)[a], +0.02 to 0.30[e]	$C_3H_7^+$ +1.27 (+0.92)	

Table D.13 is continued on the following page.

Cyclic Alkane (C_nH_{2n})	Product ion, ΔH_r^{ϕ} (eV), $C_nH_{2n} + H_3O^+ \rightarrow$			
	$C_nH_{2n-1}^+ + H_2 + H_2O$	$C_iH_{2i-1}^+ + C_{n-i}H_{2(n-i)+2} + H_2O$	$C_iH_{2i+1}^+ + C_{n-i}H_{2(n-i)} + H_2O$	$C_iH_{2i}^+ + C_{n-i}H_{2(n-i)+1}^+ + H_2O$
Cyclohexane C_6H_{12}	$C_6H_{11}^+$ +0.26 (+1.42)[a], +0.25 to +0.64[e]	$C_4H_7^+$ +1.07 (+1.03)[a] +0.31 to +0.39[e]	$C_3H_7^+$ +1.43 (+1.07)[a] +1.15[b] +1.14 to +3.26[e] $C_4H_9^+$ +1.13[a]	
Cyclooctane C_8H_{16}	*c*-$C_8H_{15}^+$ -0.77[d]	*s*-$C_4H_7^+$ +0.11[d] *s*-$C_5H_9^+$ -0.52[d] *s*-$C_6H_{11}^+$ -0.89[d]	*s*-$C_4H_9^+$ +0.47[d] *s*-$C_5H_{11}^+$ +0.46[d]	*s*-$C_4H_8^+$ +2.39[d] *s*-$C_5H_{10}^+$ +2.40[d] *s*-$C_6H_{12}^+$ +2.32[d]
Methylcyclopentane	$C_6H_{11}^+$ ~+0.092 (+1.25)[a]	$C_2H_3^+$ +2.67[a] $C_3H_5^+$ +1.88 (+1.36)[a] $C_4H_7^+$ +0.90 (0.86)[a] $C_5H_9^+$ -0.098 (+0.43)[a], -0.64 to -0.11[e]	$C_3H_7^+$ +1.26 (0.90)[a] $C_4H_9^+$ +0.96[a]	
Methylcyclohexane C_7H_{14}	$C_7H_{13}^+$ -0.29 (*c*-)[d], -0.30[c]	$C_4H_7^+$ +0.64 (*s*-)[d], +0.58[c] *t*-$C_5H_9^+$ -0.05[d] $C_6H_{11}^+$ -0.19 (+0.97)[a], -0.21 (*c*-)[d], -0.52[c], -0.11[e]	$C_3H_7^+$ +1.01[c] $C_4H_9^+$ +0.37 (*t*-)[d], +0.48[c]	*s*-$C_4H_8^+$ +2.88[d] *s*-$C_5H_{10}^+$ +2.90[d]
Butylcyclohexane $C_{10}H_{20}$		$C_3H_5^+$ +1.59 (+1.81)[a] $C_4H_7^+$ +1.14 (1.04)[a] $C_6H_{11}^+$ -0.11 (+1.05)[a]	$C_4H_9^+$ +0.24[a]	

Taking the example of methylcyclohexane, the reaction of H_3O^+ was observed to produce 95 % $C_7H_{13}^+$ (+ H_2 + H_2O) and 5 % $C_7H_{15}^+$ (+H_2O) in the SIFT at 298 K (Table D.11). The measured rate of removal of reactants was 7 x 10^{-10} cm^3 s^{-1} (Table D.11), if it is assumed that the dissociative reaction proceeds *via* the non-dissociative product and that dissociation of the non-dissociative product is relatively rapid, the rate of non-dissociative proton transfer is 7 x 10^{-10} cm^3 s^{-1}. Španěl *et al* (1995b) calculated a collisional rate constant of 2.2 x 10^{-9} cm^{-3} s^{-1} using the results of Su and Chesnavich trajectory calculations (§ 2.4.1.4, Eq. 2.49 – 2.54). Substituting these values in to Eq. D.14 gives a ΔH_r of 2.84 kJ mol^{-1} (0.03 eV). If the reaction to form $C_7H_{13}^+$ occurs by hydride transfer the rate constant of non-dissociative reaction only should be employed in Eq. D.14. Španěl *et al* (1995b) estimate this to be 3.5 x 10^{-11}, 5 % of the overall reaction rate, this results in a ΔH_r of 10.26 kJ mol^{-1} (0.11 eV). Španěl *et al* (1995b) derived proton affinities of 693.3 kJ mol^{-1} (7.19 eV) and 686.2 kJ mol^{-1} (7.11 eV) by substitution of the derived enthalpies of reaction into Eq. 2.89. Given the uncertainty in reaction mechanism Španěl *et al* (1995b) cite the proton affinity of water as an upper limit to the proton affinity presumably because, neglecting entropy, an efficiency of close to one would be expected if the proton affinity were greater than that of water (assuming non-dissociative proton transfer processes dominate). The proton affinity of cyclohexane was calculated by Španěl *et al* (1995a) by deriving the enthalpy of reaction of CS_2H^+ with cyclohexane from Eq. D.14. This reaction produces $C_6H_{11}^+$ and $C_6H_{13}^+$, it was assumed that $C_6H_{11}^+$ is produced by dissociation of the non-dissociative product and the measured rate of disappearance of reactants was employed in Eq. D.14. The resultant ΔH_r was then inputted into Eq. D.15 (analogous to Eq. 2.89) to derive the proton affinity of cyclohexane.

$$\Delta H_r = PA(CS_2) - PA(c - C_6H_{12}) \qquad \text{(D.15)}$$

Here the possibility of a non-negligible entropy is considered and the rate constants derived from Španěl *et al* (1995b) are input into Eq. 2.90 to derive Gibbs free energy of non-dissociative proton transfer of H_3O^+ and methylcyclohexane. Gas basicities are then derived by substitution of Gibbs free energies of non-dissociative proton transfer into Eq. 2.89 (Table D.10).

The reaction of cyclopropane (C_3H_6) is exothermically and entropically favourable. The Gibbs free energy of cyclopropane reaction with H_3O^+ is -0.64 and the reaction is efficient in SIFT at ~298 K (Table D.10 and D.11). Protonated cyclopropane is cyclic and the reaction does not involve ring opening, (Chong and Franklin, 1972).

The proton affinity of cyclohexane is less than that of water and the reaction with H_3O^+ is endothermic. There is a positive entropy change but the Gibbs free energy is greater than the threshold at which proton transfer reactions generally become efficient (-0.21 eV, Bouchoux 1996), the reaction is inefficient at 298 K (Table D.10 and D.11). It is probable that both products of reaction at 298 K, $C_6H_{13}^+$ and $C_6H_{11}^+$, retain a cyclic structure (Španěl *et al* 1995a, Table D.13).

Španěl *et al* (1995a) derived efficiencies and product distributions for reactions of cyclopropane and cyclohexane with H_3O^+, CS_2H^+, $C_2H_3^+$, $OCSH^+$, HCO^+, CH_5^+, N_2H^+, H_3^+ and ArH^+ at 298 K, with which reaction is increasingly exoergic. Proton transfer to cyclopropane is exothermic from all the reagent ions studied by Španěl *et al* (1995a) and all reactions were efficient. The reactions of cyclohexane with H_3O^+ and CS_2H^+ were inefficient, given the thermokinetic relationship generally observed in proton transfer reactions this suggests the reactions are endothermic, assuming entropy is negligible, as suggested by the revised lower proton affinity of cyclohexane derived by Španěl *et al* (1995a). The reactions of cyclohexane with $C_2H_3^+$, $OCSH^+$, HCO^+, CH_5^+, N_2H^+, H_3^+ and ArH^+ are exothermic using either value of cyclohexane proton affinity and were found to be efficient.

The reaction of H_3O^+ with cyclooctane is exothermic to a similar degree as cyclopropane yet the reaction is inefficient at 298 K. The reaction of methylcyclohexane is close to thermoneutral or slightly exothermic and the reaction is inefficient at 298 K. Considering the proton affinities of Midey *et al* (2003), the entropies of the non-dissociative H_3O^+ proton transfer reactions of cyclooctane and methylcyclohexane must be < -14.8 x 10^{-4} eV K^{-1} if the general thermokinetic relationship of proton transfer applies (i.e. ΔG_r^{Φ} of non-dissociative transfer is >-0.21 eV since the reaction is inefficient). A more significant entropy and or activation energy barrier than generally found in proton transfer reactions (§ 2.6) may exist due to rearrangement of the cyclic compounds. There does not seem to be a large entropy/energy barrier to the reaction of cyclohexane with H_3O^+, however this reaction does not appear to involve ring-opening, less dissociation and re-arrangement occurs than in the reactions of methylcyclohexane and cyclooctane with H_3O^+.

Midey *et al* (2003) measured the efficiencies and product distributions from cyclooctane and methylcyclohexane at 298 K, 400 K and 500 K using VT-SIFT (Table D.12). In a similar manner to the efficiencies of acyclic alkane reactions with H_3O^+ (§ D.1.1, Arnold *et al* 1998) the efficiencies of these cyclic alkane reactions with H_3O^+ decreased with the increase in temperature from 298 K to 400 K and then remained constant (Table D.12). The temperature

dependencies of the rate constants for reaction of H_3O^+ with methylcyclohexane and cyclooctane were $T^{-1.34}$ and $T^{-1.6}$ (smaller than that of the acyclic alkane reaction rate constants, § D.1.1). At 300 K the association product forms 1 % and 30 % of products from the reactions of methylcyclohexane and cyclooctane respectively and is not observed at the higher temperatures (Table D.12). As with the acyclic alkanes the negative temperature dependence of the overall rate possibly arises from the dissociation of the association product ($M.H_3O^+$) back to reactants ($M + H_3O^+$) at the higher temperature and the negative temperature dependence of association reaction rates (Midey *et al* 2003).

The increase in energy in the PTR-MS is similar to the increase in energy resulting from the increase in temperature of SIFT to 400 K and 500 K: $\langle E_r \rangle$ of H_3O^+ with methylcyclohexane at 400 K and 500 K is increased by 0.18 and 0.39 eV respectively relative to at 300 K (Midey *et al* 2003). $\Delta\langle E_r \rangle$ of H_3O^+ with methylcyclohexane in the PTR-MS at *E/N* 120 – 140 Td (T_{dt} 298 K in an air buffer) is 0.28 – 0.42 eV. $\langle E_r \rangle$ of H_3O^+ with cyclooctane at 400 K and 500 K is increased by 0.20 and 0.45 eV respectively relative to at 300 K (Midey *et al* 2003). $\Delta\langle E_r \rangle$ of H_3O^+ with cyclooctane in the PTR-MS at *E/N* 120 – 140 Td (T_{dt} 298 K in an air buffer) is 0.29 – 0.42 eV. Thus, assuming the distribution of the additional energy is not important, the association product of cyclooctane and methylcyclohexane with H_3O^+ is also likely to become increasingly unstable in the PTR-MS under normal operating conditions. Indeed Warneke *et al* (2003) did not observe any association product from the reaction of methylcyclohexane in the PTR-MS at *E/N* of 106 Td. The efficiency of the reactions of cyclooctane and methylcyclohexane are therefore likely to decrease in the PTR-MS relative to SIFT at 298 K as in the VT-SIFT at elevated temperatures. The increased pressure and change in buffer will also affect the rate of the three-body association. At the increased water vapour VMRs in the PTR-MS reverse reactions between the non-dissociative products and water may be increased, if the non-dissociative reactions are endoergic the rate of non-dissociation is also likely to increase in VT-SIFT at elevated temperatures and in PTR-MS. Given the large number of dissociative reactions occurring alongside non-dissociation and the uncertainty in Gibbs free energies of reactions, it is difficult to predict how the overall rate of reaction will vary at energies above those studied in VT-SIFT, i.e. at which the association product is not stable/does not govern the rate of reaction.

As in the reaction of alkenes at thermal energies of SIFT at 298 K the association reaction (Eq. D.5), non-dissociative reaction (Eq. D.6) and dissociation to a carbocation and alkene

(Eq. D.7) are observed from the reactions of un-substituted cycloalkanes with H_3O^+ under thermal conditions of SIFT at ~298 K. The products of dissociation to a carbocation and alkane (Eq.D.8) and dissociation by loss of hydrogen (or hydride transfer), Eq. D.16, are also observed from the reaction of un-substituted cycloalkanes with H_3O^+ at 298 K

$$C_nH_{2n} + H_3O^+ \rightarrow C_nH_{2n-1}^+ + H_2 + H_2O \qquad \text{(D.16)}$$

As with the C_3H_6 alkene, the product of the exothermic non-dissociation reaction, cyclic $C_3H_7^+$ (m/z 43), is the only product of cyclopropane reaction with H_3O^+ in SIFT at 300 K (Table D.11). The reaction of cyclohexane with H_3O^+ produces $C_6H_{13}^+$ (m/z 85) by non-dissociation as in the reaction of hexene but also $C_6H_{11}^+$ (m/z 83) by dissociative loss of hydrogen and/or hydride transfer (Table D.11). The dissociative reaction to produce $C_6H_{11}^+$ from cyclohexane is endothermic by +0.26 to + 1.42 eV depending on the structure of the $C_6H_{11}^+$ ion (Table D.13), the enthalpy of dissociation to $C_6H_{11}^+$ from hexene is -0.58 to +0.58 eV depending on the structure of the $C_6H_{11}^+$ ion. It is possible that a larger energy barrier to dissociation exists to the dissociation of hexene. $\left\langle E_r^{SIFT} \right\rangle$ and /or a positive entropy term may contribute to the dissociative reaction of cyclohexane to form $C_6H_{11}^+$.

As in the reaction of octene at 300 K, cyclooctane reacts with H_3O^+ predominantly by non-dissociation to form $C_8H_{17}^+$ (m/z 113) and dissociation *via* Eq. D.7 to form $C_5H_{11}^+$ (m/z 71). $C_8H_{16}.H_3O^+$ (m/z 131) is also a major product of the exothermic cyclooctane reaction with H_3O^+ whereas the association product is not observed from the exothermic reaction of octene, this is consistent with an entropy/energy barrier associated with ring opening to form $C_8H_{17}^+$ from cyclooctane. Additional minor products are observed from the cyclooctane reaction with H_3O^+ at m/z 69 and m/z 111 corresponding to $C_5H_9^+$ formed by dissociation *via* Eq. 3.34 and $C_8H_{15}^+$ formed by Eq.D.16 (Table D.12). As generally observed in the reaction of alkenes the dissociation reaction where the neutral contains the double bond and $C_5H_{11}^+$ is formed dominates over that in which the cation, $C_5H_9^+$, contains the double bond.

The formation of $C_5H_{11}^+$ is endothermic by 0.46 eV (Table D.13) and assuming entropy is negligible or negative its formation at 298 K suggests dissociation of $C_8H_{17}^+$ is collisional activated as observed in alkane reactions (§ D.1.1, Midey *et al* 2003). Though $\left\langle E_r^{SIFT} \right\rangle$ (Eq. 3.18) is 0.27 eV at 298 K (Midey *et al* 2003) and less than the endothermicity of the dissociation to $C_5H_{11}^+$. Arnold *et al* (1998) observed endothermic dissociation of octane to $C_4H_9^+$ and $C_5H_{11}^+$ 298 K at ~0.60 mbar in helium (§ D.1.1). The endothermic dissociation reaction of octene to form $C_4H_9^+$ has also been observed at 298 K at a slightly higher pressure of 0.93 mbar in helium (Diskin *et al* 2002, § D.1.2) but $C_4H_9^+$ was not observed

from the reaction of cyclooctane (Table D.11). The other product ions from the reaction of cyclooctane and H_3O^+; $C_8H_{17}^+$, $C_8H_{15}^+$, $C_5H_9^+$ are produced by exothermic reactions (Table D.13). The dissociative reaction to form $C_6H_{11}^+$ is also exothermic but this product ion was not observed at 298 K. This may indicate an entropy or energy barrier greater than the sum of the exothermicity of the non-dissociative reaction (0.65 eV) and $\left\langle E_r^{SIFT} \right\rangle$ (0.27 eV) exists (assuming the reaction proceeds *via* the non-dissociative product and that collisional stabilisation and loss of energy in inactive modes such as radiation are negligible). $\left\langle E_r^{SIFT} \right\rangle$ (Eq. 3.18) is insufficient to overcome the endothermicity of other dissociation reactions considered (Table D.13, Midey *et al* 2003).

The reaction of the substituted cycloalkane methylcyclohexane and H_3O^+ at ~ 300 K produces mainly cyclic $C_7H_{13}^+$ (m/z 97) by exothermic elimination of hydrogen (Eq. D.16). The more exothermic non-dissociative reaction product, $C_7H_{15}^+$, is a minor product. Midey *et al* (2003) could not find a stable cyclic structure corresponding to $C_7H_{15}^+$ (m/z 99) and suggest the reaction involves ring opening. The non-dissociative reaction is therefore likely to involve a larger barrier than the elimination of hydrogen. Association forming $C_7H_{14}.H_3O^+$ (m/z 117) and exothermic dissociation to $C_6H_{11}^+$ (m/z 83) by loss of methane have also been observed (Table D.11 and D.12). The enthalpy of the dissociative reaction to form $C_5H_9^+$ is close to zero (Table D.13) and the $\left\langle E_r^{SIFT} \right\rangle$ (Eq. 3.18) of 0.24 eV (Midey *et al* 2003) is sufficient to overcome it yet $C_5H_9^+$ is not observed. Unlike production of $C_6H_{11}^+$ and $C_7H_{13}^+$ the reaction to produce $C_5H_9^+$ involves ring opening and a more significant entropy/energy barrier may exist. $\left\langle E_r^{SIFT} \right\rangle$ (Eq. 3.18) is insufficient to overcome the endothermicity of other dissociation reactions considered (Table D.13, Midey *et al* 2003).

The product distributions from the reaction of H_3O^+ with some cycloalkanes in the PTR-MS have been measured by Warneke *et al* (2003) at the slightly lower normal operating *E/N* of 106 Td and are displayed in Table D.14. Reactions of cycloalkanes with various reagent ions have been measured (Milligan *et al* 2002, Španěl *et al* 1995b) and as well as the VT-SIFT data (Midey *et al* 2003, Table D.12) provide insight into possible products from the cycloalkanes not studied by Warneke *et al* (2003) under the elevated energies of PTR-MS and the product distributions of those studied by Warneke *et al* (2003) at higher *E/N*.

The product distributions from the reaction of cyclopropane with various reagent ions are displayed in Figure D.8 as a function of the change in energy relative to reaction with H_3O^+. The enthalpies of dissociative reactions with H_3O^+ to form $C_3H_5^+$ and $C_2H_3^+$ are shown as

approximations of the energy required for formation; these are similar to the thresholds employed by Španěl *et al* (1995a). The product distributions at an increase in energy relative to reaction with H_3O^+ at 298 K of 0.45 eV correspond to the reaction of cyclopropane with $C_2H_3^+$. The product distributions from this reaction do not conform to the trends generally observed as this reaction appears to proceed *via* more exothermic hydride transfer to form $C_3H_5^+$ and C_2H_4 rather than by dissociative proton transfer to form $C_3H_5^+$, C_2H_2 and H_2 (Španěl *et al* 1995a). Therefore these product distributions are not useful in approximation of product distributions at elevated energies in the PTR-MS and are ignored. The dashed lines indicate the consequent change in product distributions $\Delta\langle E_r \rangle$ of H_3O^+ with cyclopropane in the PTR-MS at *E/N* 120 – 140 Td (T_{dt} 298 K in an air buffer) is 0.25 – 0.37 eV (Figure 3.4), from Figure D.8 this suggests the non-dissociative product at m/z 43 will form > 90 % of the products and $C_3H_5^+$ will form a small percentage of total product ions. However the abundance of $C_3H_5^+$ may not increase linearly from zero as the change in energy relative to reaction with H_3O^+ at 298 K increases above zero as indicated by the dashed line, rather abundance will increase above zero above some threshold at which there is sufficient energy available for reaction. The enthalpy of the dissociation reaction to $C_3H_5^+$ (0.55 eV) is a first approximation of the threshold (Figure D.8). The sum of $KE^r_{c.m.}$ of H_3O^+-cyclopropane (0.18 eV to 0.24 eV, Figure 3.2) and $KE^b_{c.m.}$ (0.16 eV to 0.22 eV, Figure 3.3) is 0.34 eV to 0.46 eV at *E/N* of 120 to 140 Td (T_{dt} 298 K in an air buffer) which is less than the enthalpy of dissociation to $C_3H_5^+$ (0.55 eV). Negative entropy may enable formation of $C_3H_5^+$ at increases in energy less than the enthalpy of the dissociation reaction. However, Warneke *et al* (2003) observed only the non-dissociative product in PTR-MS at *E/N* 106 Td ($\Delta\langle E_r \rangle$ is 0.19 eV if T_{dt} is ~298 K, Figure 3.4). Formation of $C_2H_3^+$ requires an increase in energy of > 2.0 eV (Figure D.8) much greater than $\Delta\langle E_r \rangle$ of H_3O^+ with cyclopropane in the PTR-MS under normal operating conditions.

The extent of cyclopropane dissociation (Figure D.8) is greater than that of propene at elevated energies (Figure D.6). The reactions of propene are less exothermic than those of cyclopropane and the dissociation may be increased due to energy released from the opening of the highly strained cyclopropane ring (Table D.9 and D.13).

Table D.14: The product distributions resulting from the reaction of a series of cyclic alkanes with H_3O^+ in the PTR-MS in synthetic air (Warneke *et al* 2003). P_{dt} denotes drift tube pressure, T_{dt} denotes drift tube temperature, V_{drift} denotes voltage applied to the drift tube and E the resultant electric field strength. Product distributions in Warneke *et al* (2003) were measured in synthetic air.

Cyclic alkane C_nH_{2n}	P_{dt} (mbar)	T_{dt} (K)	V_{drift} (V)	E (Vcm^{-1})	E/N (Td)	Observed Product Distribution: Product Ion (m/z): **Percentage of Product Total** $C_nH_{2n} + H_3O^+ \rightarrow$ $C_nH^+_{2n+1} + H_2O$	$C_iH^+_{2i+1} + C_{n-i}H^+_{2(n-i)} + H_2O$
Cyclopropane C_3H_6	2.4	NS	NS	NS	106	$C_3H_7^+$ (43): **100**	
Cyclopentane C_5H_{10}	2.4	NS	NS	NS	106	$C_5H_{11}^+$ (71): **100**	
Methylcyclopentane C_6H_{12}	2.4	NS	NS	NS	106	$C_6H_{13}^+$ (85): **100**	
Methylcyclohexane C_7H_{14}	2.4	NS	NS	NS	106	$C_7H_{15}^+$ (99): **14**	$C_4H_9^+$ (57): **86**

Similar fragmentation patterns are observed in EI-MS of cyclopropane to those in high energy proton transfer reactions of cyclopropane. The parent ion forms 25.9 % of the product ions from EI-MS of cyclopropane, $C_3H_5^+$ 22.9 %, $C_2H_3^+$ 9.0 %, at the higher energies $C_3H_3^+$ is also observed (17.3 %) and minor product ions form 24.9 % of the signal (Mallard and Linstrom 2005). No such dissociation is expected at the lower energies in normally operated PTR-MS.

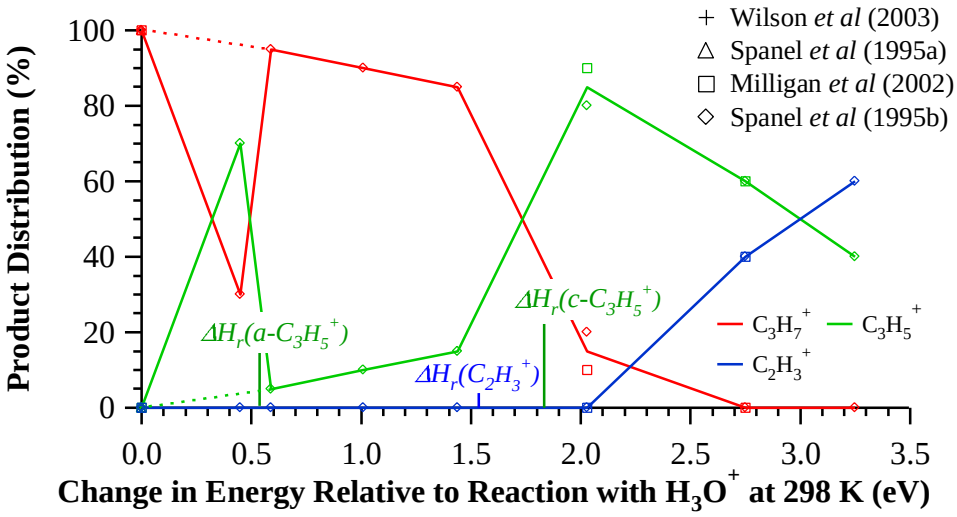

Figure D.8: Product distributions resulting from the reaction of cyclopropane with H_3O^+ (Wilson *et al* 2003, Milligan *et al* 2002, Španěl *et al* 1995a,b), CS_2H^+, $C_2H_3^+$, $OCSH^+$, HCO^+, CH_5^+, N_2H^+, H_3^+ and ArH^+ in SIFT at 298 K in helium carrier gas (Milligan *et al* 2002, Španěl *et al* 1995a). The change in energy relative to reaction with H_3O^+ is the difference in gas basicities of H_3O^+ and the reagent ion neutral (H_2O, CS_2, C_2H_2, OCS, CO, CH_4, N_2, H_2 and Ar). ΔH_r (F^+) denotes the standard enthalpy of the reaction of H_3O^+ with cyclopropane to form the fragment, F^+. ΔH_r (F^+) is an indication of the energy required for the abundance of F^+ to increase above zero. *a* denotes that the value of ΔH_r (F^+) corresponds to allyl F^+, *c* denotes that the value corresponds to cyclic F^+. Values of ΔH_r (F^+) are taken from Milligan *et al* 2002 (Table D.13).

The product distributions from the reactions of cyclohexane with various reagent ions are displayed in Figure D.9. Product distributions are given as a function of change in energy relative to reaction with H_3O^+ at ~298 K. As in the reaction of cyclopropane the product distributions from the reaction of $C_2H_3^+$ do not follow the general trends. It is suggested that $C_6H_{11}^+$ is formed from $C_2H_3^+$ by direct hydride transfer producing C_2H_4 as opposed to C_2H_2 + H_2 by dissociative proton transfer which is less exothermic (Španěl *et al* 1995a). Therefore these product distributions are neglected in approximation of product distributions at elevated energies in the PTR-MS the dashed lines indicate the consequent of change in product distributions.

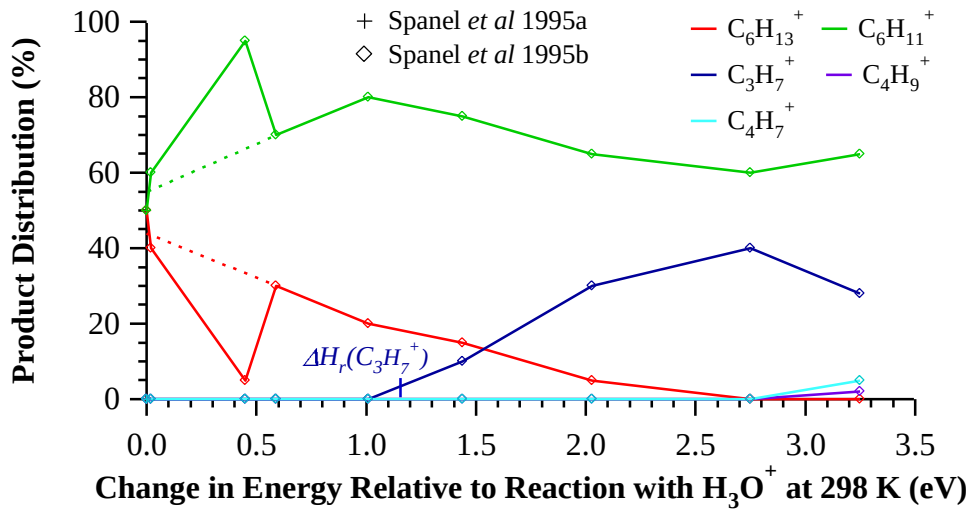

Figure D.9: Product distributions resulting from the reaction of cyclohexane with H_3O^+, CS_2H^+, $C_2H_3^+$, $OCSH^+$, HCO^+, CH_5^+, N_2H^+, H_3^+ and ArH^+ in SIFT at 298 K in helium carrier gas (Španěl *et al* 1995 a,b). The change in energy relative to reaction with H_3O^+ is the difference in gas basicities of H_3O^+ and the reagent ion neutral (H_2O, CS_2, C_2H_2, OCS, CO, CH_4, N_2, H_2 and Ar). ΔH_r $(C_3H_7^+)$ denotes the standard enthalpy of the reaction of H_3O^+ with cyclohexane to form the fragment, $C_3H_7^+$. ΔH_r $(C_3H_7^+)$ is an indication of the energy required for the abundance of $C_3H_7^+$ to increase above zero and was derived from the analogous threshold in Španěl *et al* 1995a (Table D.13).

$\Delta\langle E_r \rangle$ of H_3O^+ with cyclohexane in the PTR-MS at *E/N* 120 – 140 Td (T_{dt} 298 K in an air buffer) is 0.28 – 0.41 eV (Figure 3.4). From Figure D.9 this suggests the non-dissociative product, $C_6H_{13}^+$ (m/z 85) will form ~ 35 % of the products and $C_6H_{11}^+$ (m/z 83) will form ~ 65 % (Mallard and Linstrom 2005). Production of $C_3H_7^+$ is unlikely at the energies in normally operated PTR-MS.

$C_6H_{11}^+$ and $C_3H_7^+$ form only 2.9 % and 0.9 % of products from EI-MS of cyclohexane, the parent ion forms 14.6 %. At the increased energy in EI-MS additional fragments are observed at m/z 69 ($C_5H_9^+$, 4.6 %), m/z 56 (20.7 %), m/z 41 ($C_3H_5^+$, 14.0 %) and m/z 27 ($C_2H_3^+$, 6.2 %) (Mallard and Linstrom 2005), this level of dissociation is not expected in the PTR-MS.

The product distributions from the reaction of cyclooctane with H_3O^+ at 298 K, 400 K and 500 K as a function of the increase in energy relative to reaction of H_3O^+ at 298 K are given in Figure D.10. $\Delta\langle E_r \rangle$ of H_3O^+ with cyclooctane in the PTR-MS at *E/N* 120 – 140 Td (T_{dt} 298 K in an air buffer) is 0.29 – 0.42 eV (Figure D.10) similar to the increase in energy in VT-SIFT at 400 and 500 K (Figure D.10). Therefore, as in VT-SIFT the associative product is not expected in normally operated PTR-MS and the non-dissociative product abundance is expected to decrease to 0-20 %, the increase in pressure and buffer may also contribute. At 500 K in VT-SIFT dissociation to $C_5H_{11}^+$ (m/z 71) and $C_4H_9^+$ (m/z 85) and small alkanes

dominate, with a large number of other dissociation products each less than 10 % of the total product ions. These product ions may therefore be expected in PTR-MS, however given the possible role of collisional activation, i.e. a third-body in these endothermic dissociation reactions, the increase in pressure and buffer are likely to affect the distributions as well as the energy in the drift tube.

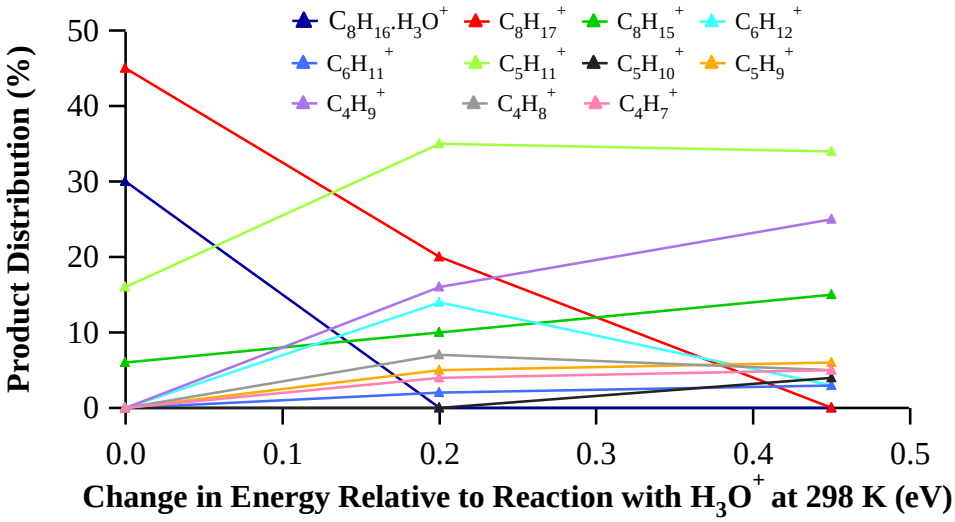

Figure D.10: Product distributions resulting from reaction of H_3O^+ with cyclooctane at 298 K, 400 K and 500 K (Midey *et al* 2003). Product distributions are given as a function of the change in energy relative to reaction with H_3O^+ at 298 K. The change in energy relative to reaction with H_3O^+ at 298 K is the increase in $\langle E_r^{SIFT} \rangle$ (Eq. 3.18) at the elevated temperature relative to 298 K. Values of $\langle E_r^{SIFT} \rangle$ at 298 K, 400 K and 500 K were taken from Midey *et al* (2003).

In EI-MS of cyclooctane a larger number of dissociation pathways are accessible, $C_4H_9^+$ (m/z 57) and $C_5H_{11}^+$ (m/z 71) form 1.9 % and 1.0 % of the product ions and $C_8H_{15}^+$ is not observed. Other product ions include m/z 27, 29, 39, 41, 42, 43, 55, 56, 67, 68, 69, 70, 82, 83, 84 and 97 (Mallard and Linstrom 2005) These product ions are not expected under the reduced energies of PTR-MS.

The product distributions from reaction of methylcyclohexane as a function of increase in energy relative to reaction at 298 K are shown in Figure D.11. $\Delta\langle E_r \rangle$ of H_3O^+ with methylcyclohexane in the PTR-MS at *E/N* 120 – 140 Td (T_{dt} 298 K in an air buffer) is 0.28 – 0.42 eV (Figure 3.4). The dominant product at this increase in energy in Figure D.10 is $C_7H_{13}^+$ ~70 % (m/z 97), other products are $C_7H_{15}^+$ (m/z 99), $C_4H_9^+$ (m/z 57) and $C_6H_{11}^+$ (m/z 83). However Warneke *et al* (2003) observed predominantly $C_4H_9^+$ (m/z 57) in the PTR-MS at *E/N* 106 Td $C_7H_{15}^+$ (m/z 99) was a minor product (Table D.14). These differences may be

due to a role of buffer molecules and differences in pressure and the of nature buffer in the PTR-MS compared to (VT-)SIFT.

The product distributions from cyclopentane in PTR-MS at *E/N* 106 Td ($\Delta\langle E_r \rangle$ 0.20 eV at T_{dt} ~ 298 K in air) were measured by Warneke *et al* (2003), the non-dissociative product was the only observed product ion (Table D.14). The proton affinity of cyclopentane and the efficiency of its reaction with H_3O^+ are unknown. The results of Warneke *et al* (2003) demonstrate that the rate is sufficient for the product ion to contribute to PTR-MS spectra. C_5H_{10} alkenes react with H_3O^+ dissociatively to form $C_3H_7^+$ (~20%) in the PTR-MS at *E/N* of 106 Td, the analogous reaction of cyclopentane is 0.36 to 0.58 eV more endothermic. Comparison with other cycloalkanes may suggest some elimination of hydrogen at the increased energies of normally operated PTR-MS. The production of $C_5H_9^+$ from the reaction of cyclopentane and H_3O^+ is endothermic by ~ 0.36 to 0.89 eV depending on the structure of $C_4H_9^+$ (Table D.13), the $\Delta\langle E_r \rangle$ of H_3O^+ with cyclopentane in the PTR-MS at *E/N* 140 Td (T_{dt} 298 K in an air buffer) is 0.40 eV (Figure 3.4), and is sufficient to overcome the endothermicity of the reaction to form $C_4H_9^+$. In EI-MS the dominant ions from cyclopentane are the parent ion (m/z 70), $C_4H_7^+$ (m/z 55), $C_3H_5^+$ (m/z 41), $C_3H_3^+$ (m/z 39) and $C_2H_3^+$ (m/z 27) and m/z 42 (Mallard and Linstrom 2005). The production of $C_4H_7^+$, $C_3H_5^+$ and $C_2H_3^+$ ions from reaction of cyclopentane with H_3O^+ are endothermic by > 0.64 eV and on this basis are unlikely in normally operated PTR-MS. However from the (VT)SIFT data it is apparent that energy barriers, entropy and/or buffer molecules and pressure are important in many reactions of cycloalkanes and product distributions can not be hypothesized from enthalpies and energies available ($\langle E_r \rangle$) alone. Not all structures of the $C_nH_{2n+1}^+$ and $C_iH_{2i-1}^+$ ions have been considered here (Table D.12) and other structures may result in more favourable enthalpies of dissociation.

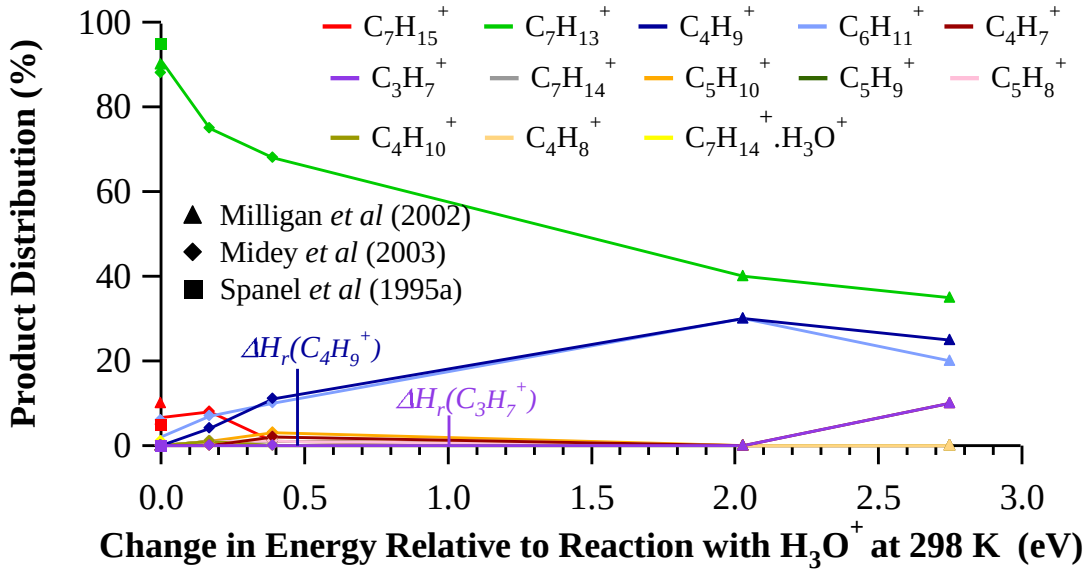

Figure D.11: Product distributions resulting from the reaction of H_3O^+ with methylcyclohexane at 298 K, 400 K and 500 K (Midey *et al* 2003). The change in energy relative to reaction with H_3O^+ at 298 K is the increase in $\left\langle E_r^{SIFT} \right\rangle$ (Eq. 3.18) at the elevated temperature relative to 298 K. Values of $\left\langle E_r^{SIFT} \right\rangle$ at 298 K, 400 K and 500 K were taken from Midey *et al* (2003). Product distributions resulting from reaction of methylcyclohexane with N_2H^+ and H_3^+ (Milligan *et al* 2002) are also shown. In this case the change in energy relative to reaction at 298 K is *GB(H_2O) –GB(reagent ion neutral)* and is 2.03 and 2.75 eV respectively. ΔH_r *(F^+)* denotes the standard enthalpy of the reaction of H_3O^+ with methylcyclohexane to form the fragment, F^+. ΔH_r *(F^+)* is an indication of the energy required for the abundance of F^+ to increase above zero. In EI-MS of methylcyclohexane the parent ion forms 7.7 % of product ions, $C_6H_{11}^+$ forms 21.0 %, $C_6H_{13}^+$ forms 0.6 %, $C_4H_9^+$ forms 1.0 % and $C_3H_7^+$ forms 1.4 %, a number of other fragments are formed (Mallard and Linstrom 2005). $C_iH_{2i-1}^+$ ions pre-dominate over $C_iH_{2i+1}^+$ ions in EI-MS of the cycloalkanes as in the EI-MS of alkenes.

The product distributions from methylcyclopentane have also been measured in the PTR-MS at *E/N* of 106 Td (Warneke *et al* 2003), only the non-dissociative reaction occurs (Table D.14). The proton affinity of methylcyclopentane and the efficiency of its reaction with H_3O^+ are unknown; evidently the rate is sufficient for product ions to contribute to PTR-MS spectra. In EI-MS the dominant product ions from methylcyclopentane are the parent ion at m/z 84, $C_5H_9^+$ (m/z 69), $C_4H_7^+$ (m/z 55), $C_3H_5^+$ (m/z 41), $C_2H_3^+$ (m/z 27) and m/z 42 and 56. Dissociation reactions of cyclopentane with H_3O^+ to form $C_4H_7^+$, $C_3H_5^+$, $C_2H_3^+$ are endothermic by > 0.86 eV (for the $C_iH_{2i-1}^+$ structures considered here) which is greater than the sum of $KE_{c.m.}^r$ of H_3O^+-methylcyclopentane (0.20 eV to 0.28 eV, Figure 3.2) and $KE_{c.m.}^b$ (0.16 eV to 0.22 eV Figure 3.3) at *E/N* of 120 to 140 Td in air at 298 K. The standard enthalpy of production of $C_5H_9^+$ from methylcyclopentane and H_3O^+ calculated here is -0.098 to +0.43 eV, depending on the structure of $C_5H_9^+$. However, as discussed, production of $C_5H_9^+$ from methylcyclohexane is close to thermoneutral (neglecting entropy) and less

than $\left\langle E_r^{SIFT} \right\rangle$ (Eq. 3.18) yet it is not observed at >1 %, although $C_5H_9^+$ formed from methylcyclopentane could retain the cyclic structure. Unlike methylcyclohexane, methylcyclopentane does not react dissociatively with H_3O^+ by elimination of hydrogen to form $C_6H_{11}^+$.

Jobson *et al* (2005) measured product distributions from butylcyclohexane ($C_{10}H_{20}$) at *E/N* of 150 Td, P_{dt} 2.4 mbar, T_{dt} 323 K and therefore *E* ~70 V cm^{-1}. Specific product distributions were not given but the dominant product was $C_6H_{11}^+$ (m/z 83) formed by loss of C_4H_{10} from the non-dissociative product. $C_6H_{11}^+$ is also the dominant peak (25.4 %) in EI-MS of butylcyclohexane (Mallard and Linstrom 2005). Significant peaks were also observed at m/z 57 ($C_4H_9^+$), m/z 97 ($C_7H_{13}^+$) and m/z 137 ($C_{10}H_{17}^+$) in the PMS, the production of which could occur without ring breakin TR-g. In EI-MS other significant peaks occur at m/z 41 ($C_3H_5^+$, 7.0 %), m/z 55 ($C_4H_7^+$, 15.8 %), m/z 67 ($C_5H_7^+$, 3.7 %) and m/z 82 (15.1 %), these fragments are not observed at the lower energies of PTR-MS.

D.1.5. Dienes and Diyenes

The gas basicities and proton affinities of various dienes and diyenes are shown in Table D.15, all are greater than those of water and the non-dissociative reactions with H_3O^+ are exothermic and exoergic. Product distributions and reaction efficiencies measured in the SIFT are reviewed in Table D.16. The product distributions of H_3O^+ reaction with a selection of dienes have been measured in the PTR-MS and are collated in Table D.17.

Table D.15: A compilation of proton affinities (*PA*), gas basicities (*GB*), potential standard enthalpy (ΔH_r^Φ), potential standard entropy (ΔS_r^Φ) and Gibbs free energies (ΔG_r^Φ) of the non-dissociative H_3O^+ reaction with dienes and diyenes. Proton affinities and gas basicities are taken from Hunter and Lias, (1998). ΔG_r^Φ and ΔH_r^Φ are calculated from Eq. 2.88 and 2.89, ΔS_r^Φ are calculated from $\Delta S_r^\Phi = \left(\Delta H_r^\Phi - \Delta G_r^\Phi\right)/T$.

Compound	*PA* (eV)	*GB* (eV)	ΔH_r^Φ (eV)	ΔS_r^Φ (x 10^{-4} eV K^{-1})	ΔG_r^Φ (eV)
Conjugated dienes:					
1,3 Butadiene	8.12	7.85	-0.96	1.81	-1.01
2-methyl-1,3-butadiene (Isoprene)	8.56	8.27	-1.40	0.77	-1.43
Cumulated dienes:					
Propan-1,2-diene	8.04	7.73	-0.87	0.52	-0.89
1,2 Butadiene	8.07	7.77	-0.91	0.66	-0.93
Diyenes:					
Butadiyne	7.64	7.39	-0.48	2.30	-0.55

Table D.16: Available reaction efficiencies and product distributions resulting from the reaction of H_3O^+ with dienes and diyenes in SIFT at ~298 K. P_{FT} denotes pressure in the flow tube, T_{FT} denotes temperature in the flow tube. k_m denotes the rate constant measured for the reaction of H_3O^+ with the diene or diyene. k_c refers to the collisional rate constant (§ 2.4.1), k_L indicates that the collisional rate constant was derived from Langevin, Gioumousis, Stevenson theory (§ 2.4.1.2, Eq. 2.34) in the cited reference. k_{SC} indicates the collisional rate constant was derived using the results of Su and Chesnavich trajectory calculations (§ 2.4.1.4, Eq. 2.49 – 2.54) in the cited reference. * indicates that the method of k_{coll} is not specified in the reference however since the dipoles of the dienes and diyenes are relatively small all rate constant calculation theories will yield a value close to k_L. k_m/k_c is the reaction efficiency (§ 2.9). δ_{k_c} denotes estimated uncertainty of the calculated collisional rate constant, δ_{k_m} denotes the estimated uncertainty of the measured rate constant. A helium carrier gas was used in all of the studies small amounts of air were added in some cases; Wang *et al* (2004a) and Španěl and Smith (1998) diluted neutral vapours using air, the dilution gas used by Španěl *et al* (1995b) was unspecified. Wilson *et al* (2003) added moist air to the flow tube. Milligan *et al* (2002) used helium alone in the flow tube, the helium was passed through a liquid nitrogen cooled zeolite resulting in a typical water vapour VMR of 150 ppb. Humidity was not specified by Španěl and Smith (1998) or Wilson *et al* (2003) though water vapour was present. Wang *et al* (2004a) performed measurements with dry air, lab air (RH 1.5 %) and humid air (RH ~6 %) (diluting the neutral vapours) no formation of $C_6H_{11}^+$ hydrates were observed in the presence of water. Humidity was not specified by Španěl *et al* (1995b).Lindinger *et al* (1998) specify measured thermal rate constants, measurement conditions are not specified.

Compound	P_{FT} (mbar)	T_{FT} (K)	k_m (x 10^{-9} m^3 s^{-1})	k_m/k_c	k_c	δ_{k_c} (%)	δ_{k_m} (%)	Observed Product Distribution : Product Ion (m/z): **Percentage of Product Total**, $R + H_3O^+ \rightarrow RH^+ + H_2O$	Reference
2-methyl-1,3-butadiene /Isoprene	[a]0.67 [b]0.67 [c]NS	[a]N/O [b]300 [c]NS	[a]2.0 [b]2.0 [c]1.3	[a]1.0 [b]1.1 [c]0.65	[a]k_{SC} [b]k_{SC} [c]k_L*	[a]20		$C_5H_9^+$ (69): [a]**100** $C_5H_9^+$ (69): [b]**100**	[a]Španěl and Smith (1998) [b]Španěl *et al* (1995b) [c]Lindinger *et al* (1998)
4-methyl-1,3-pentadiene	0.9	296 - 300						$C_6H_{11}^+$ (83): **100**	Wang *et al* (2004a)
Propan-1,2-diene /Allene	[c]0.61 [d]0.64	[c]298 [d]300±5	[c]1.4 [d]1.4	[c]0.88 [d]1.0	[c]k_L* [d]k_{SC}		[d]15	$C_3H_5^+$ (41): **100** $C_3H_5^+$ (41): **100**	Wilson *et al* (2003) Milligan *et al* (2002)
Butadiyne/ Diacetylene	0.61	298	1.6	0.89	k_L*			$C_4H_3^+$ (51): **100**	Wilson *et al* (2003)

Table D.17 The product distributions resulting from the reaction of a series of dienes with H_3O^+ in the PTR-MS. **E* was not specified in reference but to give the stated *E/N* of ~120 Td at the given P_{dt} of 2.00 mbar and T_{dt} of 313 K *E* must be approximately 55.5 V cm^{-1}. l_{dt} of ~ 10 cm was derived from the given *t* of 110 µs and *E/N* of 120 Td giving V_{drift} ~ 555 V ** Specific values of, P_{dt} and T_{dt} during the measurements of 2-methyl-1, 3-butadiene dissociation were not given, however a P_{dt} of 1.8 - 2.1 mbar and a temperature of 303 – 333 K was specified for measurements within the reference. The length of the drift tube was not specified, but a high sensitivity Ionicon Analytik PTR-MS was employed so a drift tube length of 9.5 cm is assumed, V_{drift} was specified. Thus given this temperature and pressure range and l_{dt} at [di]a V_{drift} of 580 V *E/N* would have been somewhere between ~122 and 156 Td at [dii]a V_{drift} of 380 V *E/N* would have been somewhere between ~67 and 86 Td. Distributions from Malekina *et al* (2007) are given as relative abundancies with the most abundant m/z normalised to 100 in reference and have been converted to percentage distributions here and are specified to one decimal place. Product distributions in Warneke *et al* (2003) were measured in synthetic air (humidity not specified), in Malekina *et al* (2007) product distributions were measured in laboratory air. Measurements by Lindinger *et al* (1998) are assumed to be made in PTR-MS, measurement conditions are not specified. The percentage abundancies of m/z 69 and m/z 39 from Malekina *et al* 2007 were calculated assuming m/z 39 and m/z 69 were the only observed product ions. The specified realtive abundancies were [i] (*E/N* 122 -156 Td) 7 at m/z 69 and [ii] (*E/N* 67-68 Td) less than 1 at m/z 39.

Diene (C_nH_{2n-2})	P_{dt} (mbar)	T_{dt} (K)	V_{drift} (V)	E (V cm^{-1})	E/N (Td)	Observed Product Distribution: Product Ion , (m/z): **Percentage of Product Total** $C_nH_{2n-2} + H_3O^+ \rightarrow$ $C_nH^+_{2n-1} + H_2O$	$C_iH^+_{2i-1} + C_{n-i}H_{2(n-i)} + H_2O$	$C_iH^+_{2i-3} + C_{n-i}H_{2(n-i)+2} + H_2O$	Reference
1,3 Butadiene (C_4H_6)	2.4	NS	NS	NS	106	$C_4H_7^+$ (55): **100**			Warneke *et al* (2003)
2-methyl-1,3-butadiene /Isoprene (C_5H_8)	[a]2.4 [b]~2.00 [c]2.00 [di, ii]1.8 - 2.1 [e]NS	[a]NS [b]~303 – 312 [c]313 [di, ii] 303 – 333 [e]NS	[a]NS [b]600 [c]555* [di]580 [dii]380 [e]NS	[a]NS [b]63.2 [c]55.5* [di]~61 [dii]~40 [e]NS	[a]106 [b]~130 [c]~120 [di]122 – 156 [dii]67 – 86 [e]NS	$C_5H_9^+$ (69) **[a]100** **[b]84±2** **[c]80** **[di]~6.5** **[dii]>99.01** **[e]100**	$C_3H_5^+$, (41) **[b]16±2** **[c]20**	$C_3H_3^+$ (39) **[di]~93.5** **[dii]<0.99**	[a]Warneke *et al* (2003) [b]Ammann *et al* (2004) [c]Karl *et al* (2007) [d]Malekina *et al* (2007)** [e]Lindinger *et al* (1998)
1,3 Hexadiene (C_6H_{10})	2.4	NS	NS	NS	106	$C_6H_{11}^+$ (83): **100**			Warneke *et al* (2003)
1,2 Butadiene (C_4H_6)	2.4	NS	NS	NS	106	$C_4H_7^+$ (55): **100**			Warneke *et al* (2003)

In SIFT the reactions all proceed at the collisional rate following the general correlation of Gibbs free energy of non-dissociative reaction and efficiency observed in proton transfer reactions (§ 2.9). The non-dissociative products are the only products observed from reaction of H_3O^+ with all of the reviewed dienes and diyene in SIFT at 298 K. All of the dienes except 2-methyl-1,3-butadiene (isoprene, C_5H_8) form only the non-dissociative protonated diene as in SIFT at 298 K.

The products of reaction of 2-methyl-1,3-butadiene with H_3O^+ in the PTR-MS are uncertain (Table D.17). Measurement of 2-methyl-1, 3-butadiene is of interest to the atmospheric (e.g. Fall 1999, Guenther *et al* 2006) and medical community (Lindinger *et al* 1998, Španěl *et al* 1999). Guenther *et al* (1995) estimated a global annual emission of 2-methyl-1,3-butadiene of 175 to 503 Tg carbon. In the decade since this estimate, a vast of number emission rate measurements have been performed and eddy covariance based flux measurements of 2-methyl-1,3-butadiene have become possible (e.g. Guenther and Hills 1998, Bowling *et al* 1998, Karl *et al* 2002b, Sprig *et al* 2005, Graus *et al* 2006, Kuhn *et al* 2007) alongside previously used enclosure methods. A large volume of research into the controlling factors behind 2-methyl-1,3-butadiene emission has also been carried out (Sharkey and Yeh 2001, Sharkey *et al* 2008). A number of studies of emissions in tropical regions, a large source of 2-methyl-1, 3-butadiene previously poorly characterised, have also been performed (e.g. Warneke *et al* 2001a, Holzinger *et al* 2002, Kuhn *et al* 2007).

Recent estimates from the Model of Emissions of Gases and Aerosols from Nature (MEGAN) place the (biogenic) annual global 2-methyl-1,3-butadiene emission at 500 to 750 Tg (440 to 660 Tg carbon) (Guenther *et al* 2006). A number of studies of emissions in tropical regions, a large source of 2-methyl-1, 3-butadiene previously poorly characterised, have also been performed (e.g. Warneke *et al* 2001a, Holzinger *et al* 2002, Kuhn *et al* 2007). Recent estimates from the Model of Emissions of Gases and Aerosols from Nature (MEGAN) place the (biogenic) annual global 2-methyl-1,3-butadiene emission at 500 to 750 Tg (440 to 660 Tg carbon) (Guenther *et al* 2006).

Terrestrial plants including trees, shrubs and crops are thought to emit >90 % of atmospheric 2-methyl-1,3-butadiene (Guenther *et al* 2006) and a large number of databases detailing emissions measured from various species are available, see for example, http://www.es.lancs.ac.uk/cnhgroup/download.html and http://www.bvoc.acd.ucar.edu. Phytoplankton blooms also emit 2-methyl-1,3-butadiene and an oceanic source of 0.1 -1.4 Tg yr^{-1} is estimated (Sinha *et al* 2007 and references therein). Soil microbes (Fall and Copley 2000) and animals including humans (Lindinger *et al* 1998, Španěl *et al* 1999) also

emit 2-methyl-1,3-butadiene. Emission from vegetation is strongly light and temperature dependent suggesting a photosynthetic link. 2-Methyl-1,3-butadiene synthesis in plants involves the conversion of a number of molecules of adenosine triphosphate (ATP) to adenosine diphosphate (ADP) using the -30 kJ mol^{-1} of Gibbs free energy released in each conversion (Sharkey and Yeh 2001, Lodish *et al* 1999). This expansion of energy in 2-methyl-1,3-butadiene synthesis suggests 2-methyl-1,3-butadiene has an important beneficial function. Researchers hypothesise that 2-methyl-1,3-butadiene production helps plants to survive rapid temperature changes and provides tolerance to reactive oxygen species such as ozone (Sharkey and Yeh 2001, Sharkey *et al* 2008). The pathways and mechanisms of control of 2-methyl-1, 3-butadiene emission are not completely understood and research is ongoing (e.g. Karl *et al* 2002a, Kreuzweiser *et al* 2002, Sharkey *et al* 2008).

2-methyl-1,3-butadiene has also been observed in the troposphere of urban and semi-urban areas using GC and PTR-MS (e.g. Kato *et al*, 2004, Filella *et al* 2006, Kuster *et al* 2004) this may be as a result of vegetation within the city and/or an anthropogenic source. 2-Methyl-1,3-butadiene is a known product of gasoline combustion (McLaren *et al* 1996) and is typically ~0.04 % of the total non-methane volatile organic compound (NMVOC) emissions from vehicles giving an estimated emission rate of 0.01 Tg based on 1992 emission rates of NMVOCs from vehicles (Guenther 1999). 2-Methyl-1,3-butadiene is also used in industrial production of rubber.

2-methyl-1, 3-butadiene is highly reactive in the troposphere. The rate constant for reaction with *OH* at 298 K is 10.4 ± 1.9 cm^3 $molecule^{-1}$ s^{-1} and the Arrhenius expression is k= (2.33±0.09) $x10^{-11}$exp [(444± 27)/T] giving a rate constant of ~1.16 x 10^{-11} cm^3 $molecule^{-1}$ s^{-1} at 277 K and a lifetime with respect to *OH* of ~2.9 h (at an average OH concentration of 8.1 ± 0.9 x 10^5 molecules cm^{-3} (Singh *et al* 2007). The reaction of 2-methyl-1,3-butadiene accounts for nearly 30 % of the *OH* removal rate (Choung and Stevens 2002). The lifetime with respect to NO_3 at a 12 h night time average concentration of 5 x 10^8 molecules cm^{-3} is 1.6 h and with respect to O_3 at a 24 h average concentration of 7 x 10^{11} molecules cm^{-3} is 1.3 days (Atkinson and Arey 1998). The major products of 2-methyl-1,3-butadiene oxidation are methyl vinyl ketone (MVK), methacrolein (MACR), 3-methylfuran and organic nitrates, methanal is also produced in the case of NO_3 and O_3 oxidation (Atkinson and Arey 1998). In addition to the affect on the oxidizing capacity of the troposphere 2-methyl-1,3-butadiene oxidation thus contributes to formation of longer living nitrogen containing compounds such as MPAN through reaction of these products as well as ozone formation in the presence of NO_x. There is evidence that 2-methyl-1,3-butadiene contributes to secondary organic aerosol (SOA) formation in low (Claeys *et al* 2004) and high (Kroll *et al* 2005) NO_x conditions.

PTR-MS measurements (alongside aerosol analysis) under high NO_x in SMOG chambers and in ambient air indicate that second generation products of 2-methyl-1,3-butadiene oxidation at m/z 45, 47, 61, 73, 75, 101, 113, 115 and 129 contribute to SOA yields of ~2 % (e.g. Ng *et al* 2006, Lee *et al* 2006, Holzinger *et al* 2007, Kleindienst *et al* 2007). The following possible compounds have been attributed to these m/z; m/z 45 acetaldehyde, m/z 47 methanoic acid, m/z 61 ethanoic acid and/or glycoaldehyde, m/z 73 methylglyoxal, m/z 75 hydroxyacetone and/or propionic acid and m/z 101 C_5 hydroxycarbonyls (Williams *et al* 2001, Warneke *et al* 2001a, Lee *et al* 2006, Holzinger *et al* 2007)

The importance of 2-methyl-1,3-butadiene in the troposphere has led to a large number of examples of the measurement of 2-methyl-1,3-butadiene using PTR-MS (e.g. Warneke *et al* 2001a, Sprig *et al* 2005, Graus *et al* 2006, Sinha *et al* 2007 etc.), the majority of these studies have considered count rates at the protonated m/z 69 alone. Warneke *et al* (2003) observed only the protonated non-dissociative product at m/z 69 (Table D.17), however the *E/N* of 106 Td (P_{dt} 2.04 mbar) employed is lower than the normally utilised *E/N* of 120 – 140 Td in the PTR-MS which corresponds to a further increase in $\langle E_r \rangle$ of 0.09 - 0.22 eV (Figure 3.4).

Ammann *et al* (2004) measured product distributions at *E/N* of ~130 Td, P_{dt} of ~ 2.0 mbar and T_{dt} of ~ 303 – 312 K (Table D.14) and report 16 % fragmentation to m/z 41 ($C_3H_5^+$) (Table D.17). Similarly Karl *et al* (2007) observed 20 % dissociation to m/z 41 at *E/N* of ~120 Td, P_{dt} 2.00 mbar and T_{dt} 313 K (Table D.17). The reaction of 2-methyl-1,3-butadiene with H_3O^+ to form $C_3H_5^+$ at m/z 41 (+ C_2H_4 + H_2O) is endothermic: Employing an enthalpy of formation of $C_3H_5^+$ of 10.12 eV to 10.32 eV calculated from the appearance energy for formation of $C_3H_5^+$ from 2-methyl-1,3-butadiene (Mallard and Linstrom 2005) gives an enthalpy of reaction of 1.12 eV to 1.32 eV. Utilising the enthalpy of formation of H^+ with the proton affinity and enthalpy of formation of propyne gives an enthalpy of formation of $C_3H_5^+$ of 10.09 eV and resultant enthalpy of reaction of 1.09 eV. Using the enthalpy of formation of H^+ with the proton affinity and enthalpy of formation of cyclopropene gives an enthalpy of formation of $C_3H_5^+$ of 10.31 eV and resultant enthalpy of reaction of 1.31 eV. Lias *et al* (1988) cite enthalpies of formation of $C_3H_5^+$ of 9.80 eV and 10.04 eV from *AE* measurements from $CH_2CH{=}CH_2$ and CH_3CCH_3 respectively resulting in enthalpies of reaction of 0.80 eV and 1.04 eV respectively. At *E/N* 120 -140 Td (T_{dt} 298 K, air buffer) $\Delta\langle E_r \rangle$ is 0.27 eV to 0.40 eV. The sum of $KE^r_{c.m.}$ of H_3O^+-C_5H_8 (0.20 eV to 0.27 eV, Figure 3.2) and $KE^b_{c.m.}$ (0.16 eV to 0.22 eV Figure 3.3) is 0.36 eV to 0.49 eV at *E/N* of 120 to 140 Td in air at 298 K. This suggests that a further ~ 0.31 to 0.83 eV (depending on the

enthalpy of dissociation) above the sum of $KE^{r}_{c.m.}$ and $KE^{b}_{c.m.}$ at 140 Td is required to overcome the endothermicity of dissociation (0.80 to 1.32 eV). If this energy comes from entropy alone, this suggests a relatively large entropy change of + 10.40 x 10^{-4} eV K^{-1} to + 27.83 x 10^{-4} eV K^{-1}. The role of buffer molecules and pressure is unknown.

Malekina *et al* (2007) investigated the fragmentation of 2-methyl-1, 3-butadiene as a function of V_{drift} and observed varying degrees of dissociation to m/z 39 ($C_3H_3^+$) (Table D.17). Unfortunately the *E/N* during measurements within this reference was not specified. Specific values of, P_{dt} and T_{dt} during the measurements of 2-methyl-1, 3-butadiene dissociation were not given, however all measurements within the reference were performed at a P_{dt} of 1.8 - 2.1 mbar and a temperature of 303 – 333 K. The length of the drift tube in the PTR-MS was not specified. A high sensitivity Ionicon Analytik PTR-MS was employed and a drift tube length of 9.5 cm is assumed. Therefore the distributions at a V_{drift} of 380 V correspond to an *E/N* in the range 67 – 86 Td, those at a V_{drift} of 580 V correspond to an *E/N* in the range of 122 – 156 Td. At a V_{drift} of 380 V the dissociation product at m/z 39 formed ~ < 1 % (specified relative abundance < 1) of the total products. At a V_{drift} of 580 V the dissociated product formed 93.5 % of the total products (relative abundance of m/z 69 was 7 and m/z 39 was the stated dominant ion, other ions were not specified and were therefore neglected here in calculation of percentage product distributions). The *E/N* range of the latter value at V_{drift} 580 V is closer to the *E/N* range of normal operation suggesting some fragmentation to m/z 39 may occur under normal operating conditions. The enthalpy of formation of $C_3H_3^+$ calculated from *AE* for the formation of $C_3H_3^+$ from 2-methyl-1,3-butadiene is 12.38 to 12.68 eV, employing these values to calculate the enthalpy of the reaction of 2-methyl-1,3-butadiene with H_3O^+ to form $C_3H_3^+$ (C_2H_6 + H_2O) gives a value of +1.97 to +2.27 eV. Lias *et al* (1988) cite enthalpies of formation of $CH_2C{\equiv}CH^+$ and $c\text{-}C_3H_3^+$ of 12.22 eV and 11.14 eV respectively giving enthalpies of reaction of 1.81 eV and 0.73 eV respectively. The reaction may occur indirectly by dissociation of $C_3H_5^+$ by elimination of H_2. The enthalpy of the reaction of H_3O^+ with C_5H_8 to give $C_3H_3^+$, H_2 and C_2H_4 is +3.22 eV to +3.68 eV where $C_3H_3^+$ is acyclic and +2.14 eV where $C_3H_3^+$ is cyclic. It is noteworthy that the O^{18} isomer of $H_3O^+.H_2O$ occurs at m/z 39 and should be subtracted for product distribution calculations. Provided humidity is constant conversely to fragments the O^{18} isomer of $H_3O^+.H_2O$ decreases with increasing *E/N*.

In EI-MS of 2-methyl-1, 3-butadiene m/z 41 and m/z 39 form 5.1 % and 11.2 % respectively of the total product ions. At the increased energy of EI-MS a number of other dissociation pathways become accessible the parent ion at m/z 68 forms only 14.1 % of the product ion

and a number of other product ions are observed at m/z 67 ($C_5H_7^+$, 21.9 %), m/z 53 ($C_4H_5^+$, 13.8 %), m/z 40 ($C_3H_4^+$, 5.7 %), m/z 27 ($C_2H_5^+$, 4.7 %) and other less dominant m/z (23.5 %) (Mallard and Linstrom 2005). The reaction of 2-methyl-1, 3-butadiene with OH^- in SIFT produces negatively charged fragment ions at both m/z 41 ($C_3H_5^-$) and m/z 39 ($C_3H_3^-$) each forming 25 % and 10 % of the total products respectively (Španel *et al* 1995b, Custer *et al* 2003). Product ions are not observed at m/z 39 or m/z 41 from the reactions of O_2^+ or NO^+ with 2-methyl-1, 3-butadiene (Španel *et al* 1995b).

The large degree of fragmentation of m/z 39 observed by Malekina *et al* (2007) at higher V_{drift} (therefore *E/N*) would suggest a significant underestimation of 2-methyl-1,3-butadiene concentrations at similar *E/N* derived using count rates at m/z 69 alone, as is current practice. Using the count rate at m/z 69 alone Warneke *et al* (2003) derived a measured sensitivity of 25.8 ncps ppb^{-1} within experimental uncertainty of the calculated sensitivity of 19.8 ncps ppb^{-1} suggesting insignificant fragmentation (recall uncertainty of the calibration standard was ~20 %, humidity is unknown). As Warneke *et al* (2003) employed an *E/N* of 106 Td this does not exclude the possibility of fragmentation at higher *E/N* (and/or temperature and pressure at fixed *E/N)*. Hayward *et al* (2002) observed a 1:1 ± 10 % ratio between volume mixing ratios of 2-methyl-1,3-butadiene calculated from count rates at m/z 69 and gravimetrically determined volume mixing ratios of the sampled calibration standard (humidity unknown), an agreement well within the uncertainties, *E/N* was not specified, P_{dt} was ~ 2.0 mbar, T_{dt} *and* V_{drift} were not specified.

A number of studies have compared ambient VMRs of 2-methyl-1,3-butadiene derived from count rates at m/z 69 using PTR-MS to VMRs determined using an alternative technique such as GC, GC-MS or OP-FTIR and are summarised in Table D.18.

All of the gradients of the plots of PTR-MS derived VMRs *versus* VMRs derived *via* an alternative technique are within experimental uncertainty equal to one, except that observed by Kato *et al* (2004). However, it cannot be concluded that dissociation does not occur: The intercepts of all of the plots, except that of the comparison of PTR-MS and GC-ITMS (Kato *et al*, 2004), are positive and between 14±3 and 212 ppt. This indicates that either the instrumental background was underestimated or that other compounds were contributing to m/z 69. Where background measurements were made a platinum catalyst was used and background measurements were performed at least every 2 hrs (Table d.18). The gradient of greater than one observed by Kato *et al* (2004) also suggests another compound is contributing to m/z 69. The presence of another compound with similar determining factors at m/z 69 may mask the fragmentation of 2-methyl-1,3-butadiene.

Table D.18 A review of comparisons of 2-methyl-1,3-butadiene VMRs derived using PTR-MS and those derived using various alternative techniques. Christian *et al* (2004) and Karl *et al* (2007) compared VMR from m/z 69 in PTR-MS to the sum of the VMRs of furan and 2-methyl-1,3-butadiene determined by FTIR. AT denotes alternative technique, P_{dt} denotes drift tube pressure, T_{dt} denotes drift tube temperature, V_{drift} denotes drift tube voltage, and E denotes the electric field strength. The correlation coefficient, r^2, gradient, *m*, and intercept, *c*, correspond to linear regressions of scatter plots of 2-methyl-1,3-butadiene VMRs, derived using the PTR-MS from count rates at m/z 69 alone, against 2-methyl-1,3-butadiene VMRs derived using the specified alternative technique (§ 3). * Sensitivities of a number of other compounds derived by calibration during this study were 25 % greater than those of Warneke *et al* (2003), thus 25 % was added to VMRs of compounds which were not calibrated for during the study, including 2-methyl-1,3-butadiene, and which were determined using sensitivities from Warneke *et al* (2003) (de Gouw *et al* 2003b). ** here *m* refers to the study average of the integrated PTR-MS excess VMRs divided by the integrated OP-FTIR excess VMRs of 2-methyl-1,3-butadiene + furan where excess VMR refers to the VMR measured during a generated fire minus the VMR prior to the fire, *n* indicates the number of fires used to derive *m* (Christian *et al* 2004).*** *m* is the slope of an *x-y* weighted orthogonal regression after Christian *et al* 2004.

Reference	Air sampled	AT	PTR-MS VMR derivation	PTR-MS sample times	AT sample times	P_{dt} (mbar)	T_{dt} (K)	V_{dirft} (V)	E (V cm^{-1})	E/N (Td)	r^2	m	c (ppt)
de Gouw *et al* (2003b)	Ship based measure-ments off the coast of New England in July/ August 2002 (NEAQS)	GC-MS (on-line)	Application of sensitivities from Warneke *et al* (2003) +25% * Humidity correction applied. Background determined by passing sampled air through a heated Pt coated quartz wool catalyst for 2.25 min every 1.4 hrs	Dwell time at m/z 69: 5 s, 2.25 min per cycle.	5 min sample every 30 min	2.4	NS	710	NS	NS	0.98	**0.97± 0.03**	14±3
de Gouw *et al* (2006)	Airborne measure-ments over NE USA, Alaska and western Canada (ICARTT)	GC analysis of canisters	Sensitivities determined by calibration (average accuracy ± 25 %) Background measured every 30 cycles (~10 min) by passing sample air through a Pt catalyst at 350°C	20 masses in total; 16 VOC masses monitored at 1 s per mass and H_3O^+, NO^+, O_2^+ & $H_3O^+.H_2O$ 17s cycle^{-1}.	5 to 25 s filling time.	NS	NS	NS	NS	NS	0.92	**0.888± 0.013**	19±2

Table D.18 is continued on the following page.

Reference	Air sampled	AT	PTR-MS VMR derivation	PTR-MS sample times	AT sample times	P_{dt} (mbar)	T_{dt} (K)	V_{dirft} (V)	E (V cm^{1})	E/N (Td)	r^2	m	c (ppt)
Warneke *et al* (2001a) and Williams *et al* (2001)	Airborne measure-ments over the tropical rainforest of Surinam in March 1998. (LBA/ CLAIRE)	GC-FID analysis of canisters	VMRs calculated (Eq. 2.10), accuracy ± 30 %). No humidity correction noted. Background determined by passing sampled air through a charcoal filter for 5 minutes every 20 minutes.	90 % of flight time 8 – 12 m/z measured every 15 – 25 s, for the remaining 10 % m/z 33 – 140 measured at 1s per m/z. PTR-MS measure-ments averaged over the period in which canister samples were collected.	NS	1.3 to 2.7	N S	NS	NS	130	0.93	**0.84**	670
Kuster *et al* (2004) and Karl *et al* (2003)	Suburban measure-ments at La Port - east of Houston August/ September 2000 (TexAQS 2000)	GC-ITMS (on-line)	Sensitivities determined by calibration with standard with an estimated uncertainty of ± 20 %. No humidity correction noted. Background measurements were performed every 30 min to 2 h. Air was passed through a Pt wool catalyst at 430°C	Sample acquisition times of the PTR-MS and three GC techniques were not identical. PTR-MS cycle length 40 – 360 s with 2 – 5 s integration times per single ion.	10 min sample every 60 min	2.5	NS	NS	NS	123	0.95	**1.03± 0.03**	~0

Table D.18 is continued on the following page.

Reference	Air sampled	AT	PTR-MS VMR derivation	PTR-MS sample times	AT sample times	P_{dt} (mbar)	T_{dt} (K)	V_{dirft} (V)	E (V cm^{-1})	E/N (Td)	r^2	m	c (ppt)
Kuster *et al* (2004) and Karl *et al* (2003)		GC-FID (on-line)			5 min sample every 33 min						0.63	**1.2 ± 0.2**	100
(continued)		GC-QMS (on-line)			5 min sample every 15 min						0.55	**0.96± 0.20**	160
Kato *et al* (2004)	Urban air west of Tokyo, November 2002	GC-FID (on-line)	VMRs calculated (Eq. 2.10) Background measurement for 30 min every 30 min using air passed through a heated Pt catalyst.	4 min averages of PTR-MS data used for comparison.	4 min samples every 4h	2	NS	590	NS	140	NS	**2.15**	212
Christian *et al* (2004)	Well mixed smoke from fires generated in a combust-ion facility.	OP-FTIR	VMRs calculated. No humidity correction applied. Uncertainty in mixing ratios ≤ ± 50 % as nominal rate constant employed. No background measurement noted.	Two measurement modes, cycle length 0.1 – 0.2 s in both. 20 ms per m/z in scan mode. 30 - 36 m/z in MID mode. Results splined to match OP-FTIR points (instrument computers synchronized).	0.83 to 6 s resolu-tion	2	NS	600	NS	130	-	**0.783 ± 0.465 (*n* = 39) ****	-

Table D.18 is continued on the following page.

Reference	Air sampled	AT	PTR-MS VMR derivation	PTR-MS sample times	AT sample times	P_{dt} (mbar)	T_{dt} (K)	V_{dirft} (V)	E (V cm^{-1})	E/N (Td)	r^2	m	c (ppt)
Karl *et al* 2007	Well mixed smoke from fires generated in a combust-ion facility from a mix of tropical plant species	FTIR	Sensitivities determined by calibration with estimated uncertainty of ± 20 %. Humidity correction applied. Background measurement performed, method and frequency not specified		0.83 to 6 s resolute-ion	2.0	313	~555	~55.5	~120	-	**1.05± 0.4*** **	-

Besides other dienes such as pentadiene there are a number of compounds which react with H_3O^+ to form products at m/z 69: The reaction of cyclopentene with H_3O^+ forms only the non-dissociative product at m/z 69 (Warneke *et al* 2003, § 3.1.2). Studies of the product distribution resulting from H_3O^+ reaction with alkynes of formula C_5H_8 could not be found but some non-dissociative reaction product at m/z 69 is likely. The lower alkynes, ethyne and propyne, react by non-dissociation alone in SIFT at 298 K (Wilson *et al* 2003, Milligan *et al* 2002) and PTR-MS (Warneke *et al* 2003). However the proton affinities of ethyne and propyne are 6.65 eV and 7.75 eV (reaction efficiencies are ~ 0.008 to 0.0085 and ~0.89 to 0.90 respectively, Wilson *et al* 2003, Milligan *et al* 2002). 2-pentyne for example has a larger proton affinity of 8.40 eV and dissociation reactions may be more thermodynamically favourable. The parent ion of 1-pentyne forms 20.3 % in EI-MS of 1-pentyne (Mallard and Linstrom 2005). Furan (c-C_4H_4O) reacts with H_3O^+ to form only the non-dissociative product at m/z 69 in SIFT (Wang *et al* 2004c) and PTR-MS at *E/N* of ~120 Td (Karl *et al* 2007). Unsaturated alcohols formula C_5H_9OH, 1-Octen-3-ol and potentially alcohols of the same formula and longer chain alcohols react partly by dissociation to $C_5H_9^+$ at m/z 69 in the PTR-MS (§ D.3.3). Pentanal and other saturated aldehydes formula $C_5H_{10}O$ and C_7 to C_9 and possibly higher aldehydes react partly by dissociation to m/z 69 in the PTR-MS (§ D.4.1). m/z 69 is also a minor dissociation product of the reaction of some longer chain alkanes (§ D.1.1), longer chain alkenes (§ D.1.2), cyclic alkanes (§ D.1.4) and monoterpenes mycene and ocimene (~3% in SIFT at ~298 K, Wang *et al* 2003, Schoon *et al* 2003).

Many of these compounds which react to form products at m/z 69 are observed in the troposphere. Furan has been observed from biomass burning using FTIR (Christian *et al* 2003, Christian *et al* 2004, Karl *et al* 2007). Christian *et al* 2004 and Karl *et al* 2007 compared the sum of 2-methyl-1,3-butadiene and furan VMRs measured with FTIR from biomass burning with VMRs calculated from count rates at m/z 69 in PTR-MS and found relatively good correlations with slopes of 0.783 ± 0.465 and 1.05± 0.4 respectively (Table D.18). Furan reacts rapidly with *OH* and will be present only in air directly influenced by biomass burning (or any other as yet unknown source of furan) (Williams *et al* 2001). Other biomass burning markers such as acetonitrile (m/z 42) could provide an indication of furan contribution.

Ciccioli *et al* (1999) have observed cyclopentene with high frequency (70 to 100 % of samples analysed) in urban areas at trace levels (0.5 % w/w of total VOC concentration which was typically 500 – 1500 μg m^{-3}) using GC-MS. Cyclopentene was observed less frequently in suburban and forest sites and VMR were below detection levels in remote areas (Ciccioli *et al* 1999). Grosjean *et al* (1998) observed mean ambient concentrations of

cyclopentene of 3.8 ± 2.7 mg m^{-3} in the city of Porto Alegre, Brazil, emission rate was approximated at 251 ± 71 t yr^{-1}. Cyclopentene was the 7th most important compound for reaction with *OH* of the 66 hydrocarbons measured; mean VMR (ppb) x reaction rate constant with *OH* at 298 K (10^{12} cm^3 molecule s^{-1}) was 91.6. Longer chain alkanes, alkenes and cycloalkanes which may make a minor contribution to m/z 69 are also found predominantly in urban areas (Ciccioli *et al* 1999) as a result of fossil fuel combustion (see for example, Friedrich and Obermeier 1999).

Ciccioli *et al* (1999) have observed pentanal with high frequency (70 to 100 % of samples analysed) in urban, sub-urban and forested areas at trace concentrations (less than 0.5 % w/w of total concentration of hydrocarbons) in urban areas and at a moderate level (5 to 0.5 % w/w of total concentration) in sub-urban and forested sites. Pentanal is emitted from anthropogenic sources such as vehicle exhausts (e.g. Smith *et al* 2004), $C_5H_{10}O$ aldehydes have been observed from senescing vegetation and freeze thaw treated leaves (Fall *et al* 2001, Karl *et al* 2005), aldehydes are also produced from atmospheric oxidation of VOCs (Atkinson 2000). Concentrations of 0.011 ppb and 0.093 ppb have been reported in rural areas and 0.10 ppb and 0.22 ppb in urban areas (Cleary *et al* 2007 and references therein).

Goldan *et al* (1993) observed volume mixing ratios of the C_5 unsaturated alcohol 2-methyl-3-buten-2-ol (MBO) using GC and GC-MS at a mountainous site in Colorado USA forested by lodgepole pine interspersed with aspen and Colorado blue spruce. MBO VMRs were five to eight times greater than 2-methyl-1,3-butadiene. MBO VMRs showed a diurnal variation similar to that of 2-methyl-1,3-butadiene and a linear regression of 2-methyl-1,3-butadiene *versus* MBO VMR from a 5-day period during the measurements resulted in a correlation coefficient of 0.88. The emission of MBO from lodgepole pine branches and needle and ponderosa pine has since been established (Fall 1999 and references therein). MBO is also produced from spruce bark beetles (Goldan *et al* 1993). Guenther *et al* (2000) estimated an annual above canopy MBO emission rate from North America of 3.2 Tg carbon compared to 29.3 Tg carbon of 2-methyl-1,3-butadiene. However MBO emission rates from many of the vast range of species from which 2-methyl-1, 3-butadiene emission rates have been established are not known. Goldan *et al* (1993) showed that cryogenic cooling of samples to remove water removes MBO, since cryogenic cooling is often involved in GC and GC-MS sampling of VOCs e.g. during pre-concentration processes, MBO may not have been observed in past measurement campaigns when present. In SIFT at 298 K 80 % of product ions from 2-methyl-3-buten-2-ol occur at m/z 69 the remainder at the protonated parent ion m/z 87 (Amelynck *et al* 2005, Schoon *et al* 2007, § 3.3.3). In the PTR-MS 71 to 81 % of product ions from 2-methyl-3-buten-2-ol occur at m/z 69, products at m/z 87 and m/z 41

($C_3H_5^+$) have been observed (Fall *et al* 2001, de Gouw *et al* 2000, Warneke *et al* 2003). The strong correlation between 2-methyl-1,3-butadiene and MBO and similar responses to light and temperature make it difficult to distinguish their contribution to m/z 69. A number of other ions may contribute to m/z 41 and 87 and these signals and the variation of the ratio of m/z 69 to them at varying *E/N* may not differentiate MBO from 2-methyl-1,3-butadiene. Since MBO is removed by cooling, passing the air sample through a water trap prior to measurement by PTR-MS establishes whether part or all of the sample is from MBO. Williams *et al* (2001) did this during measurements over the tropical rainforest of Surinam and observed no change in the signal indicating no MBO was present.

OH oxidation of 2-methyl-3-butan-2-ol produces predominantly acetone, propanal, glycoaldehyde, 2-hydroxy-2-methyl-propanal, methanal and organic nitrates (Ferranto *et al* 1998, Alvarado *et al* 1999). The extent of correlation of VMR from m/z 69 with the products of 2-methyl-1,3-butadiene oxidation (first and second generation) such as MVK and MACR at m/z 71 may help determine the identity of m/z 69, though other molecules may also contribute to these masses (§ 3.7) and e.g. MVK and MACR have additional sources such as automobile exhausts (Biesenthal and Shepson 1997). The difference in lifetimes of possible contributors to m/z 69 may provide insight; Williams *et al* (2000b) examined variability lifetime relationships in air masses 0-1 km above the tropical rainforest of Surinam. The variability of short-lived compounds is generally greater than that of long-lived compounds. Williams *et al* (2000b) compared variability, in this case the natural logarithm of the standard deviation of the VMR, with lifetime of a range of (O)VOCs some of which had been measured using GC and some with PTR-MS; a generally good trend was observed. However, 2-methyl-1,3-butadiene VMRs measured with GC and PTR-MS did not follow the general trend. The variability of the GC derived VMR was greater than that derived from PTR-MS (m/z 69) and closer to that which might be expected from the general trend. It is possible that longer living compounds contributed to m/z 69 and/or that the detection limit of the PTR-MS was underestimated and variability not accurately quantified (Williams *et al* 2000b). Other compounds at m/z 69 may mask fragmentation of 2-methyl-1,3-butadiene.

Given the importance of 2-methyl-1,3-butadiene in the troposphere, further work is needed to establish the extent of 2-methyl-1,3-butadiene fragmentation (and/or dimerisation) over a range of *E/N*, humidities, temperature at fixed *E/N* and pressures at fixed *E/N* to ensure accurate quantification using PTR-MS.

D.1.6 The Reaction of Dienes and Diyenes in the Presence of Water.

The proton affinity of 2-methyl-1,3-butadiene (Table D.15) is approximately the same as that of $H_3O^+(H_2O)$ (8.57 eV) and proton transfer occurs with a reaction efficiency of 1.13 in SIFT at 298 K (Španěl and Smith 1995c). The non-dissociative product was the only observed product of reaction with $H_3O^+(H_2O)$, no product was observed at m/z 87 corresponding to $C_5H_8.H_3O^+$ (Španel and Smith 1995c). Since the proton affinity of 2-methyl-1, 3-butadiene is less than $H_3O^+(H_2O)_n$ where $n \geq 2$, no proton transfer reaction occurs. The dipole of 2-methyl-1, 3-butadiene is relatively small and it does not react with any of the $H_3O^+(H_2O)_n$ n=1-3 clusters by ligand switching (potentially followed by collisional dissociation to MH^+ and H_2O) (Španel and Smith 1995c, Warneke *et al* 2001b). Warneke *et al* (2001b) observed a decrease in the measured sensitivity of 2-methyl-1,3-butadiene with increasing humidity from 43 ncps ppb^{-1} at 20 % relative humidity to 40 ncps ppb^{-1} at 100 % relative humidity in PTR-MS at P_{dt} 2.5 mbar, T_{dt} 296 K and E 65 V cm^{-1} (E/N ~106 Td) . At an increased pressure of 3.0 mbar, T_{dt} 296 K and E 65 V cm^{-1} and thus reduced E/N (~89 Td) the sensitivity at 20 % relative humidity was 30 ncps ppb^{-1} and at 100 % 19 ncps ppb^{-1}. If 2-methyl-1, 3-butadiene were reacting with all of the $H_3O^+(H_2O)_n$ n=1-3 clusters the measured sensitivity would expected to be approximately unchanged with humidity. The humidity dependence of the measured sensitivity indicates that the elevated energy in the PTR-MS is not sufficient to overcome the endothermicity of reaction with the larger $H_3O^+(H_2O)n$ clusters. The reduction in sensitivity at increased pressure and reduced E/N is due to the consequent increase in $H_3O^+(H_2O)_n$ ($n > 1$) clusters and consequent reduction in reactive reagent ions (H_3O^+ and $H_3O^+(H_2O)$ in the case of 2-methyl-1, 3-butadiene). Jobson *et al* (2005) compared measured and calculated sensitivities in calibrations using dry nitrogen, nitrogen at 46 % RH and nitrogen at 75 % RH. The measured sensitivity increased as the sum of H_3O^+ and $H_3O^+(H_2O)$ ion counts increased. The calculated sensitivity was derived using H_3O^+ count rates alone, the ratio of measured to calculated sensitivity increased with humidity from 1.01 ± 0.04 in dry nitrogen to 1.24 at 75 % RH. This also indicates $H_3O^+(H_2O)$ reacts with 2-methyl-1,3-butadiene and that exclusion of $H_3O^+(H_2O)$ count rates in the calculated sensitivity results in underestimation of the sensitivity.

The known proton affinities of the other dienes and diyene considered (Table D.15) are less than that of $H_3O^+(H_2O)_n$ $n \geq 1$ and no proton transfer reaction is expected. The dipole moments of these molecules are relatively small (~ 0 to 0.413 D) and ligand switching is unlikely to occur (§ 2.6).

D.2 Aromatics

The proton affinities and gas basicities of various aromatics and the enthalpies, entropies and Gibbs free energies of non-dissociative proton transfer from H_3O^+ are shown in Table D.19. Reaction efficiencies and product distributions observed from the reaction of a range of aromatic compounds with H_3O^+ observed in SIFT at 298 K are reviewed in Table D.20. The Gibbs free energy of reaction of the alkylbenzenes, naphthalenes and phenolic compounds with H_3O^+ are much less than – 0.43 eV (Table 3.19) and reactions are efficient at 298 K (Table D.20). Only the non-dissociative products are observed at 298 K.

Table D.19: A compilation of proton affinities (*PA*), gas basicities (*GB*), potential standard enthalpy (ΔH_r^Φ), potential standard entropy (ΔS_r^Φ) and Gibbs free energies (ΔG_r^Φ) of the non-dissociative H_3O^+ reaction with alkylbenzenes and phenolic compounds. DMB denotes dimethylbenzene and TMB denotes trimethylbenzene. Proton affinities and gas basicities are taken from Hunter and Lias, (1998) unless otherwise specified; [a]values are experimentally determined values from van Beelen *et al* (2004), [b]values are calculated (*ab initio* G3(MP2)) values from van Beelen *et al* (2004) and correspond to carbon four, *GB* values were obtained from *PA* and entropies of protonation. ΔG_r^Φ and ΔH_r^Φ are calculated from Eq. 2.88 and 2.89, ΔS_r^Φ are calculated from $\Delta S_r^\Phi = \left(\Delta H_r^\Phi - \Delta G_r^\Phi\right)/T$.

Compound	*PA* (eV)	*GB* (eV)	ΔH_r^Φ (eV)	ΔS_r^Φ (x 10^{-4} eV K^{-1})	ΔG_r^Φ (eV)
Benzene	7.78	7.52	-0.62	2.09	-0.68
Toluene	8.13	7.84	-0.96	1.15	-1.00
1, 2 – DMB (*o*-xylene)	8.25	7.96	-1.09	1.15	-1.12
1, 3 – DMB (*m*-xylene)	8.42	8.15	-1.26	1.77	-1.31
1, 4 – DMB (*p*-xylene)	8.23	7.95	-1.07	1.18	-1.11
Ethylbenzene	8.17	7.88	-1.01	1.15	-1.04
1, 3, 5 TMB	8.67	8.38	-1.50	1.18	-1.54
n-Propylbenzene	8.19	7.90	-1.03	1.15	-1.06
1-methylethyl-benzene (*iso*-propylbenzene)	8.20	7.92	-1.04	1.15	-1.08
n-butylbenzene	8.21	7.92	-1.05	1.15	-1.08
Naphthalene	8.32	8.08	-1.16	2.61	-1.24
1-methylnaphthalene	8.65	8.35	-1.49	0.52	-1.51
2-methylnaphthalene	8.62	8.32	-1.46	0.52	-1.48
Phenol	8.47	8.15	-1.31	0.00	-1.31
2-methylphenol	8.62[a]	8.29[a]	-1.46	-0.35	-1.45
(*o*-cresol)	8.54[b]	8.22[b]	-1.38	0.00	-1.38
3-methylphenol	8.72[a]	8.38[a]	-1.55	-0.35	-1.54
(*m*-cresol)	8.65[b]	8.28[b]	-1.49	-1.67	-1.44
4-methylphenol	8.44[a]	8.10[a]	-1.27	-0.35	-1.26
(*p*-cresol)	8.39[b]	8.03[b]	-1.23	-1.34	-1.19
Phenolmethanol (benzyl alcohol)	8.07	7.75	-0.90	0.24	-0.91

D.2.1 Alkylbenzenes

Product distributions derived from the alkylbenzene reactions with H_3O^+ under elevated energy conditions in the VT-SIFT, PTR-MS and using reagent ions of lower proton affinity indicate that, when observed, dissociation occurs predominantly *via* one or more of five pathways: Eq. D.17 – D.21 :

$$M + H_3O^+ \rightarrow (M - H)^+ + H_2 + H_2O \tag{D.17}$$

$$M + H_3O^+ \rightarrow (M - CH_3)^+ + CH_4 + H_2O \tag{D.18}$$

$$C_nH_{2n-6} + H_3O^+ \rightarrow C_7H_7^{\ +} + C_{n-7}H_{2(n-7)+2} + H_2O \tag{D.19}$$

$$C_nH_{2n-6} + H_3O^+ \rightarrow C_6H_7^{\ +} + C_{n-6}H_{2(n-6)} + H_2O \tag{D.20}$$

$$C_nH_{2n-6} + H_3O^+ \rightarrow C_6H_6 + C_{n-6}H^+_{2(n-6)+1} + H_2O \tag{D.21}$$

The formation of $C_7H_7^+$ tropylium ions from organics containing a benzyl group and of the type $C_6H_5CH_2X$ is well established in EI-MS. The stability of the ions such as this in which the aromatic ring remains intact lies in the ability of the ring to delocalize the positive charge (Ducket and Gilbert 2000, Harwood and Claridge 1997). The standard enthalpies of some non-dissociative and dissociative reactions of alkylbenzenes with H_3O^+ are given in Table D.21.

In EI-MS of benzene, the parent ion forms 38.8 % of the signal. Other dominant products are observed at m/z 77 (11.0 %), m/z 51 (8.6 %), m/z 50 (8.1 %), m/z 52 (7.3 %) and m/z 39 (4.3 %) (Mallard and Linstrom 2005). The aromatic ring remains intact in the more dominant fragment at m/z 77 ($C_6H_5^+$). The other ions in which the aromatic ring is broken are unlikely to be formed at the lower energies in the PTR-MS due to the aforementioned stability of the protonated aromatic ring and energy required for opening. The dissociation reaction of benzene with H_3O^+ to form $C_6H_5^+$ at m/z 77 (Eq. D.17) is endothermic by ~2.7 eV (Table D.21). The proton transfer reaction of benzene with N_2H^+ and H_3^+ was studied by Milligan *et al* (2002), and the reaction with $C_2H_3^+$, $OCSH^+$, HCO^+, CH_5^+, N_2H^+, H_3^+ and ArH^+ was studied by Španěl *et al* (1995a) the non-dissociative product was the only product observed from all reactions. The increase in energy relative to reaction with H_3O^+ at 298 K resulting from the increase in exothermicity due to these changes in reagent ion is 0.45 to 3.25 eV, this compares with $\Delta\langle E_r \rangle$ of 0.27 eV to 0.41 eV at *E/N* of 120 Td to 140 Td (T_{dt} 298 K in air), hence dissociative products are unlikely to be observed in the PTR-MS under normal operating conditions.

Table D.20: Available reaction efficiencies and product distributions resulting from the reaction of H_3O^+ with various aromatics in SIFT at ~298 K. P_{FT} denotes pressure in the flow tube, T_{FT} denotes temperature in the flow tube. k_m denotes the rate constant measured for the reaction of H_3O^+ with the aromatic compound. k_c refers to the collisional rate constant (§ 2.4.1), k_L indicates that the collisional rate constant was derived from Langevin, Gioumousis, Stevenson theory (§ 2.4.1.2, Eq. 2.34) in the cited reference. k_{SC} indicates the collisional rate constant was derived using the results of Su and Chesnavich trajectory calculations (§ 2.4.1.4, Eq. 2.49 – 2.54) in the cited reference. * indicates that the method of k_{coll} is not specified in the reference. k_m/k_c is the reaction efficiency (§ 2.9). δ_{k_c} denotes estimated uncertainty of the calculated collisional rate constant, δ_{k_m} denotes the estimated uncertainty of the measured rate constant. DMB denotes dimethylbenzene and TMB denotes trimethylbenzene. A helium carrier gas was used in all cases small amounts of air were added by Španěl and Smith (1998); Španěl and Smith (1997), Španěl and Smith (1998) and Wang *et al* (2004b) used air to dilute VOC vapours. Milligan *et al* (2002) used helium alone in the flow tube, the helium was passed through a liquid nitrogen cooled zeolite resulting in a typical water vapour VMR of 150 ppb. Humidity was not specified by Španěl and Smith (1997), Španěl and Smith (1998), Španěl *et al* (1995a) or Španěl *et al* (1995b). Water vapour was present in the measurements of Španěl and Smith (1998). Wang *et al* (2004b) performed measurements with dry air, lab air (RH 1.5 %) and humid air (RH ~6 %) (diluting the neutral vapours) results tabulated here were measured under dry conditions variations in the presence of water are discussed in the text. *Lindinger *et al* (1998) specify measured thermal rate constants, no measurement conditions are specified.

Compound	P_{FT} (mbar)	T_{FT} (K)	k_m (x 10^{-9}m^3 s^{-1})	k_m/k_c	k_c	δ_{k_c} (%)	δ_{k_m} (%)	Observed Product Distribution : Product Ion (m/z): **Percentage of Product Total**, $R + H_3O^+ \rightarrow RH^+ + H_2O$	Reference
Benzene C_6H_6	[a]0.67 [b]0.67 [c]0.64 [d]0.67	[a]300 [b]N/O [c]300±5 [d]300	[a]1.8, [b]1.9, [c]1.3 [d]1.8 [e]2.1	[a]1.0 [b]1.0, [c]0.68, [d]0.94 [e]1.1		[b]20	[c]15[d]2 0	$C_6H_7^+$ (79): [a, b, c, d]**100**	[a]Španěl *et al* (1995b), [b]Španěl and Smith (1998), [c]Milligan *et al* (2002), [d]Španěl et al (1995a) [e]Lindinger *et al* (1998)*
Toluene $C_6H_5(CH_3)$	[a]0.67 [b]0.67 [c]0.64	[a]300 [b]N/O [c]300±5	[a]2.3, [b]2.2, [c]1.3 [d]2.1	[a]1.0 [b]1.0 [c]0.59 [d]0.95		[b]20	[c]15	$C_7H_9^+$ (93): [a, b, c]**100**	[a]Španěl *et al* (1995b), [b]Španěl and Smith (1998), [c]Milligan *et al* (2002) [d]Lindinger *et al* (1998)*
1, 2 – DMB (*o*-xylene) $C_6H_4(CH_3)_2$	0.67	N/O	2.4	1.0		20		$C_8H_{11}^+$ (107): **100**	Španěl and Smith (1998)

Table D.20 is continued on the following page.

Compound	P_{FT} (mbar)	T_{FT} (K)	k_m (x 10^{-9}m^3 s^{-1})	k_m/k_c	k_c	δ_{k_c} (%)	δ_{k_m} (%)	Observed Product Distribution : Product Ion (m/z): **Percentage of Product Total**, $R + H_3O^+ \rightarrow RH^+ + H_2O$	Reference
1, 3 – DMB (*m*-xylene) ($C_6H_4(CH_3)_2$)	0.67	N/O	2.3	1.0		20		$C_8H_{11}^+$ (107): **100**	Španěl and Smith (1998)
1, 4 – DMB (*p*-xylene) $C_6H_4(CH_3)_2$	0.67	N/O	2.2	1.0		20		$C_8H_{11}^+$ (107): **100**	Španěl and Smith (1998)
Ethylbenzene $C_6H_5(CH_2CH_3)$	0.67	N/O	2.4	1.0		20		$C_8H_{11}^+$ (107): **100**	Španěl and Smith (1998)
1, 2, 3 – TMB $C_6H_3(CH_3)_3$	0.67	N/O	2.5	1.0		20		$C_9H_{13}^+$ (121): **100**	Španěl and Smith (1998)
1, 2, 4 – TMB $C_6H_3(CH_3)_3$	0.67	N/O	2.4	1.0		20		$C_9H_{13}^+$ (121): **100**	Španěl and Smith (1998)
1, 3, 5 – TMB $C_6H_3(CH_3)_3$	0.67	N/O	2.3	1.0		20		$C_9H_{13}^+$ (121): **100**	Španěl and Smith (1998)
Propylbenzene $C_6H_5(CH_2CH_2CH_3)$	0.67	N/O	2.5	1.0		20		$C_9H_{13}^+$ (121): **100**	Španěl and Smith (1998)
Naphthalene $C_{10}H_8$	0.64	300±5						$C_{10}H_9^+$ (129): **100**	Milligan *et al* (2002)
1-methylnaphthalene $C_{10}H_7(CH_3)$	0.64	300±5						$C_{11}H_{11}^+$ (143): **100**	Milligan *et al* (2002)
2-methylnaphthalene $C_{10}H_7(CH_3)$	0.64	300±5						$C_{11}H_{11}^+$ (143): **100**	Milligan *et al* (2002)
Phenol C_6H_5OH	0.67	N/O						$C_6OH_7^+$ (95): **100**	Španěl and Smith (1997)
2-methylphenol (*o*-cresol) $C_6H_4OH(CH_3)$	1.00	296-300						$C_7OH_9^+$ (109): **100**	Wang *et al* (2004b)
3-methylphenol (*m*-cresol) $C_6H_4OH(CH_3)$	1.00	296-300						$C_7OH_9^+$ (109): **100**	Wang *et al* (2004b)

Table D.20 is continued on the following page.

Compound	P_{FT} (mbar)	T_{FT} (K)	k_m (x 10^{-9}m^3 s^{-1})	k_m/k_c	k_c	δ_{k_c} (%)	δ_{k_m} (%)	Observed Product Distribution : Product Ion (m/z): **Percentage of Product Total**, $R + H_3O^+ \rightarrow RH^+ + H_2O$	Reference
4-methylphenol (*p*-cresol) $C_6H_4OH(CH_3)$	1.00	296-300						$C_7OH_9^+$ (109): **100**	Wang *et al* (2004b)
Phenolmethanol (Benzyl alcohol) $C_6H_5(CH_2OH)$	1.00	296-300						$C_7OH_9^+$ (109): **100**	Wang *et al* (2004b)
4-Ethylphenol $C_6H_4OH(CH_2CH_3)$	1.00	296-300						$C_8OH_{11}^+$ (123): **100**	Wang *et al* (2004b)
1-Phenylethanol $C_6H_5(CH_2CH_2OH)$	1.00	296-300						$C_8OH_{11}^+$ (123): **100**	Wang *et al* (2004b)
2-Phenylethanol $C_6H_5(CH_2CH_2OH)$	1.00	296-300						$C_8OH_{11}^+$ (123): **100**	Wang *et al* (2004b)

The product distributions observed from reaction of various aromatics with H_3O^+ in the PTR-MS and PTR-TOF-MS are displayed in Table D.22. The non-dissociative product is the only product observed from benzene reaction in PTR-MS at *E/N* 106 Td (P_{dt} 2.4 mbar) and PTR-TOF-MS at *E/N* 165 Td (P_{dt} 7.09 mbar, T_{dt} 313 K).

The proton transfer reaction of toluene has been studied at temperatures up to 1200 K with H_3O^+ using VT-SIFT and HTFA (P_{FT} ~0.7 mbar in helium carrier gas, Midey *et al*, 2002) and with N_2H^+ and H_3^+ at 298 K (Milligan *et al*, 2002), the results are summarised in Figure D.12, reaction efficiency was within experimental uncertainty of one at all temperatures.

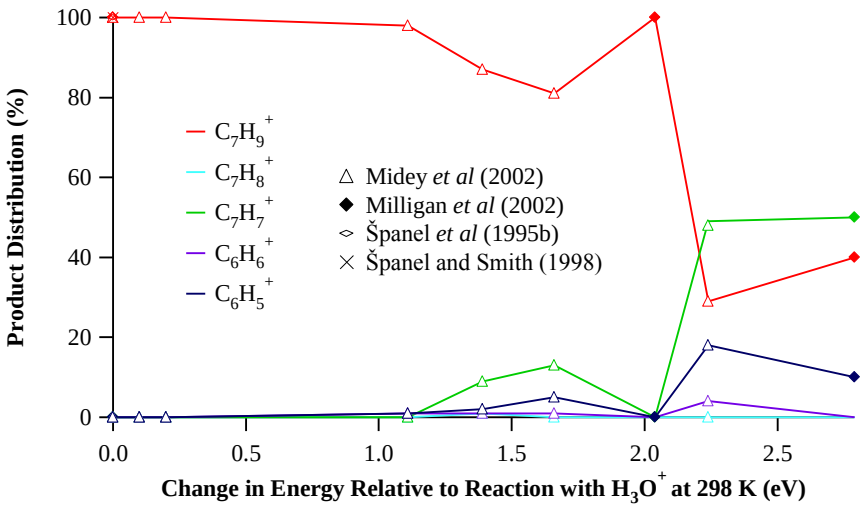

Figure D.12: Product distributions resulting from the reaction of H_3O^+ with toluene at 298 K to 1200 K (Midey *et al* 2002). Other values of product distributions at ~298 K were taken from Milligan *et al* (2002), Španěl and Smith (1998) and Španěl *et al* (1995b). The change in energy relative to reaction with H_3O^+ at 298 K is the increase in $\langle E_r^{SIFT} \rangle$ (Eq. 3.18) at the elevated temperature relative to 298 K. Values of $\langle E_r^{SIFT} \rangle$ at 298 K to 1200 K were taken from Midey *et al* (2002). Product distributions resulting from reaction of toluene with N_2H^+ and H_3^+ (Milligan *et al* 2002) are also shown. In this case the change in energy relative to reaction at 298 K is *GB(H_2O) –GB(reagent ion neutral)* and is 2.03 and 2.75 eV respectively. Points are joined to guide the eye only.

At increases in energy relative to reaction with H_3O^+ at 298 K of up to 0.2 eV the non-dissociative product ($C_7H_9^+$) remains the sole product and at a change of 1.1 eV $C_7H_9^+$ forms greater than 98 % of the products. Comparing this with the approximate $\Delta\langle E_r \rangle$ in the PTR-MS at T_{dt} 298 K in air (Figure 3.4) indicates the non-dissociated product at m/z 93 will form greater than 98 % of the product at *E/N* of up to ~200 Td. PTR-MS and PTR-TOF-MS

Table D.21 The standard (298 K) enthalpy of reaction of non-dissociative and dissociative proton transfer reactions of some alkylbenzenes with H_3O^+. DMB denotes dimethylbenzene, TMB denotes trimethylbenzene. Values derived from [a]Milligan *et al* (2002), [b]Midey *et al* (2002), [c]calculation using proton affinities (Hunter and Lias, 1988) and where applicable standard enthalpies of formation (Mallard and Linstrom 2005), [d]calculation from enthalpies of formation and appearance energies (Mallard and Linstrom 2005). Standard enthalpies of formation of $C_2H_5^+$, $C_3H_7^+$ and $C_4H_9^+$ derived from the proton affinities and standard enthalpies of formation of ethene, propene and 2-butene respectively and are 9.41 eV, 8.34 eV and 8.07 eV respectively. The standard enthalpy of formation of $C_6H_7^+$ was derived from the standard enthalpy of formation and proton affinity of benzene and is 9.00 eV. Neutrals of formula C_nH_{2n+2} were taken to be *n*-alkanes, formula C_nH_{2n} were taken to be alkenes with the double bond between carbons one and two and C_6H_6 corresponds to benzene.

Compound	ΔH_r^{Φ} (eV) $M + H_3O^+ \rightarrow$					
	$MH^+ + H_2O$	$(M-H)^+ + H_2 + H_2O$	$(M-CH_3)^+ + CH_4 + H_2O$	$C_7H_7^+ + C_nH_{2n+2} + H_2O$	$C_6H_7^+ + C_nH_{2n} + H_2O$	$C_6H_6 + C_{n-6}H^+_{2(n-6)+1} + H_2O$
Benzene (C_6H_6)	$C_6H_7^+$ -0.62[a,c]	$C_6H_5^+$ +1.88 to +3.61[d]				
Toluene (C_7H_8)	$C_7H_9^+$ -0.96[a,b,c]	$C_7H_7^+$ -0.41[a], -0.36[b], -0.42 to -0.78[d]	$C_6H_5^+$ +1.70[a], +1.76[b], +2.54 to +2.74[d]			
Ethylbenzene (C_8H_{10})	$C_8H_{11}^+$ -1.01[b,c]		*Reaction is the same as that in the adjacent column*	-0.91[b] -1.26 to -0.059 [d]	+0.48[c] +0.53[b]	$C_2H_5^+$ +1.20[c]
1, 2 – DMB (*o*-xylene, C_8H_{10})	$C_8H_{11}^+$ -1.09[c]	$C_8H_9^+$ +0.23 to +0.33[d]	*Reaction is the same as that in the adjacent column*	-0.0088 to +0.94[d]	+0.59[c]	$C_2H_5^+$ +1.32[c]
1, 4 – DMB (*p*-xylene, C_8H_{10})	$C_8H_{11}^+$ -1.07[c]	$C_8H_9^+$ +0.28 to +1.28[d]	*Reaction is the same as that in the adjacent column*	-0.06 to +1.04[d]	+0.60[c]	$C_2H_5^+$ +1.33[c]
1, 3 – DMB (*m*-xylene, C_8H_{10})	$C_8H_{11}^+$ -1.26[c]	$C_8H_9^+$ +0.58 to +1.48[d]	*Reaction is the same as that in the adjacent column*	-0.42 to +1.22[d]	+0.61[c]	$C_2H_5^+$ +1.33[c]

Table D.21 is continued on the following page.

Compound	ΔH_r^{Φ} (eV) $M + H_3O^+ \rightarrow$					
	$MH^+ + H_2O$	$(M-H)^+ + H_2 + H_2O$	$(M-CH_3)^+ + CH_4 + H_2O$	$C_7H_7^+ + C_nH_{2n+2} + H_2O$	$C_6H_7^+ + C_nH_{2n} + H_2O$	$C_6H_6 + C_{n-6}H^+_{2(n-6)+1} + H_2O$
Propylbenzene (C_9H_{12})	$C_9H_{13}^+$ -1.03[b, c]			-0.79[b] -0.19 to -1.01[d]	+0.37[c] +0.42[b] +0.55[c]	$C_3H_7^+$ +0.36[c] *s*-$C_3H_7^+$ +0.44[b] $C_3H_7^+$ 0.54[c]
1, 2, 3 – TMB (C_9H_{12})						
1, 2, 4 – TMB (C_9H_{12})					+0.60[c]	$C_3H_7^+$ 0.59[c]
Butylbenzene ($C_{10}H_{14}$)	$C_{10}H_{15}^+$ -1.05[c]			-0.94 to +0.15	+0.38[c]	$C_4H_9^+$ +0.31[c]

Table D.22: The product distributions resulting from the reaction of a series of alkylbenzenes with H_3O^+ in the PTR-MS (Warneke *et al* 2003, Jobson *et al* 2005, Rogers *et al* 2006, Malekina *et al* 2007) and CIR-TOF-MS (§ 2.8) (Blake *et al* 2006, Wyche *et al* 2007). Product distributions in Warneke *et al* (2003) were measured in synthetic air (humidity not specified), in Malekina *et al* (2007) product distributions were measured in laboratory air and in Blake *et al* (2006) product distributions were measured in dry nitrogen (thereby reducing O_2^+). Wyche *et al* (2007) specify the percentage abundance of the ion employed for quantification of the compound in the smog chamber experiments within the reference, the remainder of the total ion signal is unspecified. *P_{dt} calculated from specified T_{dt}, E and E/N, Wyche *et al* (2007) specify P_{dt} of 7 – 8 mbar for measurements within the reference. **Distributions from Malekina *et al* (2007) are given as relative abundancies with the most abundant m/z normalised to 100 and have been converted to percentage distributions here and are specified to one decimal place. Specific values of, P_{dt} and T_{dt} during the measurements of alkylbenzene dissociation were not given by Malekina *et al* (2007), however a P_{dt} of 1.8 - 2.1 mbar and a temperature of 303 – 333 K was specified for measurements within the reference, the length of the drift tube was not specified, but a high sensitivity Ionicon Analytik PTR-MS was employed so a drift tube length of 9.5 cm is assumed, V_{drift} was specified 580 V thus E/N would have been somewhere between ~122 and 156 Td.***A T_{dt} of 323 K, P_{dt} of 2.1 mbar and E/N of 150 Td were specified by Jobson *et al* (2005) for sensitivity and diesel exhaust measurements within the reference and are assumed to apply for product distribution measurements, E was derived from these values.****V_{drift} given but l_{dt} unknown therefore E calculated from the specified P_{dt}, T_{dt} and E/N. DMB denotes dimethylbenzene, TMB denotes trimethylbenzene. Measurements by Lindinger *et al* (1998) are assumed to be made in PTR-MS measurement conditions are not specified.

Compound	P_{dt} (mbar)	T_{dt} (K)	V_{drift} (V)	E (V cm^{-1})	E/N (Td)	Observed Product Distribution: Product Ion (m/z): **Percentage of Product Total** $R + H_3O^+ \rightarrow RH^+ + H_2O$				Reference
						$RH^+ + H_2O$	$(R-H)^+ + H_2 + H_2O$	$C_7H_7^+ + C_nH_{2n+2} + H_2O$	$C_6H_7^+ + C_nH_{2n} + H_2O$	
Benzene	[a]2.4 [b]7.09* [c]NS	[a]NS [b]313 [c]NS	[a]NS [b]2700 [c]NS	[a]NS [b]270 [c]NS	[a]106 [b]165 [c]NS	$C_6H_7^+$ (79): **[a, b, c]100**				[a]Warneke *et al* (2003) [b]Blake *et al* (2006) [c]Lindinger *et al* (1998)

Table D.22 is continued on the following page.

Compound	P_{dt} (mbar)	T_{dt} (K)	V_{drift} (V)	E (V cm^{-1})	E/N (Td)	Observed Product Distribution: Product Ion (m/z): **Percentage of Product Total** $R + H_3O^+ \rightarrow RH^+ + H_2O$				Reference
						$RH^+ + H_2O$	$(R-H)^+ + H_2 + H_2O$	$C_7H_7^+ + C_nH_{2n+2} + H_2O$	$C_6H_7^+ + C_nH_{2n} + H_2O$	
Toluene	[a]2.4 [b]7.09 [c]7.95 [d]1.8 -2.1 [e]NS	[a]NS [b]313 [c]313 [d]303 – 333 [e]NS	[a]NS [b]2700 [c]2700 [d]580 [e]NS	[a]NS [b]270 [c]270 [d]NS [e]NS	[a]106 [b]165 [c]147 [d]122 – 156 [e]NS	$C_7H_9^+$ (93): **[a, b, c, d, e]100**				[a]Warneke *et al* (2003) [b]Blake *et al* (2006)* [c]Wyche *et al* (2007)* [d]Malekina *et al* (2007)** [e]Lindinger *et al* (1998)
DMB (xylene - isomer not specified)	[a]1.8 - 2.1 [b]NS	[a]303 – 333 [b]NS	[a]580 [b]NS	[a]NS [b]NS	[a]122 – 156 [b]NS	$C_8H_{11}^+$ (107): **[a]62.4** **[b]100**		$C_7H_7^+$ (91): **[a]18.8**	$C_6H_7^+$ (79): **[a]18.8**	[a]Malekina *et al* (2007)** [b]Lindinger *et al* (1998)
1, 2 – DMB (*o*-xylene)	2.4	NS	NS	NS	106	$C_8H_{11}^+$ (107): **99.7**	$C_8H_9^+$ (105): **0.3**			Warneke *et al* (2003)
1, 3 – DMB (*m*-xylene)	2.4	NS	NS	NS	106	$C_8H_{11}^+$ (107): **100**				Warneke *et al* (2003)
1, 4 – DMB (*p*-xylene)	2.4	NS	NS	NS	106	$C_8H_{11}^+$ (107): **100**				Warneke *et al* (2003)

Table D.22 is continued on the following page.

Compound	P_{dt} (mbar)	T_{dt} (K)	V_{drift} (V)	E (V cm^{-1})	E/N (Td)	Observed Product Distribution: Product Ion (m/z): **Percentage of Product Total** $R + H_3O^+ \rightarrow RH^+ + H_2O$				Reference
						$RH^+ + H_2O$	$(R-H)^+ + H_2 + H_2O$	$C_7H_7^+ + C_nH_{2n+2} + H_2O$	$C_6H_7^+ + C_nH_{2n} + H_2O$	
Ethylbenzene	[a]2.4 [b]2.1 [c]1.9	[a]NS [b]323 [c]~295 - 300	[a]NS [b]NS [c]600	[a]NS [b]~70 [c]66.5	[a]106 [b]150 [c]145	$C_8H_{11}^+$ (107): **[a]98,** **[b]60,** **[c]68**			$C_6H_7^+$ (79): **[a]2,** **[b]40,** **[c]32**	[a]Warneke *et al* (2003) [b]Jobson *et al* (2005)*** [c]Rogers *et al* (2006)****
Propylbenzene	[a]2.4 [b]1.9	[a]NS [b]~295 - 300	[a]NS [b]600	[a]NS [b]66.5	[a]106 [b]145	$C_9H_{13}^+$ (121): **[a]91,** **[b]36**			$C_6H_7^+$ (79): **[a]9,** **[b]64**	[a]Warneke *et al* (2003) [b]Rogers *et al* (2006)****
1-methylethyl-benzene (*iso*-propylbenzene)	2.4	NS	NS	NS	106	$C_9H_{13}^+$ (121): **44**			$C_6H_7^+$ (79): **56**	Warneke *et al* (2003)
1-ethyl-2-methyl-benzene (2-ethyltoluene)	2.4	NS	NS	NS	106	$C_9H_{13}^+$ (121): **100**				Warneke *et al* (2003)

Table D.22 is continued on the following page.

Compound	P_{dt} (mbar)	T_{dt} (K)	V_{drift} (V)	E (Vcm^{-1})	E/N (Td)	Observed Product Distribution: Product Ion (m/z): **Percentage of Product Total** $R + H_3O^+ \rightarrow RH^+ + H_2O$				Reference
						$RH^+ + H_2O$	$(R-H)^+ + H_2 + H_2O$	$C_7H_7^+ + C_nH_{2n+2} + H_2O$	$C_6H_7^+ + C_nH_{2n} + H_2O$	
1-ethyl-3-methyl-benzene (3-ethyltoluene)	2.4	NS	NS	NS	106	$C_9H_{13}^+$ (121): **100**				Warneke *et al* (2003)
1-ethyl-4-methyl-benzene (4-ethyltoluene)	2.4	NS	NS	NS	106	$C_9H_{13}^+$ (121): **100**				Warneke *et al* (2003)
1, 2, 3 – TMB	2.4	NS	NS	NS	106	$C_9H_{13}^+$ (121): **100**				Warneke *et al* (2003)
1, 2, 4 – TMB	2.4	NS	NS	NS	106	$C_9H_{13}^+$ (121): **100**				Warneke *et al* (2003)
1, 3, 5 – TMB	2.4	NS	NS	NS	106	$C_9H_{13}^+$ (121): **100**				Warneke *et al* (2003)
n-butylbenzene	2.4	NS	NS	NS	106	$C_{10}H_{15}^+$ (135): **95**			$C_6H_7^+$ (79): **5**	Warneke *et al* (2003)
s-butylbenzene	2.4	NS	NS	NS	106	$C_{10}H_{15}^+$ (135): **100**				Warneke *et al* (2003)
t-butylbenzene	2.4	NS	NS	NS	106	$C_{10}H_{15}^+$ (135): **50**			$C_6H_7^+$ (79): **50**	Warneke *et al* (2003)
1,2 diethylbenzene	2.4	NS	NS	NS	106	$C_{10}H_{15}^+$ (135): **100**				Warneke *et al* (2003)
1,3 diethylbenzene	2.4	NS	NS	NS	106	$C_{10}H_{15}^+$ (135): **100**				Warneke *et al* (2003)
1,4 diethylbenzene	2.4	NS	NS	NS	106	$C_{10}H_{15}^+$ (135): **100**				Warneke *et al* (2003)
1,2,4,5 tetramethylbenzene	2.4	NS	NS	NS	106	$C_{10}H_{15}^+$ (135): **100**				Warneke *et al* (2003)

derived product distributions confirm $C_7H_9^+$ is the only observed product at *E/N* of 106 Td (P_{dt} 2.4 mbar) to 165 Td (P_{dt} 7.09 mbar, T_{dt} 313 K) (Table D.22). It is noteworthy that on a thermodynamic basis the formation of $C_7H_7^+$ would be expected ($\Delta H^{\Phi}_{r\_298K}$ = ~- 0.39 eV, Table D.21), the lack of $C_7H_7^+$ at room temperature and elevated energies of PTR-MS and VT-SIFT is indicative of an energy barrier. Midey *et al* (2002) experimentally determined an activation energy of +0.86 eV. It is not clear whether the reaction proceeds *via* a direct mechanism (hydride transfer) or *via* loss of hydrogen from $C_7H_9^+$, the activation energy could correspond to formation of $C_7H_7^+$ from $C_7H_9^+$ or from $C_7H_8^+$ and H_3O^+ directly. The role of collisions with buffer molecules (and therefore pressure) is unclear and the pressure dependence at fixed energies in the PTR-MS requires investigation. In a similar manner, at the elevated energies of toluene reaction with H_3O^+ in HTFA at 1200 K, and in the more exothermic reaction of toluene with H_3^+ (Figure D.12) in EI-MS m/z 91 ($C_7H_7^+$) forms 39.1 % of the product ions from toluene the parent ion forms 30.9 %. Other fragments in which the aromatic ring is opened are minor; m/z 65 4.7 %, m/z 39 4.2 %, m/z 63 2.9 % and minor products totalling 18.7 % (Mallard and Linstrom 2005). This degree of fragmentation is not expected at the energies available in conventional PTR-MS.

The reaction of ethylbenzene and propylbenzene with H_3O^+ have also been studied at temperatures from 298 K to 1000 K in VT-SIFT and HTFA (P_{FT} ~0.7 mbar in helium carrier gas, Midey *et al* 2002), the results are shown in Figure D.17 and D.18.

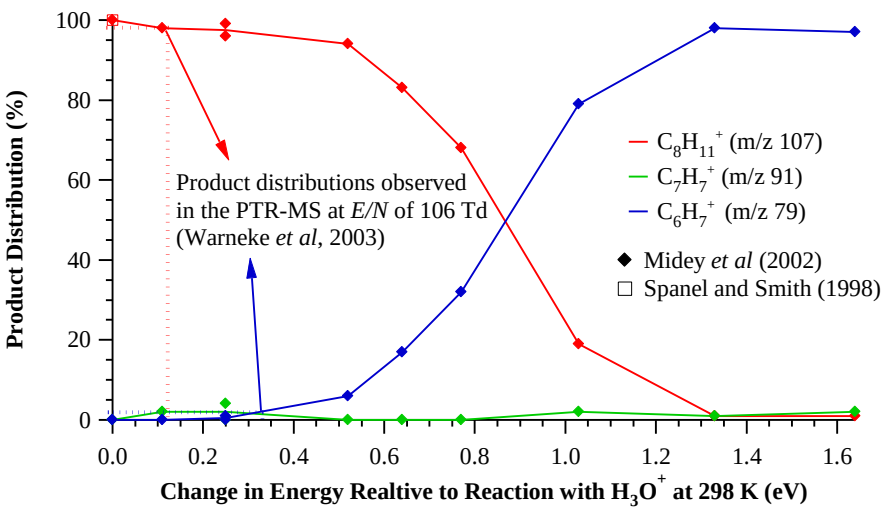

Figure D.13: Product distributions resulting from H_3O^+ reaction with ethylbenzene as a function of the change in energy relative to reaction with H_3O^+ at 298 K. Distributions were measured in VT-SIFT and HTFA and the change in energy corresponds to $<E_r>$ (Eq. 3.18) at the elevated temperature relative to 298 K. The percentage abundancies of fragments in the PTR-MS at *E/N* 106 Td (P_{dt} 2.4 mbar, Warneke *et al* 2003, Table D.22) are shown; $C_8H_{11}^+$ 98 %, $C_6H_7^+$ 2 % corresponding to $<E_r>$ in the range of ~ 0.11 to 0.33 eV.

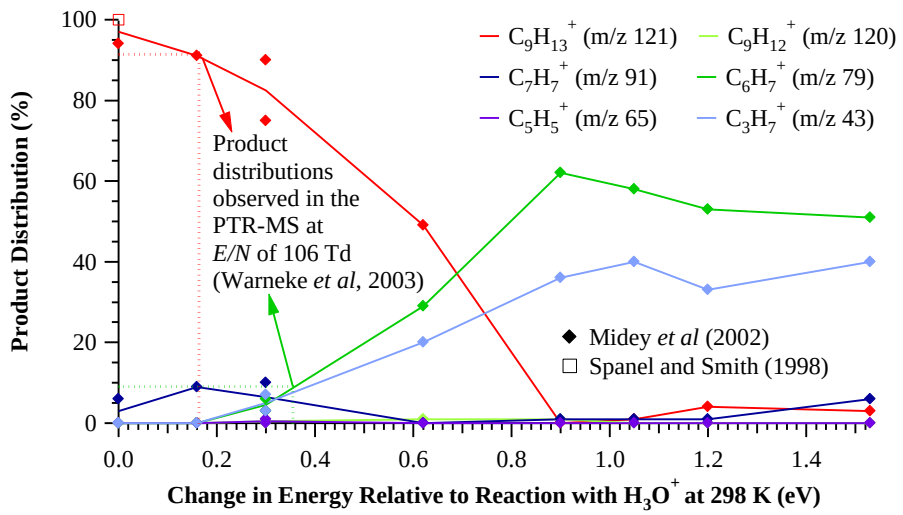

Figure D.14: Product distributions resulting from H_3O^+ reaction with *n*-propylbenzene as a function of the change in energy relative to reaction at 298 K. Distributions were measured in VT-SIFT and HTFA and the change in energy corresponds to $\langle E_r \rangle$ (Eq. 3.18) at the elevated temperature relative to 298 K. The percentage contribution of fragments in the PTR- MS at *E/N* 106 Td (P_{dt} 2.4 mbar, Warneke *et al* 2003, Table D.22) are shown; $C_9H_{13}^+$ 91 %, $C_6H_7^+$ 9 % corresponding to $\langle E_r \rangle$ in the range of ~ 0.16 to 0.36 eV.

The reaction efficiencies were within experimental uncertainty of one at all temperatures. Despite the exoergicity of $C_7H_7^+$ formation from ethylbenzene and propylbenzene reaction with H_3O^+ (Table D.19) this dissociative product does not form more than 10 % of the products in either reaction across the temperature range. Evidently entropy considerations and/or an activation energy barrier prevent significant formation of the dissociation product up to $\Delta\langle E_r \rangle$ of 1.6 eV, formation in the PTR-MS under normal operating conditions is unlikely. Warneke *et al* (2003) did not observe any $C_7H_7^+$ formation from ethylbenzene or propylbenzene (Table D.20) at the slightly lower than normal *E/N* of 106 Td (P_{dt} 2.4 mbar). The formation of $C_7H_7^+$ is also exothermic for the butylbenzene and 1, 2-dimethyl-benzene, Warneke *et al* (2003) did not observe $C_7H_7^+$ from the reaction of these or any of the studied alkylbenzenes at *E/N* of 106 Td (P_{dt} 2.4 mbar). Lindinger *et al* (1998) did not observe any $C_7H_7^+$ formation from toluene or dimethylbenzene. Malekina *et al* (2007) found that $C_7H_7^+$ contributed ~19 % of the products formed from dimethylbenzene reaction with H_3O^+. The exact *E/N* used during this measurement is not given but the range of operating conditions specified for the measurements correspond to an *E/N* of 122 - 156 Td (Table D.22), the $\Delta\langle E_r \rangle$ (Eq. 3.21) for a neutral reactant of molecular mass 106 g mol^{-1} at *E/N* of 120 to 160 Td (T_{dt} 298 K in air) is 0.28 to 0.58 eV (Figure 3.4). In comparison $C_7H_7^+$ from the reaction of ethylbenzene with H_3O^+ is not more than 5 % of the total product ions up to $\Delta\langle E_r \rangle$ of 1.6

eV. The enthalpy of the dissociative reaction with H_3O^+ to form $C_7H_7^+$ is less favourable for dimethylbenzene than ethylbenzene though there is a large degree of uncertainty in the value (Table D.20). In EI-MS $C_7H_7^+$ (m/z 91) forms a greater percentage of the product ions from ethylbenzene (40.9 %) than from 1,2, 1,3 and 1,4 dimethylbenzene (34.0 %, 28.1 % and 33.4 % respectively) (Mallard and Linstrom 2005). Further experimental investigation of fragmentation of dimethylbenzene at *E/N* of greater than 106 Td is required. At the elevated energies of EI-MS $C_7H_7^+$ (m/z 91) is the dominant ion from toluene (39.1 %), ethylbenzene, 1, 2, 1, 3 and 1, 4 dimethylbenzene and propylbenzene (53.5 %) (Mallard and Linstrom 2005). In an analogous manner to $C_7H_7^+$ formation from ethylbenzene and dimethylbenzenes $(M\text{-}CH_3)^+$ ions are observed in EI-MS of larger alkylbenzenes; for example $C_8H_9^+$ at m/z 105 is the dominant product ion from the trimethylbenzenes forming 34.2 %, 34.5 % and 29.5 % from 1, 3, 5 – , 1 , 2, 3 – and 1 , 2, 4 – trimethylbenzene respectively, the ion is observed to a much lesser extent (2.0 %) from propylbenzene (Mallard and Linstrom 2005). Fragmentation of larger alkylbenzenes *via* Eq. 3.2 may occur at higher energies in the PTR-MS (*E/N* > 106 Td).

$C_6H_7^+$ (m/z 79) was the dominant fragment (Eq. 3.4) from ethylbenzene and propylbenzene in VT-SIFT and HTFA up to 1200 K (Midey *et al* 2002, Figure D.13 and D.14). Likewise $C_6H_7^+$ is the only dissociation product observed from the reaction of C_2 – C_4 monosubstitbuted alkylbenzenes in the PTR-MS at *E/N* 106 Td (P_{dt} 2.4 mbar, Table D.20, Warneke *et al*, 2003). The reactions are endothermic (Table D.19) and do not occur at 298 K. Midey *et al* (2002) experimentally determined activation energies of 0.53 eV and 0.47 eV for formation of $C_6H_7^+$ from ethylbenzene and propylbenzene respectively. The enthalpies of some reactions of C_8H_{10} with H_3O^+ are displayed in Figure D.15.

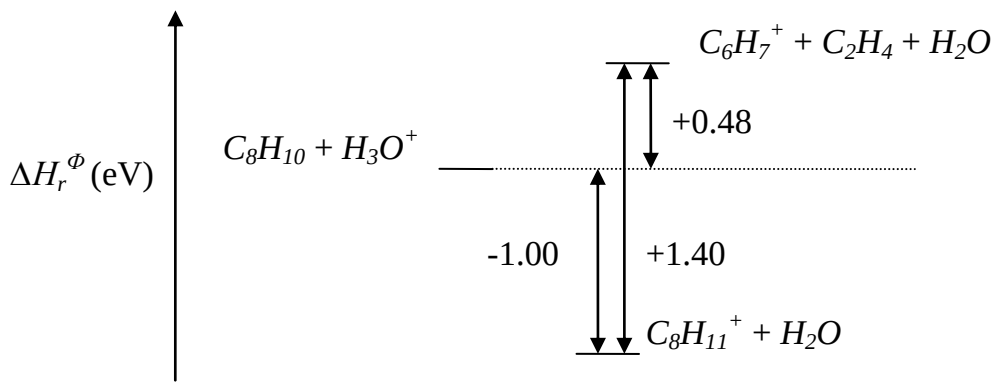

Figure D.15: The enthalpies of reactions of C_8H_{10} with H_3O^+.

The activation energy is less than the endothermicity of dissociation of $C_8H_{11}^+$ to $C_6H_7^+$ (+ CH_4) and approximately equal to that of the reaction of H_3O^+ with C_8H_{10} to produce $C_6H_7^+$ (+ CH_4 + H_2O) directly, suggesting the reaction occurs directly rather than *via* $C_8H_{11}^+$ (Midey *et al* 2002). Similarly the activation energy for formation of $C_6H_7^+$ from propylbenzene and H_3O^+ is less than the endothermicity of dissociation of $C_9H_{13}^+$ to $C_6H_7^+$ + CH_4 (~1.44 eV) and approximately equal to the endothermicity of the direct reaction (~0.42 eV, Table D.21) suggesting the reaction occurs directly rather than *via* $C_9H_{13}^+$. $C_6H_7^+$ is first observed (6 %) from ethylbenzene and propylbenzene at $\Delta\langle E_r \rangle$ of 0.52 ($\langle E_r \rangle$ 0.75 eV, Midey *et al* 2002) and 0.30 eV ($\langle E_r \rangle$ 0.55 eV, Midey *et al* 2002) when there is sufficient energy to overcome the activation energy (~endothermicity) of dissociation.

The product distributions observed from ethylbenzene and propylbenzene reaction in the PTR-MS at *E/N* 106 Td (Warneke *et al*, 2003) correspond to $\Delta\langle E_r \rangle$ of 0.11 – 0.33 eV (mean 0.22 eV) and 0.16 – 0.36 eV (mean 0.26 eV) respectively, the $\Delta\langle E_r \rangle$ (Eq. 3.21) at *E/N* of 106 Td (T_{dt} 298 K in air) is ~0.21 eV. Increasing fragmentation to $C_6H_7^+$ is observed at increasing $\langle E_r \rangle$ (Figures D.13 and D.14), however VT-SIFT data combined with anticipated $\Delta\langle E_r \rangle$ at normal operating *E/N* of 120 – 140 Td indicate fragmentation to $C_6H_7^+$ of less than 20 %. PTR-MS data at *E/N* 106 Td (Table D.22) suggests increased dissociation to $C_6H_7^+$ may be observed when the mono-substituent is branched. $C_6H_7^+$ is observed from the reactions ethyl-, propyl- and butylbenzene with H_3O^+ in the PTR-MS at *E/N* of 106 Td (P_{dt} 2.4 mbar Table D.22, Warneke *et al* 2003). No dissociation to $C_6H_7^+$ is observed where there is more than one substituent to the benzene ring at *E/N* 106 Td (P_{dt} 2.4 mbar Table D.22, Warneke *et al* 2003). This is unsurprising given the increased endothermicity, complexity of reaction and implicit level of re-arrangement. Malekina *et al* (2007) observed a $C_6H_7^+$ fragment of ~ 19 % from H_3O^+ reaction with dimethylbenzene at an *E/N* in the range of 122 – 154 Td. Experimental investigation is required to determine the *E/N* at which $C_6H_7^+$ formation from H_3O^+ reaction (Eq. 3.4) becomes viable for di, tri and tetra substituted alkylbenzenes. In the absence of alternative techniques such as GC the fragmentation of higher alkylbenzenes to $C_6H_7^+$ (m/z 79) may lead to overestimation of benzene VMR. In EI-MS $C_6H_7^+$ (m/z 79) is only a minor product ion and differences in its percentage abundance from different isomers are small; e.g. the percentage abundance from ethylbenzene is 2.0 % 1, 2-dimethylbenzene 2.2 %, 1, 3-dimethylbenzene 2.2 %, 1, 4-dimethylbenzene 2.3 % and from propylbenzene is 0.6 %, 1, 3, 5-trimethylbenzene 2.3 %, 1,

2, 3-trimethylbenzene 3.4 % and 1 , 2, 4-trimethylbenzene 3.5 % (Mallard and Linstrom 2005).

The dissociation reaction to form benzene and $C_{n-6}H^{+}_{2(n-6)+1}$ is endothermic for ethylbenzene, dimethylbenzene, propylbenzene and butylbenzene. However the reaction becomes increasingly favourable as number of carbons in the substituent increases and the standard enthalpy of reaction for propylbenzene and butylbenzene are similar to that for formation of $C_6H_7^+$ (Table D.21). $C_3H_7^+$ was observed from the reaction of propylbenzene with H_3O^+ in VT-SIFT and HTFA at $\Delta\langle E_r \rangle$ of 0.30 eV ($\langle E_r \rangle$ 0.55 eV) onwards, increasing with increasing temperature (Figure D.14, Midey *et al* 2002). Midey *et al* (2002) experimentally derived an activation energy of 0.38 eV which is less than the endothermicity of dissociation of $C_9H_{13}^+$ to form $C_3H_7^+$ + C_6H_6 and approximately equal to the endothermicity of the direct reaction from C_9H_{12} + H_3O^+ of ~0.44 eV, suggesting a direct reaction occurs. No $C_3H_7^+$ was produced from propylbenzene reaction with H_3O^+ in the PTR-MS at *E/N* of 106 Td (P_{dt} 2.4 mbar Table D.22, Warneke *et al* 2003). The $\Delta\langle E_r \rangle$ (Eq. 3.21) of propylbenzene is 0.21 eV at *E/N* of 106 Td (T_{dt} 298 K in air) less than that at which $C_3H_7^+$ was observed in VT-SIFT (Midey *et al* 2002). The sum of $KE^{r}_{c.m.}$ of H_3O^+-propylbenzene (0.17 eV) and $KE^{b}_{c.m.}$ (0.13 eV) at *E/N* of 106 Td and T_{dt} of 298 K in air is 0.30 eV and insufficient to overcome the activation energy of the reaction to form $C_3H_7^+$. The results of VT-SIFT and HTFA reactions of propylbenzene with H_3O^+ (Figure D.14) suggest that at the higher $\Delta\langle E_r \rangle$ associated with normal operating PTR-MS at *E/N* of 120 – 140 Td for propylbenzene ($\Delta\langle E_r \rangle$ ~0.29 - 0.42 eV at T_{dt} 298 K in air) minor fragmentation to $C_3H_7^+$ may occur.

$C_4H_9^+$ was not observed from the butylbenzene reaction at *E/N* of 106 Td (P_{dt} 2.4 mbar, Table D.22, Warneke *et al* 2003) but may occur at normal operating *E/N* of 120 Td to 140 Td where $\Delta\langle E_r \rangle$ is 0.29 to 0.43 eV (T_{dt} 298 K in air) and is sufficient to overcome the endothermicity of the reaction (0.31 eV, Table D.21) depending on the existence/size of any energy barrier and the loss of energy in inactive modes such as radiation. In EI-MS of alkylbenzenes the $C_{n-6}H^{+}_{2(n-6)+1}$ product ion is minor for example $C_2H_5^+$ at m/z 29 forms <0.15 % of product ions from 1, 2-dimethylbenzene, 1, 3-dimethylbenzene and 1, 4-dimethylbenzene and is not observed from ethylbenzene (Mallard and Linstrom 2005). Similarly $C_3H_7^+$ (m/z 43) is only 0.03 % of the total product ions from EI-MS of 1, 3, 5 –

trimethylbenzene and is not observed from 1, 2, 3 – or 1, 2, 4 – trimethylbenzene or propylbenzene (Mallard and Linstrom 2005). Warneke *et al* (2003) derived measured and calculated sensitivities for benzene, toluene, ethylbenzene, 1, 2 -, 1, 3 - and 1, 4 - dimethylbenzene applying the product distributions reviewed in Table D.21 to derive the measured sensitivity. All of the measured and calculated sensitivities were within the uncertainties except that of 1, 2 – dimethylbenzene for which a measured sensitivity of 10.2 ncps ppb^{-1} was obtained compared to a calculated sensitivity of 22.2 ncps ppb^{-1}, this may indicate an underestimation of the fragmentation. VMRs of benzene and toluene in a calibration standard derived from ion counts at m/z 79 and m/z 93 respectively in the PTR-MS by Ammann *et al* (2004) were within experimental uncertainty of gravimetrically determined concentrations substantiating the lack of fragmentation of these compounds. The sensitivities of the alkylbenzenes are humidity dependent. Differences in measured and calculated sensitivities have been observed as a result of dissociation of $H_3O^+(H_2O)$ clusters between the drift tube and detection region resulting in overestimation of H_3O^+ reagent ions and overestimation of the calculated sensitivity (§ D.2.2)

A number of comparisons of VMRs of benzene derived from GC measurements and those derived from count rates at m/z 79 in PTR-MS have been performed and are summarized in Table D.23. The gradients obtained are all approximately equal to one given the uncertainties, this concurs with the discussed lack of fragmentation from benzene in the PTR-MS. Ammann *et al* (2004) also observed good agreement between PTR-MS and GC obtained VMR, a linear regression was not shown. Small positive intercepts have been observed in a number of studies (Table D.23) this is possibly an indication that other compounds are contributing to m/z 79. Warneke *et al* (2005) compared PIT-MS derived benzene VMRs with on-line GC-MS and obtained a large gradient of 2.35 and r^2 of 0.76. This was partially attributed to a change in pump and consequently lower pressure in the detection region resulting in greater dissociation of $H_3O^+(H_2O)$ to H_3O^+ between the drift tube and detection after the initial calibration, though the instrument had been re-calibrated. It is possible that contributions from other compounds to m/z 79 were partly responsible for the large gradient and relatively low correlation coefficient, though the intercept is small (Table D.23). As discussed above ethylbenzenes and propylbenzenes fragment to m/z 79 in the PTR-MS (Table D.22). GC-PTRMS measurements have shown contributions from ethylbenzene and propylbenzenes at m/z 79 (e.g. de Gouw *et al* 2003a, de Gouw and Warneke 2007, Karl *et al* 2007). Rogers *et al* (2006) subtracted the contribution of ethylbenzene and propylbenzene fragments from count rates at m/z 79 using the known product distribution of ethylbenzene and propylbenzene (Table D.22) and count rates at the

non-dissociative product masses. GC measurements showed that ethylbenzene and propylbenzene were a relatively constant fraction of the C_8H_{10} and C_9H_{12} alkylbenzenes respectively and their contributions to m/z 107 and 121 could be derived and used to calculate contribution to m/z 79 from the known product abundancies. This resulted in a good agreement between GC and PTR-MS derived VMRs of benzene (Table D.23).

A number of studies have compared VMRs of toluene obtained from PTR-MS and GC techniques (de Gouw and Warneke 2007 and references therein, Christian *et al* 2004, Roger *et al* 2006). The gradients of scatter plots of PTR-MS derived VMRs *versus* GC derived VMRs are generally in agreement within the uncertainties, and correlation coefficients > 0.90. The intercepts of these plots are variable; negative intercepts of - 2 ppt and - 66 ppt were obtained by Rogers *et al* (2006) and Warneke *et al* (2001b) respectively, conversely positive intercepts of 100 ppt and 23 ppt were obtained by Kuster *et al* (2004) and de Gouw *et al* (2004) respectively, these differences may reflect variability in the accuracy of instrument background measurements. Other compounds may contribute to m/z 93 (§ 3.7) resulting in a positive intercept. Toluene was the only compound observed at m/z 93 in GC-PTR-MS measurements in urban air samples in Colorado (Warneke *et al* 2003, de Gouw and Warneke 2007) and Utrecht (de Gouw *et al* 2003a), in remote air at the Sonnblick Observatory in the Austrian Alps (de Gouw *et al* 2003a) and air samples influenced by tropical biomass burning (Karl *et al* 2007). Kato *et al* (2004) derived a gradient of 0.52 and intercept of 158 ppt. Rogers *et al* (2006) obtained a gradient of 1.40 and intercept of 18 ± 6 ppt. Otherwise gradients of ~1 and relatively good correlation coefficients are consistent with a lack of toluene fragmentation in the PTR-MS.

Table D.23 A review of comparisons of benzene VMRs derived using PTR-MS and those derived using various alternative techniques. AT denotes alternative technique, P_{dt} denotes drift tube pressure, T_{dt} denotes drift tube temperature, V_{drift} denotes drift tube voltage, and E denotes the electric field strength. The correlation coefficient, r^2, gradient, m, and intercept, c, correspond to linear regressions of scatter plots of benzene VMRs, derived using the PTR-MS from count rates at m/z 79, against benzene VMRs derived using the specified alternative technique (§ 3). *m corresponds to the ratio of VMRs from GC analysis of canister samples to those from the PTR-MS averaged over the time which the canister was filled. **Rogers *et al* (2006) subtracted the contribution of C_2 alkylbenzenes and C_3 alkylbenzenes fragments from count rates at m/z 79 using GC measurements of C_2 alkylbenzenes and C_3 alkylbenzenes and known product distributions (Table D.22).

Reference	Air sampled	AT	PTR-MS VMR derivation	PTR-MS sample times	AT sample times	P_{dt} (mbar)	T_{dt} (K)	V_{dirft} (V)	E (V cm^{-1})	E/N (Td)	r^2	m	c (ppt)
Warneke *et al* (2001b)	Ambient air at Cabauw, the Netherlands	GC-FID analysis of canisters	Sensitivities determined by calibration (accuracy ~ ± 20 %) over a range of humidities.	NS	15s filling time analysed within 1 week.	2.5	NS	NS	NS	NS	0.91	**0.82**	106
de Gouw *et al* (2003b)	Ship based measure-ments off the coast of New England in July/ August 2002 (NEAQS)	GC-MS (on-line)	Sensitivity determined by calibration (accuracy ~ ± 15 %). Humidity correction applied. Background determined by passing sampled air through a heated Pt coated quartz wool catalyst for 2.25 min every 1.4 hrs	Dwell time at m/z 79: 5s, 2.25 min per cycle.	5 min sample every 30 min	2.4	NS	710	NS	NS	0.93	**1.12 ± 0.08**	NS

Table D.23 is continued on the following page.

Reference	Air sampled	AT	PTR-MS VMR derivation	PTR-MS sample times	AT sample times	P_{dt} (mbar)	T_{dt} (K)	V_{dirft} (V)	E (V cm^{-1})	E/N (Td)	r^2	m	c (ppt)
Kato *et al* (2004)	Urban air west of Tokyo, November 2002	GC-FID (on-line)	VMRs calculated (Eq. 2.10) Background measurement for 30 min every 30 min using air passed through a heated Pt catalyst.	4 min averages of PTR-MS data used for comparison.	4 min samples every 4 h	2	NS	590	NS	140	NS	**0.82**	26
Kuster *et al* (2004) and Karl *et al* (2003)	Suburban measure-ments at La Port - east of Houston August/ September 2000 (TexAQS 2000)	GC-ITMS (on-line)	Sensitivities determined by calibration with standard with an estimated uncertainty of ± 20 %. No humidity correction noted. Background measurements were performed every 30 min to 2 h. Air was passed through a Pt wool catalyst at 430°C	Sample acquisition times of the PTR-MS and three GC techniques were not identical. PTR-MS cycle length 40 – 360 s with 2 – 5 s integration times per single ion.	10 min sample every 60 min	2.5	NS	NS	NS	123	0.94	**0.85± 0.01**	~0
		GC-QMS (on-line)			5 min sample every 15 min						0.89	**0.97± 0.10**	~0

Table D3.23 is continued on the following page.

Reference	Air sampled	AT	PTR-MS VMR derivation	PTR-MS sample times	AT sample times	P_{dt} (mbar)	T_{dt} (K)	V_{dirft} (V)	E (V cm^{-1})	E/N (Td)	r^2	m	c (ppt)
de Gouw *et al* (2004)	Asian air masses transported toward North America in airborne measure-ments (ITCT 2K2)	GC analysis of canisters	Sensitivities determined by calibration (accuracy ± 15 %), humidity correction not noted. Background measurement performed method and frequency not specified.	NS	NS	NS	NS	NS	NS	NS	0.92	**1.04 ± 0.05**	15
Christian *et al* (2004)	Well mixed smoke from fires generated in a combustion facility.	GC	VMRs calculated. No humidity correction applied. Uncertainty in mixing ratios ≤±50 % as nominal rate constant employed. No background measurement noted.	Two measure-ment modes, cycle length 0.1 – 0.2 s in both. 20 ms per m/z in scan mode. 30 - 36 m/z in MID mode.	Filling time ~10 s filling time with respect to PTR-MS recorded All cans analysed 2- 3 months after collection	2	NS	600	NS	130	-	~1.2*	-

Table D.23 is continued on the following page.

Reference	Air sampled	AT	PTR-MS VMR derivation	PTR-MS sample times	AT sample times	P_{dt} (mbar)	T_{dt} (K)	V_{dirft} (V)	E (V cm^{-1})	E/N (Td)	r^2	m	c (ppt)
de Gouw *et al* (2006)	Airborne measure-ments over NE USA, Alaska and western Canada (ICARTT)	GC analysis of canisters	Sensitivities determined by calibration (accuracy > ± 15 %), no humidity correction noted. Background measured every 30 cycles (~10 min) by passing sample air through a Pt catalyst at 350°C.	20 masses in total; 16 VOC masses monitored at 1 s per mass and H_3O^+, NO^+, O_2^+ & $H_3O^+.H_2O$ 17s cycle^{-1}.	5 to 25 s filling time.	NS	NS	NS	NS	NS	0.87	**1.08 ± 0.02**	12.8 ± 1.4
Rogers *et al* (2006)	Mexico City metropolitan air in spring 2003 (MCMA)	GC-FID analysis of canist-ers	Sensitivities determined by calibration (accuracy ± 15 %), humidity correction applied.** Background measurement was performed by passing the sample through a Pt catalyst heated to 400°C for 60 cycles after 600 cycles of ambient measurement.	12 masses monitored at 0.1s per m/z plus drift tube temperature and pressure resulting in a measure-ment cycle just under 2 s.	Collected for 1-3 hrs throughout a 24 h day. Analysis performed within 24 h of collection	1.9	~295 - 300	600	NS (~60 to 70)	145	0.98	**0.96**	7

D.2.2 The Reaction of Alkylbenzenes in the Presence of Water.

Toluene, benzene, the C_8H_{10} alkylbenzenes and propylbenzene have proton affinities less than that of $H_3O^+(H_2O)$ (8.57 eV). The dipole moments of the alkylbenzenes are relatively small suggesting ligand switching will not occur. Španěl and Smith (1995c) did not observe any reaction between toluene and $H_3O^+(H_2O)_n$ n=1 to 3 at 298 K in SIFT. Španěl and Smith (2000) conclude that when M is an aromatic hydrocarbon, MH^+ hydrates are not formed at a significant rate in SIFT either by ligand switching reactions of M with $H_3O^+(H_2O)$ or by association of MH^+ with H_2O. Midey *et al* (2002) studied the reaction efficiencies and product distributions from the reaction of $H_3O^+(H_2O)$ with toluene, ethylbenzene and propylbenzene in VT-SIFT and HTFA in helium (P_{FT} ~0.7 mbar). The reaction efficiencies of $H_3O^+(H_2O)$ reactions with toluene, ethylbenzene and propylbenzene were 0.53, 0.96 and 0.95 respectively at 298 K, all were within uncertainty ~ 1 at temperatures >500 K. No ligand switching products ($M.H_3O^+$) were observed which may indicate the reaction does not occur or that dissociation to MH^+ and H_2O occurs following ligand switching. At 298 K the non-dissociative (MH^+) product is the predominant product from the reaction of toluene, ethylbenzene and propylbenzene with $H_3O^+(H_2O)$ with small amounts of (0.18 %, 0.17 % and 0.14 % respectively) the association product , $H_3O^+(H_2O)M$, at 500 K the non-dissociative product is the only product of reaction; some dissociation is observed at higher temperatures. The $\langle E_r \rangle$ at 298 K are just greater than the endothermicities of the non-dissociative reactions of toluene, ethylbenzene and propylbenzene with H_3O^+ (H_2O). $\langle E_r \rangle$ may contribute to the large efficiencies despite the endothermicity though this would leave the products ~ internally cold, entropy and/or collisions with buffer may also contribute (Midey *et al* 2002).

The sum of $KE^b_{c.m.}$ (0.15 eV) and $KE^r_{c.m.}$ of toluene, ethylbenzene and propylbenzene with $H_3O^+(H_2O)$ in the PTR-MS at E/N 130 Td (T_{dt} 298 K in air) are 0.37 eV, 0.38 eV and 0.39 eV respectively compared to endothermicities of non-dissociative reactions of 0.44 eV, 0.40 eV and 0.38 eV respectively. Thus given the results of Midey *et al* (2002) at E/N of 130 Td or higher, efficient reactions producing mainly the non-dissociative product may be expected since there is sufficient energy to overcome the endothermicities (the energy of the neutral alkylbenzene also contributing). However the role of pressure and the nature of buffer may affect the reaction (Midey *et al* 2002). Warneke *et al* (2001b) observed decreasing measured sensitivity for benzene and toluene with increasing humidity and the consequently increasing relative abundance of $H_3O^+(H_2O)$ and decreasing relative abundance of H_3O^+ in the PTR-MS

at *E/N* 106 Td (P_{dt} 2.5 mbar, *E* 65 V cm^{-1} and T_{dt} 296 K). The decrease in sensitivity may be a result of the decrease in H_3O^+ reagent ions. Such a humidity dependence of the measured sensitivity was not observed for compounds which react with $H_3O^+(H_2O)_n$ (n=1-3) clusters since count rates of reagent ions are unchanged as H_3O^+ and $H_3O^+(H_2O)_n$ (n=1-3) clusters are reagent ions (§ 2.6). Jobson *et al* (2005) compared measured and calculated sensitivities for benzene, toluene, 1, 4 – dimethylbenzene and 1, 2, 4 – trimethylbenzene in calibration standards diluted in dry nitrogen, nitrogen at 46 % RH and nitrogen at 75 % RH at *E/N* of 150 Td, P_{dt} 2.1 mbar, T_{dt} 323 K and therefore *E* ~70 V cm^{-1}. The results are shown in Table D.24

Table D.24: The ratio of measured to calculated sensitivities for alkylbenzenes in a calibration standard diluted with nitrogen of varying relative humidity at *E/N* of 150 Td, P_{dt} 2.1 mbar and T_{dt} 323 K (therefore *E* ~70 V cm^{-1}) from Jobson *et al* (2005). DMB denotes dimethylbenzene and TMB denotes trimethylbenzene.

Compound	Ratio of measured to calculated sensitivities in calibrations in:		
	Dry N_2	N_2 46 % RH	N_2 75 % RH
Benzene	1.00 ± 0.04	0.96	1.04
Toluene	0.96 ± 0.03	0.96	1.08
1, 4 – DMB	0.96 ± 0.03	0.96	1.12
1, 2, 4 – TMB	0.88 ± 0.02	0.86	1.05

Calculated sensitivities were derived taking H_3O^+ as the reagent ions, a ratio of measured to calculated sensitivity greater than one in humid samples may suggest the calculated sensitivity is an underestimate and the alkylbenzenes react with $H_3O^+(H_2O)$, the ratio would then be expected to increase with humidity. The ratios observed were less than or equal to one and approximately unchanged in dry nitrogen and nitrogen at a relative humidity of 46 %. The values of less than one may result from the differences in actual and measured H_3O^+ count rates due to dissociation of $H_3O^+(H_2O)$ between the drift tube and detection. The ratios in 75 % RH were greater than one and slightly increased relative to the lower humidity conditions most noticeably for 1, 4 – DMB and 1, 2, 4 – TMB. This may be indicative of some degree of reaction with $H_3O^+(H_2O)$ at the higher *E/N* and T_{dt}.

D.2.3 Phenolic Compounds

The known proton affinities of the phenolic compounds listed in Table D.19 are greater than that of water and the non-dissociative reaction is exothermic. The reactions of H_3O^+ with the phenolic compounds listed in Table D.20 produce only the non-dissociative product and are assumed to proceed efficiently at thermal 298 K in SIFT (Wang *et al* 2004b, Španěl and Smith 1997). Lindinger *et al* (1998) report formation of the non-dissociative product from the reaction of H_3O^+ with phenol but measurement conditions were not specified. No other

measurements of the product distributions from phenol or the methyl-phenols in the PTR-MS could be found. Although no fragmentation of these compounds is observed in SIFT (Wang *et al* 2004b, , Španěl and Smith 1997, Table D.20) the elevated energy and differing buffer and pressure conditions in the PTR-MS may lead to fragmentation. Critchley *et al* (2004) have measured 2, 6 - diisopropyl phenol (propofol) in the PTR-MS and SIFT, only the non-dissociative product was observed in SIFT but dissociation to m/z 137 and m/z 95 occurred in the PTR-MS. m/z 137 corresponds to protonated 2 (1methylethyl)-phenol (C_9-$H_{13}O^+$) formed by loss of C_3H_6 from protonated 2, 6 – diisopropyl phenol, it is suggested that m/z 95 is protonated phenol and is formed by loss of a further C_3H_6 molecule from $C_9H_{13}O^+$ (Critchley *et al* 2004). Further dissociation of the protonated phenol fragment was not observed. The possible fragments of phenol and methyl-phenols at the elevated energies of PTR-MS should be considered:

The thermodynamics of various possible reactions of some phenolic compounds are given in Table D.25. In EI-MS the parent ion of phenol (m/z 94) is the most abundant product ion forming 34.0 % of the total ion products. The most dominant fragments are; m/z 66 (13.1 %), m/. 65 (9.0 %), m/z 39 (8.2 %) and m/z 40 (3.9 %) (Mallard and Linstrom 2005). The formation of these fragment ions involves opening of the aromatic ring and, as observed in alkylbenzene measurements (§ D.2.1), this is unlikely at the energies available in normally operated PTR-MS. Analogy with alcohols may suggest loss of water from protonated phenol to form $C_6H_5^+$ (m/z 77) in the PTR-MS. However the carbon oxygen bond of phenols is much stronger than that in alcohols and this reaction is endothermic by ~ 1.4 eV (Table D.25) which compares with a sum of $KE^b_{c.m.}$ (0.16 – 0.22 eV) and $KE^r_{c.m.}$ phenol-H_3O^+ (0.21 – 0.28 eV) of 0.37 to 0.57 eV at *E/N* of 120 to 140 Td at T_{dt} 298 K in air (Figures 3.2 and 3.3). m/z 77 forms only 0.3 % of the total product ions in EI-MS of phenol. Karl *et al* (2007) compared VMR at m/z 95 in PTR-MS (*E/N* ~120 Td, P_{dt} 2.0 mbar, T_{dt} 313 K) with VMR of phenol measured using FTIR in air from controlled laboratory fires. A linear regression of PTR-MS versus FTIR VMRs yielded a gradient of 1.02 ± 0.15. If significant fragmentation were occurring PTR-MS VMRs from m/z 95 would be expected to be less than those derived using FTIR producing a gradient of less than one. Although contributions from other compounds may mask the fragmentation GC-PTRMS results suggested only vinyl furan (~15 % of the total signal at m/z 95) and another unidentified compound were contributing to m/z 95 in addition to phenol and the contribution was small (Karl *et al* 2007). Christian *et al* (2004) compared VMR from m/z 95 in PTR-MS with those of phenol measured with OP-FTIR and found good agreement at high mixing ratios. a linear regression of PTR- MS versus OP-FTIR VMRs yielded a gradient 1.13 ± 0.077 and r^2 of 0.82, indicating any

fragmentation of phenol was minor though the gradient of greater than one and r^2 of less than one suggest some contributions from other compounds.

In EI-MS of 2-methyl-phenol and 3-methyl-phenol the parent ions form 27.7 % and 24.1 % of the total ion products respectively. The dominant fragments from EI-MS of 2-methyl-phenol and 3-methyl-phenol are m/z 107 (18.6 % and 23.0 % respectively), m/z 79 (7.0 % and 8.4 % respectively) and m/z 77 (6.1 % and 7.8 % respectively) (Mallard and Linstrom 2005).

The formation of $C_6H_5^+$ at m/z 77 from H_3O^+ reactions with the methyl-phenols are endothermic by ~2.2 eV (Table D.25) and formation is unlikely at the energies available in normally operated PTR-MS. The formation of $C_6H_7^+$ at m/z 79 from reactions of methyl-phenols with H_3O^+ are endothermic by ~ 0.45 eV (Table D.25) this compares with a sum of $KE^b_{c.m.}$ (0.16 – 0.28 eV) and $KE^r_{c.m.}$ methyl-phenol-H_3O^+ (0.21 – 0.39 eV) of 0.37 to 0.67 eV at *E/N* of 120 to 160 Td at T_{dt} 298 K in air (Figures 3.2 and 3.3), thus it is possible that this fragment will occur at the higher *E/N*. However the rearrangement implicit in formation of $C_6H_7^+$ and CH_2O may result in an energy/entropy barrier and the effects of pressure and buffer are unknown. The formation of $C_7H_7O^+$ from H_3O^+ reactions with methyl-phenols are only slightly endothermic (~0.10 eV Table D.25) and energy in the drift tube is sufficient to overcome this endothermicity. It is noteworthy that hydrogen loss from the alkylbenzene aromatics involve significant energy barriers and the energy required for hydrogen loss is greater than that needed to overcome the endothermicity of reaction, for example hydrogen loss from toluene does not occur in SIFT or PTR-MS despite being exothermic.

The loss of water and formation of $C_7H_7^+$ (m/z 91) from methyl-phenol may be expected by analogy with alcohols (§ 3.1) and the reaction is exothermic (Table D.25). However the lack of formation in SIFT at 298 K (Table D.20, Wang *et al* 2004b) indicates an energy/entropy barrier exists. The *OH* group of phenol is *ortho*, *para* directing toward electrophilles (Clayden *et al* 2001) and *ab initio* calculations of van Beelen *et al* (2004) indicate carbon 4(*para*) has the highest proton affinity in 2- and 3-methyl-phenol and carbon 2 and 4 (*ortho* and *para*) have similar proton affinities in 4-methyl-phenol. This indicates protonation does not occur at the oxygen suggesting loss of water from protonated methyl-phenol is less likely than loss from protonated alcohols. m/z 91 forms only 1.7 % and 1.6 % of total product ions from EI-MS of 2- and 3-methyl-phenol respectively. Another possible fragmentation pathway from methyl-phenol in which the ring remains intact is formation of $C_6H_5O^+$ (m/z 93), production of $C_6H_5O^+$ from reactions of methyl-phenols with H_3O^+ are endothermic by

Table D.25: The standard (298 K) enthalpy of reaction of non-dissociative (Table D.19) and dissociative proton transfer reactions of various phenollic compounds with H_3O^+. Values derived from [a]proton affinities and where applicable standard enthalpies of formation, [b]enthalpies of formation, ion enthalpies of formation taken from Lias *et al* 1988, [c]Španěl and Smith (1997), [d]enthalpies of formation and appearance energies. The enthalpies of formation of the neutral phenolics, propene, methanal, methanol, methane, hydrogen and water were taken from Mallard and Linstrom (2005). $C_6H_7^+$ is taken to be protonated benzene. Proton affinities were taken from Hunter and Lias (1998) with the exception of those of 2-, 3- and 4-methyl-phenol which were taken from Van Beelen *et al* (2004). Propofol refers to 2,6-diisopropyl phenol.

Compound	Product ion, ΔH_r^{ϕ} (eV), $M + H_3O^+ \rightarrow$						
	$MH^+ + H_2O$	$(M-OH)^+ + 2H_2O$	$(M-H)^+ + H_2O + H_2$	$(M-CH_3)^+ + H_2O + CH_4$	$(M-CH_3O)^+ + H_2O + CH_3OH$	$(M-CHO)^+ + H_2O + CH_2O$	$(M-C_3H_5)^+ + H_2O + 2C_3H_6$
Phenol (C_6H_6O)	$C_6H_7O^+$ (m/z 95) -1.31[a]	$C_6H_5^+$ (m/z 77) +1.52[b], +1.41[c] +1.23 to +2.96[d]	$C_6H_5O^+$ (m/z 93) +1.26[b]				
2-methyl-phenol (*o*-cresol, C_7H_8O)	$C_7H_9O^+$ (m/z 109) -1.46, -1.38[a]	$C_7H_7^+$ (m/z 91) -0.51 to -0.31[d]	$C_7H_7O^+$ (m/z 107) +0.18[d]	$C_6H_5O^+$ (m/z 93) +0.81[b]	$C_6H_5^+$ (m/z 77) +2.17[b]	$C_6H_7^+$ (m/z 79) +0.45[a], +1.01[d]	
3-methyl-phenol (*m*-cresol C_7H_8O)	$C_7H_9O^+$ (m/z 109) -1.55 -1.49[a]	$C_7H_7^+$ (m/z 91) -0.44 to -0.34[d]	$C_7H_7O^+$ (m/z 107) +0.15 to +1.38[d]	$C_6H_5O^+$ (m/z 93) +0.85[b]	$C_6H_5^+$ (m/z 77) +2.21[b]	$C_6H_7^+$ (m/z 79) +0.49[a]	
4-methyl-phenol (*p*-cresol C_7H_8O)	$C_7H_9O^+$ (m/z 109) -1.27 -1.23[a]	$C_7H_7^+$ (m/z 91) -0.08 to +0.08[d]	$C_7H_7O^+$ (m/z 107) +0.08[d]	$C_6H_5O^+$ (m/z 93) +0.78[b]	$C_6H_5^+$ (m/z 77) +2.14[b]	$C_6H_7^+$ (m/z 79) +0.42[a]	
Propofol ($C_{12}H_{18}O$)							$C_6H_7O^+$ (m/z 95) +0.65[a]

~0.8 eV. m/z 93 forms less than 1 % of product ions from EI-MS of the methyl-phenols (Mallard and Linstrom 2005).

A comparison of GC-MS derived VMRs of 2-methylphenol and 3-methylphenol with VMRs at m/z 109 in the PTR-MS in Paris City air in May 2007 was performed by Gros *et al* (2007). The variability and observed levels did not compare well. VMRs from m/z 109 were higher than those obtained from GC-MS and another as yet unidentified compound appeared to contribute to m/z 109 correlating well with signals at m/z 131 and 150. Thus no information with regard methyl-phenol fragmentation can be obtained from this comparison.

D.2.4 The Reaction of Phenolic Compounds in the Presence of Water

The phenollic compounds have relatively large dipoles and ligand switching reactions with $H_3O^+(H_2O)_n$ $n=1\text{-}3$ are likely. Wang *et al* (2004b) observed product ions at m/z corresponding to $MH^+(H_2O)_n$ n=1 and 2 from 2-, 3-, 4-methyl-phenol, 4-ethyl-phenol and 2-hydroxyphenol in SIFT at 298 K in the presence of water. The dihydrate abundance increased with increasing humidity and the monohydrate abundance decreased. These ions may be formed by ligand switching of neutral M with $H_3O^+(H_2O)$ or three-body association of MH^+ with water. Association reaction rates may be reduced in the PTR-MS due to the elevated energies though the increased pressure and polyatomic buffer may increase stabilization slightly. Dissociation of the $MH^+(H_2O)_n$ n=1 and 2 hydrates to MH^+ and H_2O may occur at the elevated energies of PTR-MS.

The proton affinities of phenol and 4-methylphenol are slightly less than that of $H_3O^+(H_2O)$ and those of 2- and 3-methylphenol are greater than that of $H_3O^+(H_2O)$. At the elevated energies of PTR-MS proton transfer from $H_3O^+(H_2O)$ to phenol and the 4-methyl-phenol may occur at an increased rate

References

Alvarado, A., E. C. Tuazon, S. M. Aschmann, J. Arey, R. Atkinson (1999) Products and mechanisms of the gas-phase reactions of OH radicals and O_3 with 2-methyl-3-buten-2-ol, *Atmospheric Environment*, **33**: 2893 – 2905.

Amelynck, C., N. Schoon, T. Kuppens, P. Bultinck, E. Arjis (2005) A selected ion flow tube study of the reactions of H_3O^+, NO^+ and O_2^+ with some oxygenated biogenic volatile organic compounds, *International Journal of Mass Spectrometry*, **247**: 1-9.

Ammann, C., C. Sprig, A. Neftel, M. Steinbacher, M. Komenda, A. Schaub (2004) Application of PTR-MS for measurements of biogenic VOC in a deciduous forest, *International Journal of Mass Spectrometry*, **239**: 87-101.

Arnold, S. T., A. A. Viggiano, R. A. Morris (1997) Rate constants and branching ratios for the reactions of selected atmospheric primary cations with *n*-octane and isooctane (2, 2, 4-trimethylpentane), *Journal of Physical Chemistry A*, **101**: 9351-9358.

Arnold, S. T., A. A. Viggiano, R. A. Morris (1998) Rate constants and product branching fractions for the reactions of H_3O^+ and NO^+ with C_2-C_{12} alkanes. *Journal of Physical Chemistry A*, **102**: 8881-8887.

Atkinson, R., J. Arey (1998) Atmospheric chemistry of biogenic organic compounds, *Accounts of Chemical Research*, **31**: 574 – 583.

Atkinson, R. (2000) Atmospheric chemistry of VOCs and NO_x, *Atmospheric Environment*, **34**: 2063 – 2101.

Blake, R. S., K. P. Wyche, A. M. Ellis, P. S. Monks (2006) Chemical ionization reaction time-of-flight mass spectrometry: Multi-reagent analysis for determination of trace gas composition, *International Journal of Mass Spectrometry*, **254**: 85-93.

Bohme, D. K., G. I. Mackay, H. I. Schiff (1980) Determination of proton affinities from the kinetics of proton transfer reactions. VII. The proton affinities of O_2, H_2, Kr, O, N_2, Xe, CO_2, CH_4, N_2O, and CO, *Journal of Chemical Physics*, **73** (10): 4976-4986.

Bonsang B., C. Boissard (1999) Chapter 6: Global Distribution of Reactive Hydrocarbons in the Atmosphere. In *Reactive Hydrocarbons in the Atmosphere*, edited by C. N. Hewitt, pages 209-265. Academic Press, London.

Bouchoux, G., J. Y. Salpin, D. Leblane (1996) A relationship between the kinetics and thermochemistry of proton transfer reactions in the gas phase, *International Journal of Mass Spectrometry and Ion Processes*. **153**: 37-48.

Bowling, D. R., A. A. Turnipseed, A. C. Delany, D. D. Baldocchi, J. P. Greenberg, R. K. Monson (1998) The use of relaxed eddy accumulation to measure biosphere-atmosphere exchange of isoprene and other biological trace gases, *Oecologia*, **116**: 306 – 315.

Chong, S-L., J. L. Franklin (1972) Heats of formation of protonated cyclopropane, methylcyclopropane, and ethane, *Journal of the American Chemical Society*, **94** (18): 6347 – 6351.

Christian, T, J., B. Kleiss, R. J. Yokelson, R. Holzinger, P. J. Crutzen, W. M. Hao, B. H. Saharjo, D. E. Ward (2003) Comprehensive laboratory measurements of biomass-burning emissions: 1. Emissions from Indonesian, African, and other fuels, *Journal of Geophysical Research*, **108** (D23, 4719): 1 – 13.

Christian, T. J., B. Kleiss, R. J. Yokelson, R. Holzinger, P. J. Crutzen, W. M. Hao, T. Shirai, D. R. Blake (2004) Comprehensive laboratory measurements of biomass-burning emissions: 2. First comparison of open path FTIR, PTR-MS, and GC-MS/FID/ECD, *Journal of Geophysical Reasearch*, **109** (D02311): 1-12

Ciccioli, P., E. Brancaleoni, M. Frattoni (1999) Chapter 5: Reactive Hydrocarbons in the Atmosphere at Urban and Regional Scales In: *Reactive Hydrocarbons in the Atmosphere*, edited by C. N. Hewitt, pages 159 – 207. Academic Press, London.

Cleary, P. A., P. J. Wooldridge, D. B. Millet, M. McKay, A. H. Goldstein, R. C. Cohen (2007) Observations of total peroxy nitrates and aldehydes: measurement interpretation and inference of OH radical concentrations. *Atmospheric Chemistry and Physics*, **7**: 1947 – 1960.

Critchley, A. T. S. Elliott, G. Harrison, C. A. Mayhew, J. M. Thompson, T. Worthington (2004) The proton transfer reaction mass spectrometer and its use in medical science: applications to drug assays and the monitoring of bacteria, *International Journal of Mass Spectrometry*, **239**: 235 – 241.

Custer, T. G., S. Kato, R. Fall, V. M. Bierbaum (2003) Negative-ion CIMS: analysis of volatile leaf wound compounds including HCN, *International Journal of Mass Spectrometry*, **223 – 224**: 427 – 446.

De Gouw, J., C. J. Howard, T. G. Custer, B. M. Baker, R. Fall (2000) Proton-transfer chemical-ionisation mass spectrometry allows real-time analysis of volatile organic compounds released from cutting and drying of crops, *Environmental Science and Technology*, **34**: 2640-2648.

De Gouw, J., C. Warneke, T. Karl, G. Eerdekens, C. van der Veen, R. Fall (2003a) Sensitivity and specificity of atmospheric trace gas detection by proton-transfer-reaction mass spectrometry, *International Journal of Mass Spectrometry*, **223 – 224**: 365 – 382.

De Gouw, J., P. D. Goldan, C. Warneke, W. C. Kuster, J. M. Roberts, M. Marchewka, S. B. Bertman, A. A. P. Pszenny, W. C. Keene (2003b) Validation of proton transfer reaction-mass spectrometry (PTR-MS) measurements of gas-phase organic compounds in the atmosphere during the New England Air Quality Study (NEAQS) in 2002, *Journal of Geophysical Research*, **108** (D21): 4682, art.-nr.: 10.1029/2003JD003863.

De Gouw, J. A., O. R. Cooper, C. Warneke, P. K. Hudson, F. C. Fehsenfeld, J. S. Holloway, G. Hübler, D. K. Nicks Jr., J. B. Nowak, D. D. Parrish, T. B. Ryerson, E. L. Atlas, S. G. Donnelly, S. M. Schauffler, V. Stroud, K. Johnson, G. R. Carmichael, D. G. Streets (2004) Chemical composition of air masses transported from Asia to the U.S. West Coast during ITCT 2K2: Fossil fuel combustion versus biomass-burning signatures, *Journal of Geophysical Research*, **109** (D23S20): 1 – 15.

De Gouw, J. A., C. Warneke, A. Siohl, A. G. Wollny, C. A. Brock, O. R. Cooper, J. S. Holloway, M. Trainer, F. C. Fehsenfeld, F. L. Atlas, S. G. Donnelly, V. Stroud, A. Lueb (2006) Volatile organic compounds composition of merged and aged forest fire plumes from Alaska and western Canada, *Journal of Geophysical Research*, **111** (D10303): 1 – 20.

De Gouw, J., C. Warneke (2007) Measurements of volatile organic compounds in the earth's atmosphere using proton-transfer-reaction mass spectrometry, *Mass Spectrometry Reviews*, **26**: 223-257.

Diskin, A. M., T. Wang, D. Smith, P. Spanel (2002) A selected ion flow tube (SIFT), study of the reactions of H_3O^+, NO^+ and O_2^+ ions with a series of alkenes; in support of SIFT-MS, *International Journal of Mass Spectrometry*, **218**: 87-101.

Dotan, I., D. L. Albritton, W. Lindinger, M. Pahl (1976) Mobilities of CO_2^+, N_2H^+, H_3O^+, $H_3O^+.H_2O$, and $H_3O^+.(H_2O)_2$ ions in N_2, *The Journal of Chemical Physics*, **65** (11): 5028-5030.

Fall, R (1999) Chapter 2: Biogenic Emissions of Volatile Organic Compounds from Higher Plants. In: *Reactive Hydrocarbons in the Atmosphere*, edited by C. N. Hewitt, pages 41-91. Academic Press, London.

Fall, R., T, Karl, A, Hansel, A, Jordan, W, Lindinger (1999) Volatile organic compounds emitted after leaf wounding: On-line analysis by proton-transfer-reaction mass spectrometry, *Journal of Geophysical Research*, **104**: 15963 - 15974

Fall, R., S. D. Copley (2000) Bacterial sources and sinks of isoprene, a reactive atmospheric hydrocarbon, *Environmental Microbiology*, **2** (2): 123 – 130.

Fall, R., T. Karl, A. Jordans, W. Lindinger (2001) Biogenic C5 VOCs: release from leaves after freeze-thaw wounding and occurrence in air at a high mountain observatory, *Atmospheric Environment*, **35**: 3905-3916.

Ferranto, C., J. J. Orlando, G. S. Tyndall (1998) Rate and mechanism of the reactions of OH and Cl with 2-methyl-3-buten-2-ol, *Journal of Geophysical Research*, **103** (D19): 25579 – 25586.

Fiaux, D. L., D. L. Smith, J. H. Futrell (1976) Internal energy effects on the reaction of H_3^+ with ethylene, *Journal of the American Chemical Society*, **98**: (19) 5773 -5780

Filella, I., J. Peñuelas (2006) Daily, weekly and seasonal time courses of VOC concentrations in a semi-urban area near Barcelona, *Atmospheric Environment*, **40**: 7752 – 7769.

Friedrich, R., A. Obermeier (1999) Chapter 1: Anthropogenic Emissions of Volatile Organic Compounds In: *Reactive Hydrocarbons in the Atmosphere*, edited by C. N. Hewitt, pages 1 – 39. Academic Press, London.

Goldan, P. D., W. C. Kuster, F. C. Fehsenfeld, S. A. Montzka (1993) The observation of a C_5 alcohol emission in a North American pine forest, *Geophysical Research Letters*, **20** (11): 1039 – 1042.

Graus, M., A. Hansel, A. Wisthaler, C. Lindinger, R. Forkel, K. Hauff, M. Klauer, A. Pfichner, B. Rappenglück, D. Steigner, R. Steinbrecher (2006) A relaxed-eddy-accumulation method for the measurement of isoprenoid canopy-fluxes using an online gas-chromatographic technique and PTR-MS simultaneously, *Atmospheric Environment*, **40**: S43-S45.

Gros, V., C. Gaimoz, C. Decuq, B. Bonsang, C. Coeur, F. Henry, F. Herrman, T. Custer, J. Williams, O. D'Argouges, R. Sarda, J. Sciarre., 2007 VOCs measurements in Paris city in May 2007 with focus on secondary organic aerosol precursors [online]. Available from: http://www.eurochamp.org/datapool/page/55/Gros.pdf. [Accessed March 2008]

Guenther, A., C. N. Hewitt, D. Erickson, R. Fall, C. Geron, T. Graedal, P. Harley, L. Klinger, M. Lerdau, W. A. McKay, T. Pierce, B. Scholes, R. Steinbrecher, R. Tellamraju, J. Taylor, P. Zimmerman (1995) A global model of natural volatile organic emisssions, *Journal of Geophysical Research*, **100**: 8873-8892.

Guenther, A., A. J. Hills (1998) Eddy covariance measurement of isoprene fluxes, *Journal of Geophysical Research*, **103** (D11): 13145 – 13152.

Guenther, A. (1999) Chapter 3: Modeling Biogenic Volatile Organic Compound Emissions to the Atmosphere. In: *Reactive Hydrocarbons in the Atmosphere*, edited by C. N. Hewitt, pages 97 – 118. Academic Press, London.

Guenther, A., C. Geron, T. Pierce, B. Lamb, P. Harley, R. Fall (2000) Natural emissions of non-methane volatile organic compounds, carbon monoxide, and oxides of nitrogen from North America, *Atmospheric Environment*, **34**: 2205 – 2230.

Guenther, A., T. Karl, P. Harley, C. Wiedinmyer, P. I. Palmer, C. Geron (2006) Estimates of global terrestrial isoprene emissions using MEGAN (Model of Emissions of Gases and Aerosols from Nature), *Atmospheric Chemistry and Physics*, **6**: 3181 – 3210.

Harwood, L. M., T. D. W. Claridge (1997) *Introduction to Organic Spectroscopy*, Oxford University Press. New York.

Hayward, S., C. N. Hewitt, J. H. Sartin, S. M. Owen (2002) Performance characteristics and applications of proton transfer reaction-mass spectrometer for measuring volatile organic compounds in ambient air, *Environmental Science and Technology*, **36**: 1554-1560.

Holzinger, R., E. Sanhueza, R. von Kuhlmann, B. Kleiss, L. Donoso, P. J. Crutzen (2002) Diurnal cycles and seasonal variation of isoprene and its oxidation products in the tropical savanna atmosphere, *Global Biogeochemical Cycles*, **16** (4): 1074, 1-13.

Holzinger, R., D. B. Millet, B. Williams, A. Lee, N. Kreisberg, S. V. Hering, J. Jimenez, J. D. Allan, D. R. Worsnop, A. H. Goldstein (2007) Emission, oxidation, and secondary organic aerosol formation of volatile organic compounds as observed at Chebogue Point, Nova Scotia, *Journal of Geophysical Research*, **112** (D10S24): 1 – 12.

Hunter, E. P. L., S. G. Lias (1998) Evaluated gas phase bascities and proton affinities of molecules: An update, *Journal of Physical Chemical Reference Data*, **27** (3): 413-656.

Hunter, K. C., A. L. L. East (2002) Properties of C-C bonds in *n*-alkanes: relevance to cracking mechanisms, *Journal of Physical Chemistry A*, **106**: 1346 -1356.

Jobson, B. T., M. L. Alexander, G. D. Maupin, G. G. Muntean (2005) On-line analysis of organic compounds in diesel exhaust using a proton transfer reaction mass spectrometer (PTR-MS), *International Journal of Mass Spectrometry*, **245**: 78 - 89.

Karl, T., R. Fall, T. N. Rosenstiel, P. Prazeller, B. Larsen, G. Seufert, W. Lindinger (2002a) On-line analysis of the $^{13}CO_2$ labeling of leaf isoprene suggests multiple subcellular origins of isoprene precursors, *Planta*, **215**: 894-905.

Karl, T. G., C. Sprig, J. Rinne, C. Stroud, P. Prevost, J. Greenberg, R. Fall, A. Guenther (2002b) Virtual disjunct eddy covariance measurements of organic compound fluxes from a subalpine forest using proton transfer reaction mass spectrometry, *Atmospheric Chemistry and Physics*, **2**: 279 – 291.

Karl, T., T. Jobson, W. C. Kuster, E. Williams, J. Stutz, R. Shetter, S. R. Hall, P. Goldan, F. Fehsenfeld, W. Lindinger (2003) Use of proton-transfer-reaction mass spectrometry to characterize volatile organic compound sources at the La Porte super site during the Texas Air Quality Study 2000, *Journal of Geophysical Research*, **108** (D16, 4508) 1 – 15.

Karl, T., F. Harren, C. Warneke, J. De Gouw, C. Grayless, R. Fall (2005) Senescing grass crops as regional sources of reactive volatile organic compounds, *Journal of Geophysical Research*, **110**: 1-11

Karl, T. G., T. J. Christian, R. J. Yoelson, P. Artaxo, W. M. Hao, A. Guenther (2007) The Tropical Forest and Fire Emissions Experiment: method evaluation of volatile organic compound emissions measured by PTR-MS, FTIR, and GC from tropical biomass burning. *Atmospheric Chemistry and Physics*, **7**: 5883 - 5897.

Kato, S., Y. Miyakawa, T. Kaneko, Y. Kajii (2004) Urban air measurements in Tokyo area and comparison with GC-FID measurements, *International Journal of Mass Spectrometry*, **235**: 103-110.

Keesee, R. G., A. W. Castleman (1986) Thermochemical data on gas-phase ion-molecule association and clustering reactions, *Journal of Physical Chemical Reference Data*, **15** (3): 1011-1071.

Kleindienst, T. E., M. Jaoui, M. Lewandowski, J. H. Offenberg, C. W. Lewis, P. V. Bhave, E. O. Edney (2007), *Atmospheric Environment*, **41**: 8288 – 8300.

Kreuzweiser, J., M. Graus, A. Wisthaler, A. Hansel, H. Rennenberg (2002) Xylem-transported glucose as an additional carbon source for leaf isoprene formation in Quercus robur, *New Phytologist*, **156**: 171-178.

Kuhn, U., M. O. Andreae, C. Ammann, A. C. Araújo, E. Brancaleoni, P. Ciccioli, T. Dindorf, M. Frattoni, L. V. Gatti, L. Ganzeveld, B. Kruijt, J. Lelieveld, J. Lloyd, F. X. Meixner, A. D. Nobre, U. Pöschl, C. Sprig, P. Stefani, A. Thielmann, R. Valentini, J. Kesselmeier (2007) Isoprene and monoterpene fluxes from Central Amazonian rainforest inferred from tower-based and airborne measurements, and implications on the atmospheric chemistry and the local carbon budget, *Atmospheric Chemistry and Physics*, **7**: 2855 – 2879.

Kuster, W. C., B. T. Jobson, T. Karl, D. Riemer, E. Apel, P. D. Goldan, F. C. Fehsenfeld (2004) Intercomparison of Volatile Organic Carbon Measurement Techniques and Data at La Porte during the TexAQS2000 Air Quality Study, *Environmental Science and Technology*, **38**: 221 – 228.

Lee, A., A. H. Goldstein, J. H. Kroll, N. L. Ng, V. Varutbangkul, R. C. Flagan, J. H. Seinfeld (2006) Gas-phase products and secondary aerosol yields from the photooxidation of 16 different terpenes, *Journal of Geophysical Research*, **111** (D17305): 1 – 25.

Lias, S. G., J. E. Bartmess, J. F. Liebman, J. L. Holmes, R. D. Levin, W. G. Mallard (1988) Gas-phase ion and neutral thermochemistry, *Journal of Physical and Chemical Reference Data*, **17** (Supplement 1): 1-861.

Lindinger, W., A. Hansel, A. Jordan (1998) On-line monitoring of volatile organic compounds at pptv levels by means of proton-transfer-reaction mass spectrometry (PTR-MS) medical applications, food control and environmental research, *International Journal of Mass Spectrometry and Ion Processes*, **173**: 191-241.

Lodish, H., A. Berk, S. L. Zipursky, P. Matsudaira, D. Baltimore, J. Darnell (1999) *Molecular Cell Biology*, W. H. Freeman and Company, New York.

Malekina, S. D., T. L. Bell, M. A. Adams (2007) PTR-MS analysis of reference and plant-emitted volatile organic compounds, *International Journal of Mass Spectrometry*, **262**: 203-210.

Mallard, W. G., P. J. Linstrom (2005) NIST Chemistry WebBook, NIST Standard Reference Database Number 69, February 2000, National Institute of Standards and Technology, Gaithersburg, MD.

McLaren, R., D. L. Singleton, J. Y. K. Lai, B. Khouw, E. Singer, Z. Wu, H. Niki (1996) Analysis of motor vehicle sources and their contribution to ambient hydrocarbon distributions at urban sites in Toronto during the Southern Ontario Oxidants Study, *Atmospheric Environment*, **30** (12) 2219 – 2232.

Meot-Ner M., F. H. Field (1976) Unimolecular thermal decomposition reactions of gaseous carbonium ions. *The Journal of Physical Chemistry*, **80** (26) 2865 – 2869.

Meot-Ner M. (1979) Chapter 6: Temperature and pressure effects in the kinetics of ion-molecule reactions. In: *Gas Phase Ion Chemistry Volume 1*, edited by M. T. Bowers, pages 197-271. Academic Press, London.

Midey, A. J., S. Williams, S. T. Arnold, A. A. Viggiano (2002) Reactions of $H_3O^+(H_2O)_{0,1}$ with alkylbenzenes from 298 K to 1200 K, *Journal of Physical Chemistry A*, **106**: 11726-11738.

Midey, A. J., S. Williams, T. M. Miller, A. A. Viggiano (2003) Reactions of O_2^+, NO^+ and H_3O^+ with methylcyclohexane (C_7H_{14}) and cyclooctane (C_8H_{16}) from 298 K to 700 K, *International Journal of Mass Spectrometry*, **222**: 413-430.

Milligan, D. B., P. F. Wilson, C. G. Freeman, M. Meot-Ner (Mautner), M. J. McEwan (2002) Dissociative proton transfer reactions of H_3^+, N_2H^+, and H_3O^+ with acyclic, cyclic and aromatic hydrocarbons and nitrogen compounds, and astrochemical implications, *Journal of Physical Chemistry*, **106**: 9745-9755

Rogers T. M., E. P. Grimsrud, S. C. Herndon, J. T. Jayne, C. E. Kolb, E. Allwine, H. Westberg, B. K. Lamb, M. Zavala, L. T. Molina, M. J. Molina, W. B. Knighton (2006) On-road measurements of volatile organic compounds in the Mexico City metropolitan area using proton transfer reaction mass spectrometry, *International Journal of Mass Spectrometry*, **252**: 26-37.

Schoon, N., C. Amelynck, L. Vereecken, E. Arjis (2003) A selected ion flow study of the reactions of H_3O^+, NO^+ and O_2^+ with a series of monoterpenes, *International Journal of Mass Spectrometry*, **229**: 231-240.

Schoon, N., C. Amelynck, E. Debie, P. Bultinck, E. Arjis (2007) A selected ion flow tube study of the reactions of H_3O^+, NO^+ and O_2^+ with a series of C_5, C_6, C_8 unsaturated biogenic alcohols, *International Journal of Mass Spectrometry*, **263**: 127-136..

Sharkey, T. D., S. Yeh (2001) Isoprene emission from plants, *Annual Review of Plant Physiology and Plant Molecular Biology*, **52**: 407 – 436.

Sharkey, T. D., A. E. Wiberley, A. R. Donohue (2008) Isoprene emission from plants: Why and how, *Annals of Botany*, **101**: 5 – 18.

Singh, S., Z. J. Li (2007) Kinetics investigation of OH reaction with isoprene at 240-340 K and 1-3 Torr using the relative rate/discharge flow/mass spectrometry technique, *Journal of Physical Chemistry A*, **111** (46): 11843 – 11851.

Sinha, V., J. Williams, M. Meyerhöfer, U. Riebesell, A. I. Paulino, A. Larsen (2007) Air-sea fluxes of methanol, acetone, acetaldehyde, isoprene and DMS from a Norwegian fjord following a phytoplankton bloom in a mesocosm experiment, *Atmospheric Chemistry and Physics*, **7**: 739-755.

Smith, D., P. Španěl, D. Dabill, J. Cocker, B. Rajan (2004) On-line analysis of diesel engine exhaust gases by selected ion flow tube mass spectrometry, *Rapid Communications in Mass Spectrometry*, **18**: 2830 – 2838.

Španěl, P., D. Smith, M. Henchman (1995a) The reactions of some interstellar ions with benzene, cyclopropane and cyclohexane, *International Journal of Mass Spectrometry and Ion Processes*, 141: 117-126.

Španěl, P., M. Pavlik, D. Smith (1995b) Reactions of H_3O^+ and OH^- ions with some organic molecules; applications to trace gas analysis in air, *International Journal of Mass Spectrometry and Ion Processes*, **145**: 177-186.

Španěl, P., D. Smith (1995c) Reactions of hydrated hydronium ions and hydrated hydroxide ions with some hydrocarbons and oxygen-bearing molecules, *Journal of Physical Chemistry*, **99**: 15551 – 15556.

Španěl, P., D. Smith (1997) SIFT studies of reactions of H_3O^+, NO^+ and O_2^+ with a series of alcohols, International Journal of Mass Spectrometry and Ion Processes, 167/168: 375-388

Španěl, P., D. Smith (1998) Selected ion flow tube studies of the reactions of H_3O^+, NO^+ and O_2^+ with several aromatic and aliphatic hydrocarbons, *International Journal of Mass Spectrometry*, **181**: 1-10.

Španěl, P., S. Davies, D. Smith (1999) Quantification of breath isoprene using the selected ion flow tube mass spectrometric analytical method, *Rapid Communications in Mass Spectrometry*, **13**: 1733-1738.

Španěl, P., D. Smith (2000) Influence of water vapour on selected ion flow tube mass spectrometric analyses of trace gases in humid air and breath, *Rapid Communications in Mass Spectrometry*, **14**: 1898-1906.

Španěl, P., J. M. van Doren, D. Smith (2002) A selected ion flow tube study of the reactions of H_3O^+, NO^+, and O_2^+ with saturated and unsaturated aldehydes and subsequent hydration of the product ions, *International Journal of Mass Spectrometry*, **213**: 163-176.

Sprig, C., A. Neftel, C. Ammann, J. Dommen, W. Grabmer, A. Thielmann, A. Schaub, J. Beauchamp, A. Wisthaler, A. Hansel (2005) Eddy Covariance measurements of biogenic VOCs during ECHO 2003 using proton transfer reaction mass spectrometry, *Atmospheric Chemistry and Physics*, **5**: 465 – 481.

Van Beelen, E. S. E., T. A. Koblenz, S. Ingemann, S. Hammerum (2004) Experimental and theoretical evaluation of proton affinities of furan, the methylphenols, and the related anisols, *Journal of Physical Chemistry A*, **108**: 2787 – 2793.

Wang, T., P. Španěl, D. Smith (2003) Selected ion flow tube, SIFT, studies of the reactions H_3O^+, NO^+ and O_2^+ with eleven $C_{10}H_{16}$ monoterpenes, *International Journal of Mass Spectrometry*, **228**: 117-126.

Wang, T., D. Smith, P. Španěl (2004a) Selected ion flow tube, SIFT, studies of the reactions of H_3O^+, NO^+ and O_2^+ with compounds released by Pseudomonas and related bacteria, *International Journal of Mass Spectrometry*, **233**: 245-251.

Wang, T., P. Španěl, D. Smith (2004b) A selected ion flow tube of the reactions of H_3O^+, NO^+ and O_2^+ with some phenols, phenyl alcohols and cyclic carbonyl compounds in support of SIFT-MS and PTR-MS, *International Journal of Mass Spectrometry*, **239**: 139-146.

Wang, T., P. Spanel, D. Smith, (2004c) A selected ion flow tube, SIFT, study of the reactions of H_3O^+, NO^+ and O_2^+ ions with several N- and O-containing heterocyclic compounds in support of SIFT-MS, *International Journal of Mass Spectrometry*, **237**: 167-174.

Warneke, C., J. Kuczynski, A. Hansel, A. Jordan, W. Vogel, W. Lindinger (1996) Proton transfer reaction mass spectrometry (PTR-MS): propanol in human breath, *International Journal of Mass Spectrometry and Ion Processes*, **154**: 61-70.

Warneke, C., R. Holzinger, A. Hansel, A. Jordan, W. Lindinger, U. Pöschl, J. Williams, P. Hoor, H. Fischer, P. J. Crutzen, H. A. Scheeren, J. Lelieveld (2001a) Isoprene and its oxidation products methyl vinyl ketone, methacrolein and isoprene related peroxides measured online over the tropical rain forest of Surinam in march 1998, *Journal of Atmospheric Chemistry*, **38**: 167-185.

Warneke, C., C. van der Veen, S. Luxembourg, J. A. De Gouw, A. Kok (2001b) Measurements of benzene and toluene in ambient air using proton-transfer-reaction mass spectrometry: calibration, humidity dependence, and field intercomparison, *International Journal of Mass Spectrometry*, **207**: 167-182.

Warneke, C., J. A. De Gouw, W. C. Custer, P. D. Goldan, R. Fall (2003) Validation of atmospheric VOC measurements by proton-transfer-reaction mass spectrometry using a gas chromatographic preparation method, *Environmental Science and Technology*, **37**: 2494-2501.

Warneke, C., S. Kato, J. A. De Gouw, P. D. Goldan, W. C. Kuster, M. Shao, E. R. Lovejoy, R. Fall, F. C. Fehsenfeld (2005) Online volatile organic compound measurements using a newly developed proton-transfer ion-trap mass spectrometry instrument during New England air quality study – intercontinental transport and chemical transformation 2004: Performance, intercompraison, and compound identification, *Environmental Science and Technology*, **39**: 5390 – 5397.

Williams, J., H. Fischer, G. W. Harris, P. J. Crutzen, P. Hoor, A. Hansel, R. Holzinger, C. Warneke, W. Lindinger, B. Scheeren, J. Lelieveld (2000b) Variability-lifetime relationship for organic trace gases: A novel aid to compound identification and estimation of HO concentrations, *Journal of Geophysical Research*, **105** (D16): 20473 – 20486.

Williams, J., U. Pöschl, P. J. Crutzen, A. Hansel, R. Holzinger, C. Warneke, W. Lindinger, J. Lelieveld (2001) An atmospheric chemistry interpretation of mass scans obtained from a proton transfer mass spectrometer flown over the tropical rainforest of Surinam, *Journal of Atmospheric Chemistry*, **38**: 133 – 166.

Wróblewski, T., L. Ziemczonek, K. Szerement, G. P. Karwasz (2006) Proton affinities of simple organic compounds, *Czechoslovak Journal of Physics*, **56**: (Suppl. B): B1110- B1115.

Wyche, K. P., R. S. Blake, A. M. Ellis, P. S. Monks, T. Brauers, R. Koppmann, A. C. Apel (2007) Technical note: performance of chemical ioniazation reaction time-of-flight mass spectrometry (CIR-TOF-MS) for the measurement of atmospherically significant oxygenated volatile organic compounds, *Atmospheric Chemistry and Physics*, **7**: 609-620.